Universidade de Aveiro

Ano 2021

Samuel

Dias Costa

Codificação de bloco espaço-tempo na habilitação de sistemas MIMO-OFDM

Space time block coding to enable MIMO-OFDM RADCOM systems

Universidade de Aveiro Departamento de Eletrónica Telecomunicações e Informática
Ano 2021

Samuel
Dias Costa

Codificação de bloco espaço-tempo na habilitação de sistemas MIMO-OFDM

Space time block coding to enable MIMO-OFDM RADCOM systems

Dissertação apresentada à Universidade de Aveiro para cumprimento dos requisitos necessários à obtenção do grau de Mestre em Engenharia Eletrónica e Telecomunicações, realizada sob a orientação científica do Professor Doutor Adão Silva, Professor Associado do Departamento de Eletrónica, Telecomunicações e Informática da Universidade de Aveiro e coorientação do Doutor Daniel Castanheira, investigador auxiliar no Instituto de Telecomunicações de Aveiro.

This work is partially funded by the European Structural and Investment Funds (FEEI) through the Competitiveness and Internationalization Operational Program - COMPETE 2020 and by National Funds through FCT -Foundation for Science and Technology under the project RETIOT (POCI-01-0145- FEDER-016432).

o júri / the jury

Presidente / President	Professor Doutor Arnaldo Silva Rodrigues de Oliveira Professor Auxiliar, Universidade de Aveiro
Vogais / Examiners Comitee	Professor Doutor Marco Alexandre Cravo Gomes Professor Auxiliar, Faculdade de Ciências e Tecnologia da Universidade de Coimbra (Arguente)
	Professor Doutor Adão Paulo Soares da Silva Professor Associado, Universidade de Aveiro (Orientador)

agradecimentos

Aqui deixo expressa a minha eterna gratidão para com aqueles que de uma forma direta ou indireta desempenharam um papel essencial na redação desta dissertação. Sem o vosso apoio e incentivo nada disto seria possível.

Primeiramente aos meus pais, Cristina e Carlos o meu obrigado por tudo fazerem para que se encontrassem reunidas todas as condições favoráveis para o meu sucesso. Não só durante esta etapa, não só durante o meu percurso académico, mas sim durante toda a minha vida. Mãe e Pai, obrigado por tornarem isto possível.

À minha namorada Mariana, obrigado por seres quem és. Obrigado pela paciência, pelo apoio e pelo carinho demonstrado ao longo de todos estes anos. És uma fonte inesgotável de força e motivação que me faz querer ser melhor a cada dia que passa, e qualquer desafio se torna fácil quando se tem alguém como tu ao lado. Agradeço igualmente aos seus pais Dulce e José, por toda a compreensão, e pelo constante apoio demonstrado nesta fase árdua.

Ao meu avô Mário, nem tudo se aprende na escola e, portanto, obrigado pelos ensinamentos, e pelo exemplo que és. Deixo também uma palavra para alguém que infelizmente já não está presente, mas jamais estará ausente, obrigado por tudo avó.

Diogo, Sandra Pedro e Samuel obrigado também pela amizade e apoio demonstrado principalmente neste último ano.

Ao meu orientador Professor Doutor Adão Silva e coorientador Doutor Daniel Castanheira obrigado pelo constante acompanhamento, pelo contributo e pela total disponibilidade sempre demonstrada. Obrigado pela partilha de conhecimento, por todo o apoio, pela ajuda e compreensão. Agradeço também ao Leonardo Lamas por todas as sugestões, pelo seu contributo e por estar sempre disponível para qualquer esclarecimento adicional. Foi um grande privilégio trabalhar com todos vós.

Por fim gostaria de agradecer à Universidade de Aveiro, ao Departamento de Eletrónica Telecomunicações e Informática e ao Instituto de Telecomunicações por providenciarem todas as condições necessárias de trabalho e aprendizagem.

A todos vós, o meu mais sincero obrigado.

palavras-chave

OFDM, MIMO, RADAR, Tarokh, RadCom, Space-Time Block Code (STBC)

resumo

A largura de banda disponível no espectro de radio frequência enfrenta uma diminuição face ao crescente número de aplicações e utilizadores. Assim, por forma a assegurar uma evolução sustentável neste campo é fulcral desenvolver estratégias que otimizem o uso do espectro. A junção das funcionalidades RADAR e comunicação num só terminal faz parte dessa estratégia. Desta forma, duas funcionalidades usualmente concorrentes pelos mesmos recursos radio, podem coexistir em cooperação, sem interferência entre ambos.

Nesta dissertação a integração dos dois sistemas é conseguida através do uso do OFDM como forma de onda comum. Através de códigos desenhados no espaço-tempo/frequência, nomeadamente a codificação de Tarokh, foi possível introduzir diversidade espacial e ortogonalidade no sistema, aumentando assim a sua robustez e permitindo o uso do conceito de antenas virtuais, que por sua vez possibilitam uma melhoria na resolução e deteção do RADAR. De forma a avaliar o desempenho do sistema desenvolveu-se uma plataforma de simulação. Nesta plataforma começou-se por considerar a deteção RADAR para sistemas com uma e múltiplas antenas, onde posteriormente se integraram as funcionalidades de comunicação. Os resultados obtidos mostraram um excelente desempenho do sistema, que devido à sua baixa complexidade, pode ser um sistema RadCom interessante para os futuros sistemas sem fios.

keywords

OFDM, MIMO, RADAR, Tarokh, RadCom, Space-Time Block Code (STBC)

abstract

The available bandwidth in the radio frequency spectrum is decreasing due to the growing number of applications and users. Therefore, in order to ensure a sustainable evolution in this area it is crucial to develop strategies to optimize the spectrum usage. Joining RADAR and communication functionalities in a single terminal represents exactly this same strategy. As such, the two functionalities, which usually compete for the same radio resources, can coexist through a cooperative relation in which they can thrive and cease to introduce interferences in between them.

In this dissertation, the integration of both systems is achieved through the use of OFDM as the common waveform. Through the space time/frequency block codes, namely the Tarokh coding it is possible to introduce spatial diversity and orthogonality to the system, therefore increasing the system's robustness and allowing to use the virtual antenna concept, which enables improved RADAR resolution and detection. In order to evaluate the system's performance, a simulation platform was developed. In these simulations we start by firstly considering RADAR detection for single and multiple antenna systems and then integrate the radar and communication functionalities. We have verified the good performance levels of the proposed system, which thanks to its low complexity can be an interesting RadCom approach for future wireless systems.

Index

List of figures

List of tables

Acronyms

1G	1st Generation
2G	2nd Generation
3G	3rd Generation
4G	4th Generation
5G	5th Generation
6G	6th Generation
AI	Artificial Inteligence
AMPS	Advanced Mobile Phone System
AWGN	Additive White Gaussian Noise
BER	Bit Error Rate
ConVex C-V2X	Connected Vehicle, Cellular-Vehicle to Anything
CP	Cyclic Prefix
CW	Continuous Wave
DOA	Direction of Arrival
EGC	Equal Gain Combining
eMBB	Enhanced Mobile BroadBand
FDM	Frequency Division Multiplexing
FFT	Fast Fourier Transform

GSM	Global System for Mobile Communications
ICI	Inter-Carrier Interference
IEEE	Institute of Electrical and Electronic Engineering
IFFT	Inverse Fast Fourier Transform
IoT	Internet of Things
ISI	Intersymbol Interference
ISM	The Industrial, Scientific and Medical
ITU	International Telecommunications Unit
LPI	Low Probability of Interception
LO	Local Oscilator
MIMO	Multiple-Input Multiple-Output
MISO	Multiple-Input Single-Output
MMS	Multimedia Message Service
mMTC	Massive Machine-Type Communications
MRC	Maximal Ratio Combining
NMT	Nordic Mobile Telephone
OFDM	Orthogonal Frequency Division Multiplexing
PDP	Power Delay Profile
PRS	Passive Radar System
PSK	Phase Shift Keying
QAM	Quadrature Amplitude Modulation

QPSK	Quadrature Phase Shift Keying
RADAR	Radio Detection and Ranging
RadCom	RADAR and Communication
RCS	Radar Cross Section
RF	Radio Frequency
SC	Selection Combining
SIMO	Single-Input Multiple-Output
SISO	Single-Input Single-Output
SMS	Short Message Service
SNR	Signal to Noise Ratio
STBC	Space Time Block Code
TACS	Total Action Communication System
UAV	Unmanned Aerial Vehicle
ULA	Uniform Linear Array
URLLC	Ultra-Reliable Low Latency Communications
V2V	Vehicle to Vehicle

Chapter 1
Introduction

The following chapter introduces the background and the present of communication and RADAR systems as well as how it can be advantageous to merge them together. The chapter is divided in three sections, the first regarding the evolution of the communication systems, followed by a section addressing the basics of a joint radar and communication system. Finally, the last section will present the motivations and the structure of the dissertation.

1.1 - Mobile communication systems

Communication at its core is part of the reason why mankind was able to create and evolve so much. The ability to transmit acquired knowledge allows us to accelerate drastically the learning process, thus increasing productivity. Ever since we learned about the role that communication plays in technological evolution, we keep working on its optimization. Early on speech turned into smoke signals, then letters, telegraph, phone and by now the focus is the mobile communications, but the idea is the same from start, transmit as much information as possible in as little time as possible.

The now well-known 4G and 5G are the product of a constant evolution ever since the first generation (1G). This was introduced in the early 1980s and was all about laying the foundations of mobile communications. As a first generation it ended up delivering satisfactory results for the time, producing an annual growth in the mobile market of thirty to fifty percent by 1990 [1]. 1G was only able to transmit analogue voice information, and its most prominent systems were advanced mobile phone system (AMPS) from USA, Nordic mobile telephone (NMT) and total access communication system (TACS) both from Europe.

The second generation (2G) emerged in the late 1980s marking the transition from analogical to digital. [2]. 2G used the global system for mobile communications (GSM) and managed to deliver short message service (SMS) and multimedia messages (MMS). In short, the novelties offered by this technology were, digital voice and simple data transfer at low rates. Later 2G would see further improvements and turn into 2.5G that would serve as a stepping stone for the third generation(3G).

Delivered in the new millennium by the International Telecommunication Union (ITU), 3G brought some new features. The new radically improved data speed represented an upgrade for the existent services like voice, SMS and MMS, which started to operate faster. At the same time 3G introduced some new features such as the video calling and internet services [3].

About ten years later the fourth generation (4G) was launched. Fueled by a growing demand of high speed and real time applications, 4G delivered ultra-broadband internet service, data speed ranges from 100 Mbps – 1.0Gbps, high speed handoff, MIMO technology and global mobility. 4G provides its users the capability of

enjoying services such as: HD voice, SMS, MMS, mobile TV, wearable devices, HD streaming, Global roaming, gaming services etc., [3].

Once more, ten years went by, and today we find ourselves in the fifth generation (5G) era, and 5G is all around us, literally. 5G depicts an ambitious project aiming to not only achieve speeds in the gigabit per second order but also to connect entire cities. In order to study the traffic of a massive IoT network in a city scenario a large-scale test took place in a dense urban environment [4]. Data was retrieved from a variety of connected devices such as water, gas and electricity meters, car accelerometers (monitoring driver behaviour) and some other devices. The numbers are presented in figure 1.

	WATER METERS	ELECTRICITY METERS	GAS METERS	VENDING MACHINES	BIKE FLEET MANAGEMENT	PAY-AS-YOU-DRIVE
Typical message size	100 bytes	100 bytes	100 bytes	150 bytes	150 bytes	150 bytes
Message interval	12 hours	24 hours	30 minutes	24 hours	30 minutes	10 minutes
Device density	10,000/km²	10,000/km²	10,000/km²	150/km²	200/km²	2,250/km²

Figure 1-Traffic characteristics of massive IoT network [4].

Along with this, and due to its popularity, it is highly unlikely that the proliferation of smart devices will cease. Smartphones, tablets, TV, sensors etc., are increasingly being used in all kinds of applications as estimated in figure 2, and with it comes the nonstop growing demand of 5G traffic.

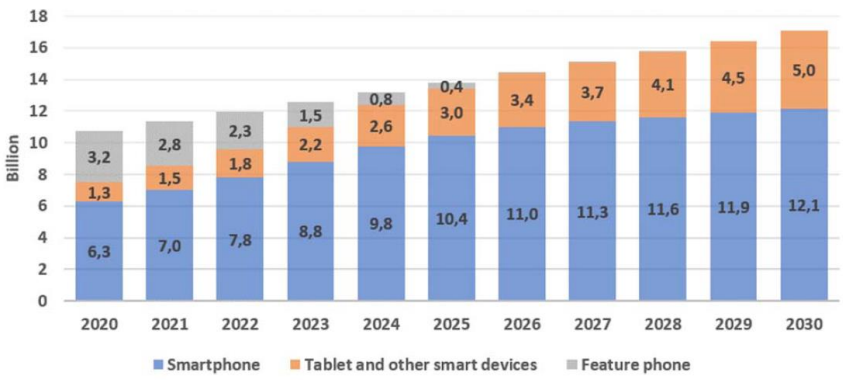

Figure 2-Estimation of global mobile subscriptions [5].

In order to succeed, 5G has not only to live up to its expectations but also has to lift the bar high enough to guarantee an immediate response to the unforeseen use cases that are expected to be revealed in the short

future. Some of the services that 5G will be providing are presented in figure 3, which sorts each service's position in terms of the defining characteristics of 5G, i.e. enhanced Mobile Broadband (eMBB), Ultra Reliable Low Latency Communications (URLLC) and massive Machine-Type Communications (mMTC).

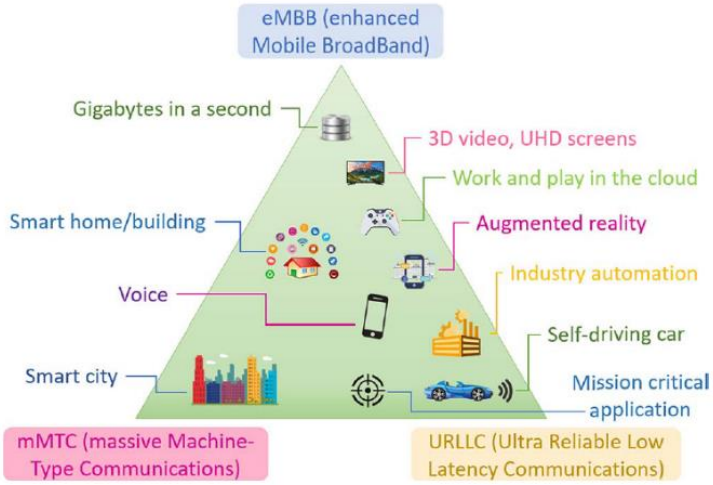

Figure 3-5G Usage scenarios [5].

The 5G promises to optimize our lifestyle by giving us the ability to be in constant communication with our surrounding devices, but for that to happen it is necessary to meet certain requirements. Below are presented the main ones [6].

- Data rate – Real time applications like gaming, streaming, augmented reality or even self-driving vehicles present a critical need of high data rates in order to function properly.
- Latency – Tightly connected to the high data rates, there is also the need to achieve minimal delays in the communication, especially for the control and automation in industry 4.0.
- Energy and cost – It is mandatory to keep energy consumption at a sustainable level as well as the costs involved.

1.2 - RadCom concept

The concept of joint radar and communications (RadCom) appears naturally given the similarities in both systems. Both rely on transmitting and receiving electromagnetic signals and retrieve information from them after a processing stage. The combining of both systems would result in a more efficient use of the radio frequency spectrum since these would share the same band. It would also mean that instead of two pieces of hardware there would only be one covering the two functionalities, thus halving the amount of necessary hardware in a system.

However, before addressing the joint RADAR communication system, it is important to understand the introductory concepts behind RADARs. What they are, what they do, how they do it, and why they are necessary.

1.2.1 RADAR introduction

Starting in the very beginning, the word RADAR besides being a palindrome, is also the acronym for radio detection and ranging. Albeit the term by itself already explains its purpose, it is important to go further. The main operation method of any RADAR revolves in the same principle: an active source illuminates a target, a receiver then collects scattered target energy and a processor generates the radar product (e.g., dots on a screen representing target detections or a synthetic aperture radar image) [7]. By comparing the signal in the transmission and the one received it is possible to estimate the channel, and with that becomes possible to retrieve parameters like range and speed.

A few decades ago, the radar technology was very associated with military equipment or large-scale civilian applications, detecting enemies and controlling air traffic were some of the major use cases of the technology. With time, although not as much as communications, radar evolved, and is not a long-range device only anymore. With the technological advance in the industry, and the amount of high frequency components available today, it can operate at medium or even short range (few meters), thus finding many uses. Although fundamental in the 'old' applications, RADARs now emerged to a lot of new applications: automotive RADARs, geophysical monitoring, surveillance and also medical applications, where RADAR is progressing and inclusively being used for breast cancer detection and tumor localization [8]. The demand for RADAR application keeps growing.

1.2.2 RadCom two-user topologies

The RadCom idea is not new [9], and has been researched for many years, consequently there are a lot of ideas and concepts already established. In order to better understand the concept, we start by addressing passive radar systems (PRS), which rely on non-cooperative signals available in the environment such as cell tower or television station signals to act as illumination sources. Research showed that these illumination sources, can efficiently be utilized to detect and track targets, for this reason, multiple algorithms have already been proposed for the PRS [10]. Since PRS rely on other transmitted signals which travel between a pair of transmit and receive antennas, the PRS presents itself as a good fit for a bistatic RADAR scheme, which we will discuss further in this work. Figure 4 presents a basic PRS bistatic scheme where it is possible to observe communication happening between a transmitter and receiver while the broadcasted signal is simultaneously being used for target detection.

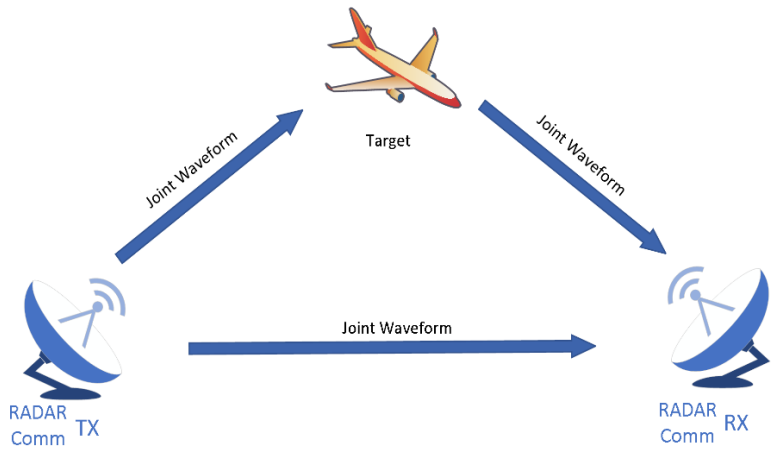

Figure 4- Bi-static broadcast channel topology.

In the other hand, active radars operate in a more independent way, actively generating a radar signal specifically designed for the sensing functionality. For instance, when a generated pulse or continuous wave is emitted, its reflected version will then be received in the same position from whence it came.

The active radars are better suited for a monostatic scheme which will be addressed further in this work. An active monostatic RadCom scheme is shown in figure 5. Here while still operating with a common waveform on both the RADAR and communication systems, the receiver device only needs to receive the processed information instead of processing it itself.

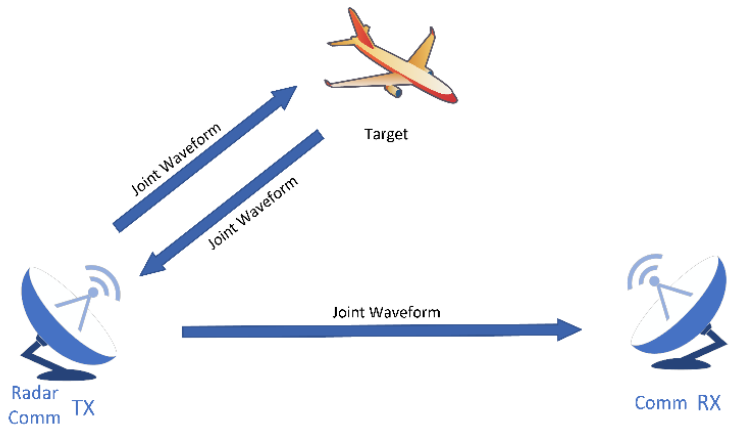

Figure 5 – Monostatic broadcast channel topology.

Both these scenarios aim to improve and simplify the current coexistence of legacy radar and wireless communications commonly designed in isolation from each other. The reason to this becomes evident by observing figure 6. It becomes clear that the two users in this system suffer from mutual interference presented as the blank arrows. Once again, the use of a shared waveform would simplify the whole process, giving the interference and RF spectrum usage problems a proper answer. The optimal thought solution is presented in figure 7, with a dynamic system capable to adapt not only to the environment but also to each device [11]. This

topology has no dedicated radar nor communications resource but dynamic elements that cooperate between themselves in order to achieve the common desired objective of simultaneously sensing and communicating.

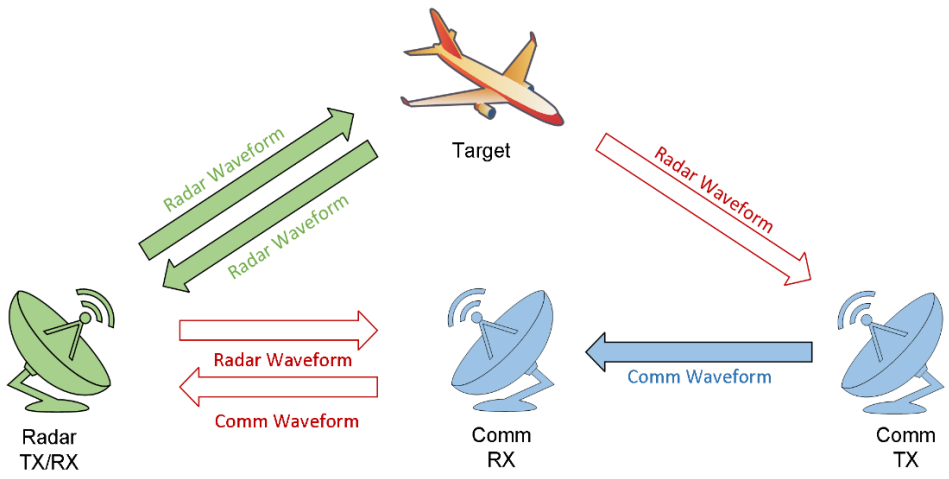

Figure 6 - Interference between radar and communications.

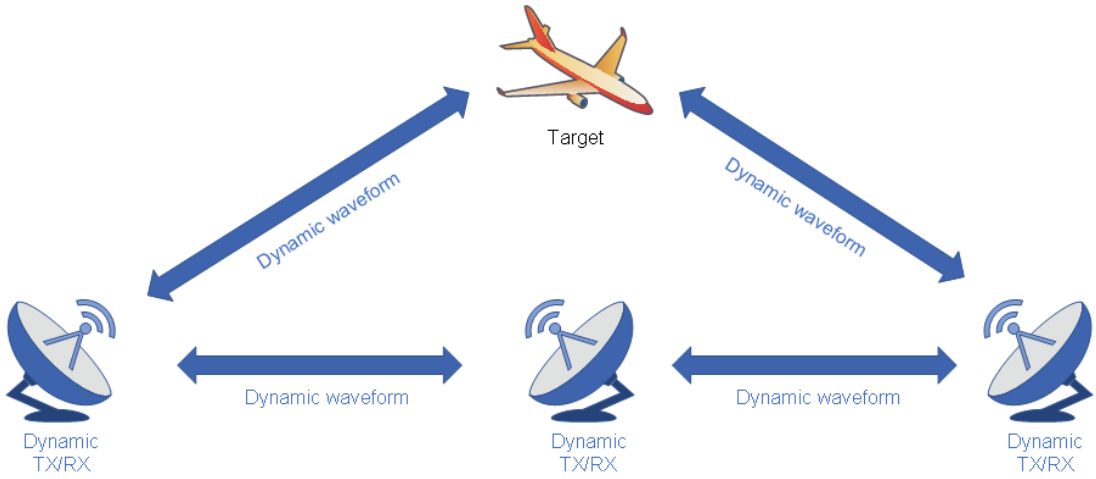

Figure 7 - Dynamic radar communication scheme.

The main concept behind a RadCom system relies in integrating the communication message within the radar waveform, or inversely integrate the sensing operation through the communication waveforms. In order to achieve either it is important to go through some key techniques from which this work cannot deviate, for instance Orthogonal Frequency Division Multiplexing (OFDM) and Multiple Input Multiple Output (MIMO) systems.

OFDM became a very popular modulation technique among the new communication standards, bringing robustness against multi-path fading, easy synchronization and equalization, and a high flexibility in system design, which allows for easily adapting the system parameters to the given channel characteristics [9]. In communications, the OFDM modulation scheme is already vastly explored and used for its capability of

enabling high bit rates and maximizing the efficiency of the bandwidth usage. As for in a radar system it will be used as a modulation for pulse compression in the receiver allowing the extraction of range and Doppler parameters. This way OFDM presents itself as the best technique to fulfill a RadCom system's needs, and the idea is to combine this concept with the MIMO technology, details about this strategy will be presented later in this document.

With a fully functional RadCom system it is expected to unlock a vast group of applications in different areas greatly linked to the automotive realm, transports and also to the military.

- **Civilian applications**: Air traffic control, long range weather RADAR, Vessel traffic service, Automotive radars for collision avoidance, Localization for Vehicular Networks, Wi-Fi Based Indoor Localization and Activity Recognition, Unmanned Aerial Vehicle (UAV) Communication and Sensing, RFID, Medical sensors. [12]
- **Military applications**: Multi-Function RF Systems, Military UAV Applications, RADAR-Assisted Low-Probability-of-Intercept (LPI) Communication [12]

The study of joint RADAR communication systems is highly sought after in the automotive sector as each vehicle sensing system has to be proven not to disturb or blind others [13]. By using a common waveform each vehicle would broadcast information instead of interference to all the nearby users. Sending information like speed, direction or even takeover intention would result in an improved collision avoidance system, better yet a general accident-avoidance network given that pedestrians would also receive information concerning nearby vehicles.

Tesla motors owned by Elon Musk holds possibly the most popular collision avoidance system. It relies on a cooperation between eight cameras, artificial intelligence (AI) processing and ultrasonic sensors. Due to this each Tesla vehicle presents futuristic capabilities such as autopilot or even full self-driving. These functionalities are continuously being improved via software updates [14]. It is important to note that a lot of cars circulating today have basic or no collision detection system at all, thus each Tesla has to also consider those and compensate by doing all the work by itself. Meaning its AI has to collect data, identify objects/vehicles/road limits in real time and act on that information. All of this translates in a demanding system with high processing power requirements. Tesla could improve and even alleviate some of this computational power by integrating a RadCom system. This would allow each vehicle to sense and identify each nearby object from the start, whether vehicle or pedestrian. By receiving processed information Tesla's AI wouldn't have to waste resources in identification algorithms since it would be pre-identified. Let us take for instance the ConVeX C-V2X (Connected Vehicle , cellular-vehicle to anything) trials made by Audi which started in December 2016 and took place in Germany [15]. This feature empowered the vehicles to receive information of its surroundings, from aquaplaning warnings to broken vehicles in the road, the vehicle was constantly receiving useful information. Furthermore, a vehicle reaching crossroads would also receive information on other vehicles approaching the same crossing. These are all features that can and should co-exist with the already present radar functionality, this is a cooperation that would enhance both the sensing and

communication operations while minimizing the amount of hardware needed. Having all the possible information at our disposal logically has a crucial importance in a future of self-driving vehicles and accident-free roads.

1.3 - Motivations and objectives

As mentioned previously, there is an ever-growing demand in terms of wireless connected devices, and that same demand brings some constraints regarding the RF spectrum. The pace at which this phenomenon is happening turned this finite resource into one of the most expensive resources. This is observable in the sharp rise of the auction price of the available RF spectrum, as of 2015, for example, mobile network operators in the United Kingdom have been required to pay a combined annual total of £80.3 million for the 900 MHz and £119.3 million for the 1800 MHz band, employed for voice and data services using a mix of 2/3/4G technologies. In Germany, the regulator Bundesnetzagentur revealed that the total in the auction of 4 frequency bands for mobile network operators exceeded 5 billion euros. Meanwhile the US Federal Communications Commission (FCC) completed its first 5G auction, with a sale of 28 GHz spectrum licenses raising $702 million [12].

Since RF spectrum is not produced nor recycled it is mandatory to ensure that its usage efficiency is maximized, hence the importance of merging two concurrent systems. This merging would also result in a reduced number of electronic devices in any of the areas where both RADAR and communications usage is relevant, this represents a benefit both economically and ecologically. With the growing number of use cases for RADAR, and the acceleration in the communication technologies becomes evident that there is a need to improvement, and as so both systems end up benefiting from the ongoing RadCom research.

As such, the objective behind this work is to further develop the cooperative relation between RADAR and communication systems, create conditions for both to not only coexist but also rely on each other to achieve better performance levels. The upcoming rise of 5G, along with the scarcity of the RF spectrum are the main drive of this also upcoming RadCom system. The ultimate goal is to find the proper waveform in order to develop a joint system through an MIMO-OFDM RADAR capable of simultaneously sensing and communicating. Recently, it was considered space-time/frequency block codes to efficiently integrate communication and RADAR functionalities [16]. It was already shown that by using the Alamouti coding scheme, the spatial diversity order is improved as in legacy communication systems, which has a favorable impact on the bit error rate (BER). Furthermore, as the Alamouti code is an orthogonal code the RADAR's angle resolution is improved through the use of the virtual array concept. However, Alamouti coding has some limitation in terms of the number of transmit antennas. Therefore, in this dissertation, we aim to overcome this limitation by extending the work in [16] for a general space-time/frequency coding scheme, namely the Tarokh codes that allows more transmit antennas. This means that the RadCom terminal will then have multiple antennas in order to be able to estimate the angle of arrival of a signal, then the Tarokh coding will be added to the system so that it can establish communication whilst performing the radar operation. Finally, a performance evaluation in several scenarios will take place through numeric simulations.

1.4 - Outline

This dissertation is composed by six chapters. This first one being an introductory chapter which starts by giving insight regarding the evolution of mobile communications. Followed by a brief overview of joint RADAR and communication systems and lastly presenting the motivations and contributions.

In chapter 2 we address RADAR basics. We start by differentiating a passive RADAR from an active RADAR and briefly introduce the topologies that suit each case. We then go through each of the possible detection scenarios, explaining when and why they happen. Next, we introduce the RADAR estimation process, here we explain the relation between certain parameters and the estimation itself. Lastly, we explain the basic differences between pulsed RADARs and continuous wave radars.

Chapter 3 is dedicated to the OFDM modulation. The operation method behind the OFDM technology is presented along with the advantages that it brings. We introduce useful concepts for the further chapters such as the OFDM frame and the distribution of the symbols through it. The cyclic prefix is also addressed in this chapter, extolling its importance. We then present the typical channel parameters of OFDM systems. Later we explain why OFDM presents a good fit for a RADAR system and how the parameters are retrieved.

Chapter 4 starts by introducing the general MIMO concept and the diversity attained from its use. Next, the MIMO configurations are presented. Two space time block codes (STBC) are then introduced, Alamouti and Tarokh, followed by the virtual antenna concept. Lastly, we merge the previously introduced OFDM concept into the MIMO domain.

Chapter 5 presents the developed work in detail. First, we briefly present the simple SISO-OFDM RADAR scenario, where the terminals are equipped with a single antenna. After, we upgrade the previous scenario by moving from a SISO to a MIMO setup. Lastly, we merge the two functionalities in the MIMO system thus obtaining the MIMO-OFDM STBC RadCom system. Throughout this evolving presentation the core concepts and mathematic processes are explained.

Chapter 6 being the last chapter presents the main conclusions of this work along with some topics for possible future work.

Chapter 2
RADAR systems

As mentioned previously the word RADAR stands for radio detection and ranging, and essentially these are the main functions of a RADAR, these fulfill the purpose of its invention. Although, more than a hundred years went by since the first RADAR presented by Christian Hülsmeyer in 1904 [17], as a result the RADAR systems became more and more sophisticated throughout the years covering additional functions besides just detection and ranging. Today we can rely on radars to estimate velocity or even the target shape and size.

This chapter serves as an introduction to radar systems in general. It starts by presenting the basic aspects of a RADAR, its working method and the most used topologies. We then present a set of possible scenarios regarding detection, where the concept of correct and incorrect detection is explained and justified. Next comes the estimation section in which it is described how the system estimates the values of range and speed as well as the resolution of each of these measurements, the mathematic expressions of these estimations are also presented in this section. An analysis of the RADAR equation and all its parameters is done, and lastly a comparison between continuous and pulsed RADAR takes place.

2.1 - Overview

The basic form of operation, common for all RADAR systems consists in transmitting electromagnetic waveforms. These waveforms propagate through space ultimately colliding onto objects which we can refer to as targets, from this collision a reflected waveform is created, and by comparing the transmitted waveform with the reflected one it becomes possible to estimate the targets parameters. The basic concept of a radar is shown in figure 8.

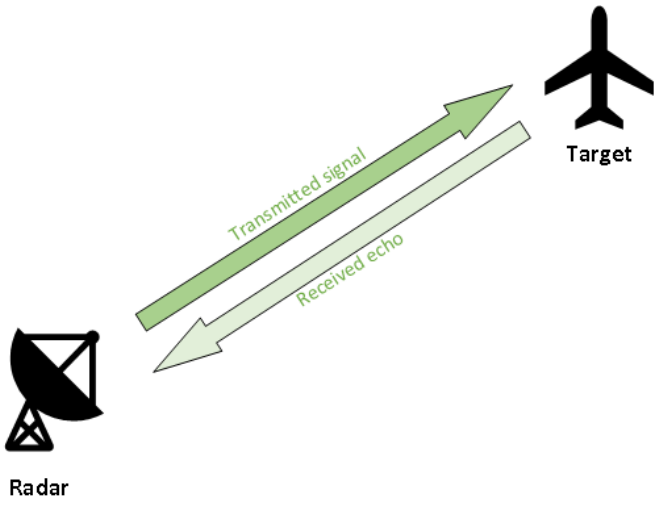

Figure 8 - Basic radar method of operation (monostatic topology).

Regarding the physical layout of a RADAR, the two main topologies have already been briefly introduced in chapter 1.2. The monostatic RADAR is shown in figure 5 for a possible RadCom scenario and in figure 8 for a radar only scenario. This scheme is composed by one device alone which comprises the two co-located components. One being the transmitter, sending a given data, and the other the receiver which will receive the reflection of the sent data. As for bistatic RADARs, these are composed by the two same components as the prior, although this time non-co-located. This topology is also shown in figure 4 for a possible RadCom scenario and in figure 9 for a radar only scenario.

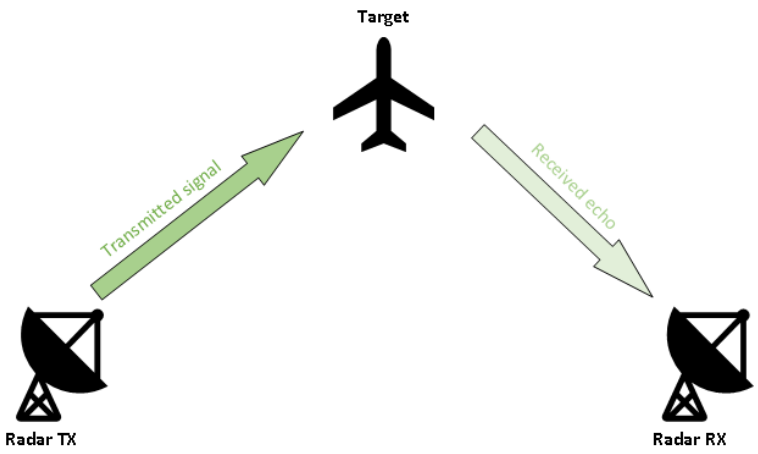

Figure 9 - Bistatic radar scheme.

Diving in further detail figure 10 shows a basic block diagram for a generic monostatic radar system. The monostatic topology is achieved by using the duplexer, this is the component responsible for the constant switching between transmission and reception, similar to a rail switch it acts as a channel, ensuring that the transmitted signal goes to the transmitter and the received signal goes to the receiver. Moreover, by doing this the duplexer also protects the receiver from the high power originated by the transmission process that could damage the receiver.

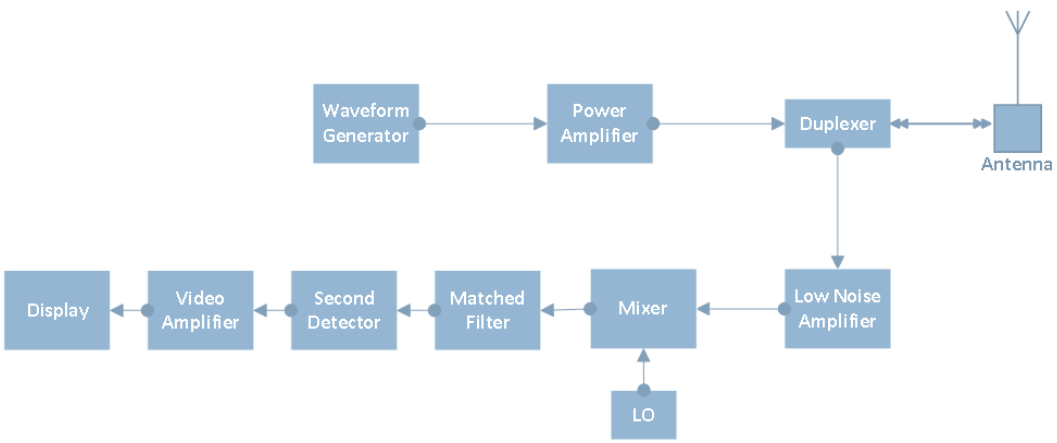

Figure 10 – Radar block diagram.

The transmitter system consists in generating a waveform at a low power level, this adds versatility to the system, since it allows an easier generation of different waveforms for different applications. After comes the amplification stage which will amplify the power of the generated waveform to a desired level, from here the amplified waveform reaches the duplexer and is transmitted through the antenna.

In the receiver, we have a very attenuated signal polluted with noise, and in order to make use of it, it is important to first have a low noise amplifier. This will provide a power gain while still reducing the signal to noise ratio (SNR). Next come the mixer with the local oscillator, these two ordinarily cooperate in order to change a signal's frequency (heterodyning process), and so here the function maintains, this block is responsible to convert the received RF signal to the desired frequency. Afterwards the matched filter will maximize the SNR by correlating the received signal with the transmitted, and from here comes another detection and amplifying stage that will end up in the displayed signal.

2.2 - Detection

RADARs gather a couple of core functions, such as target detection and range estimation, besides this, and as mentioned, they are capable of estimating speed and size as well. Some are also able to distinguish the number of targets in its operation range. The subsection below seeks to explain how the detection happens.

By definition, detection is the act of identifying or accessing a target or information. This function provided perhaps the main motivation in the emergence of RADAR systems. However, there is a variety of scenarios for detection, this process might or might not translate what is happening in the real world, and those situations also have to be accessed and explained. As so, to begin with, we can separate the scenarios based on its outcome: Correct detection or Incorrect detection. The correct detection then splits in other two sub scenarios.

1st – Correct detection of a target: In this sub scenario, a target is present and the received signal confirms its presence, with the amplitude of the returning signal surpassing the presence threshold.

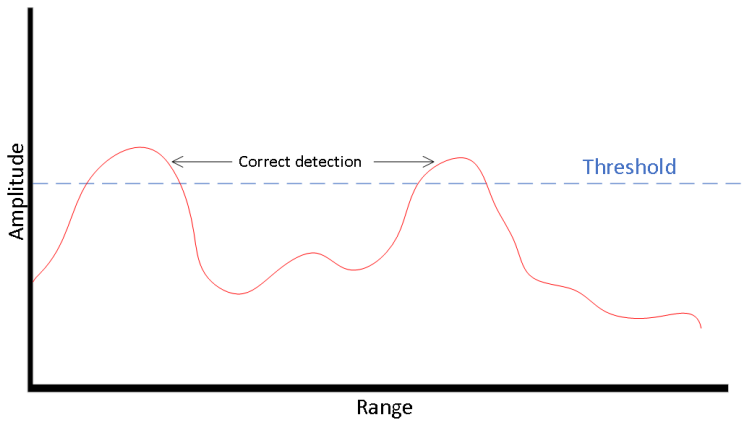

Figure 11 - Correct detection case.

2nd – Correct non detection: This time the radar has no target in its range, and the information received goes accordingly, showing no peaks above the presence threshold.

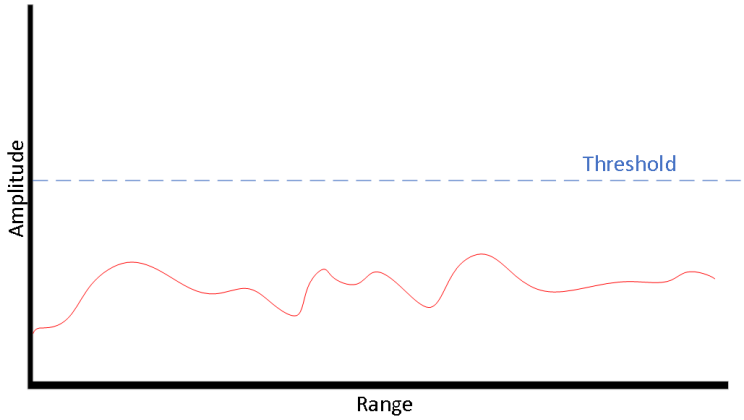

Figure 12 - Correct non-detection case.

Similarly, to the correct scenarios, the incorrect detection is also doubled.

1st – Incorrect detection of a target, false positive: Happens when the radar shows the presence of a non-existent target, this can happen due to high levels of noise / clutter.

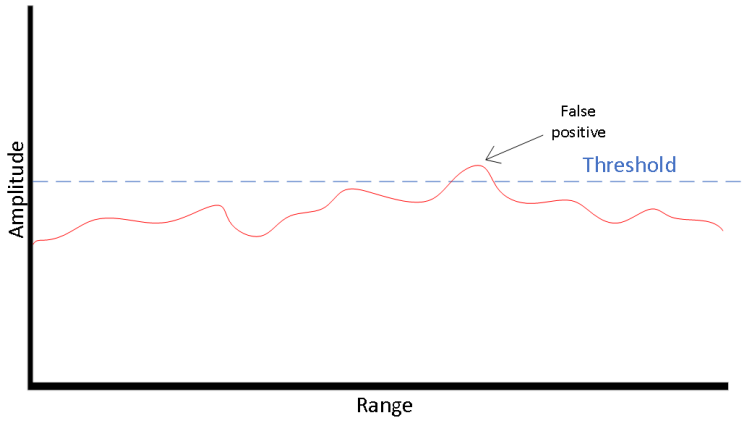

Figure 13 - Incorrect detection case.

2nd – Incorrect absence of target: In this case the target(s) is present but the radar fails to confirm that information, this happens when the peak amplitude in the received signal is too low and does not reach the threshold level. Heavy attenuation is the main cause of this phenomenon.

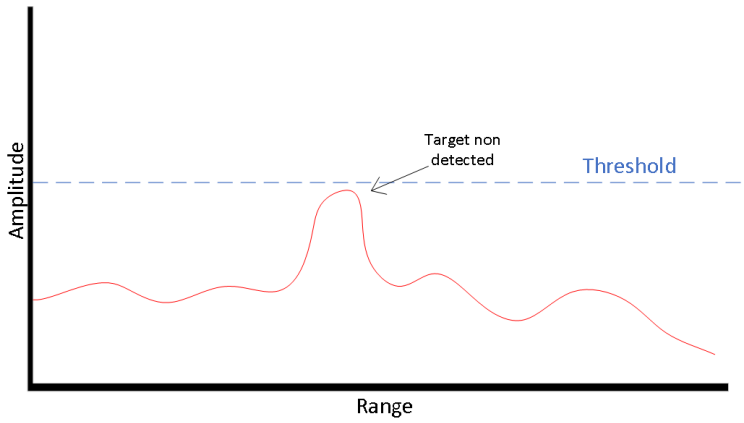

Figure 14 - Incorrect non-detection case.

2.3 - Estimation

The following subsection aims to explain how the target parameters are estimated, and describes the functions behind each measurement.

Range

The ability to estimate the distance between the radar and the target is heavily tied to the time it takes for the waveform to reach the target and come back to the radar.

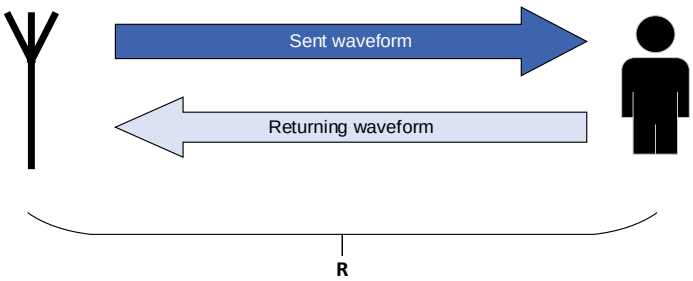

Figure 15 - Signal two way trip.

In this two-way trip, since we are dealing with an electromagnetic wave, happens at the speed of light ($c_0 = 3\times10^8 m/s$), from here assuming t_d as the time it takes for the wave to travel twice the range R , we can estimate the said range using the following expression.

$$R = \frac{t_d c_0}{2} \tag{2.1}$$

Speed (from Doppler)

In order to understand how RADARs compute the speed of a target, it is essential to comprehend the Doppler effect. The Doppler effect is actually something that we experience quite often, namely every time a

vehicle passes near us with a moderate velocity, the difference between the sound heard when the vehicle is approaching and when is going away is none other than the expression of the Doppler effect itself.

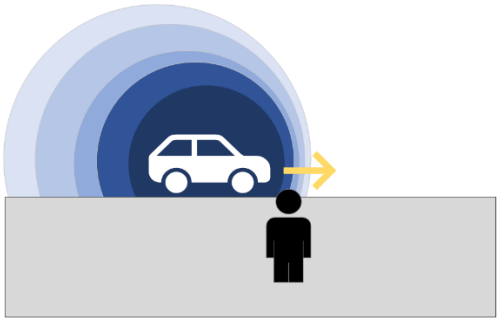

Figure 16 - Doppler effect (approaching).

The reason why this happens is because if the vehicle was static in relation to the observer, the sound heard would also be 'static', but by moving, the waves generated propagate in space differently. While the vehicle is approaching, the observer will sense consecutive waves with a higher frequency, since the distance between vehicle observer is constantly reducing, this is depicted in figure 16. In the other hand when the vehicle is going away the opposite happens, and as so the observer senses the waveforms with a lower frequency as shown in figure 17.

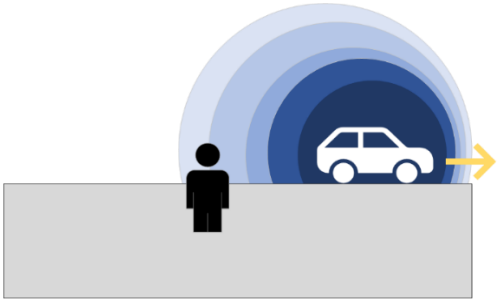

Figure 17 - Doppler effect (leaving).

In this example we used a vehicle as a waveform source, but this effect is transversal to all scenarios, obviously including RADARs. Ultimately the Doppler effect is expressed by a change in frequency or wavelength, this change or better yet shift can then be quantified and expressed by:

$$f_D = \frac{2v}{\lambda} \tag{2.2}$$

Where f_D represents the doppler shift and v is the radial velocity (relative speed of the wave source).

Resolution (both cases)

In both these measurements it is important to have the proper resolution as it can translate a distortion of the reality into the processed data. For instance, the range resolution is what makes possible for a RADAR to distinguish two targets that are close together. Meaning that a wrong range resolution can result in incorrect

identification, detecting one target when it should be detecting two. This obviously represents a critical failure which can have catastrophic consequences if we are considering planes as targets for instance.

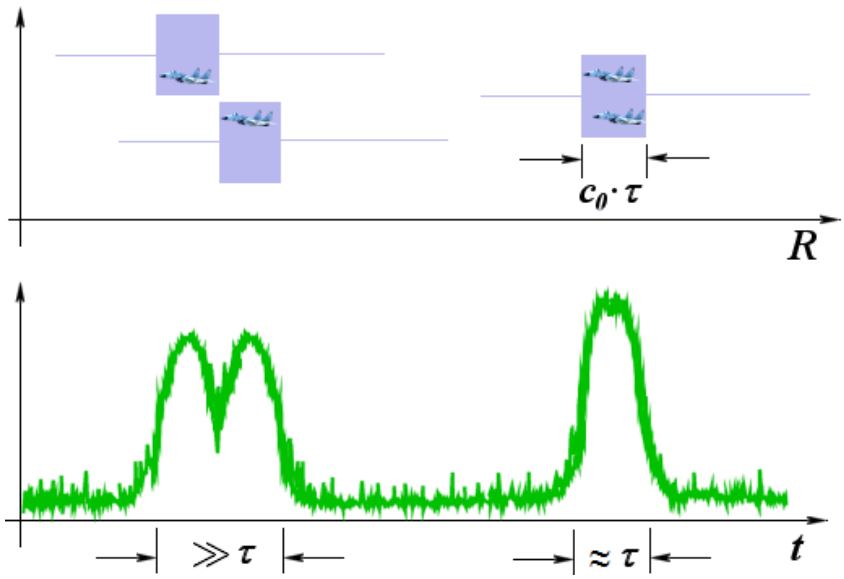

Figure 18 -Importance of range resolution [18].

The range resolution depends on the pulse width. Theoretically a RADAR should be able to distinguish targets that are separated by half of the pulse width time τ . The bandwidth $B = 1/\tau$ naturally also plays a role in range resolution, given that the more resolution we want to achieve, the more bandwidth has to be used as shown in figure 19.

In order to achieve better resolution, pulse compression methods are used. Short pulses result in higher bandwidth and better resolution, however, it also results in less received energy. This can turn into a problem since it can lead to miss detection of targets. Therefore, we need increased bandwidth and not so short pulses. This way we can modulate the pulse, for instance in frequency or phase. Therefore, the ability to compress the pulse itself is dependent on the bandwidth of the transmitted pulse. The receiver will need at least the same amount of bandwidth to process the echoes received. In figure 19 we can observe that as we push the range resolution to lower values, (making the radar capable of distinguishing objects with smaller and smaller distances in between them) we also have to increase the bandwidth drastically. This relation is also verified in the expression (2.3).

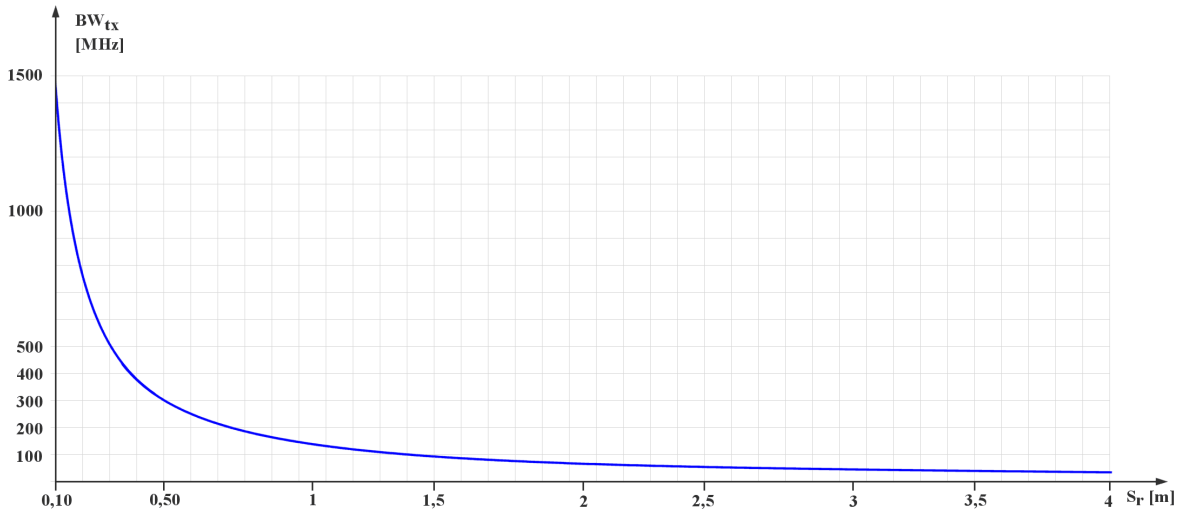

Figure 19- Bandwidth by Range resolution [18].

The resolution expression is then given by:

$$\Delta R = \frac{\tau c_0}{2} = \frac{c_0}{2B} \tag{2.3}$$

As seen in the expression there is an inverse proportion relation between bandwidth and pulse width, this is the reason why we have to sacrifice bandwidth for resolution or vice versa. A long pulse can have the same bandwidth (resolution) as a short pulse, but it has to be modulated in frequency or phase [19].

The same happens to velocity. The Doppler resolution translates the ability of a RADAR to distinguish targets with different radial velocities within a same distance from the RADAR. Again, as with the range, it is crucial to be able to calculate the speed at which a target is moving in order to avoid accidents. The Doppler resolution depends on the observation time T_{Obs}, the more time the effect is observed the better resolution gets, as so the expression is given by:

$$\Delta f_D = \frac{1}{T_{Obs}} \tag{2.4}$$

2.4 - RADAR Equation

Perhaps the most useful description of the factors influencing a RADAR's performance is obtained through the RADAR equation [20]. This equation presents a deterministic model that relates received echo power to transmitted power in terms of a variety of system design parameters [21].

Assuming a scenario with a directive antenna with a radiating power of P_t in all directions, we can picture that imagining a sphere with a growing radius R_S centered in the antenna. Although since the antenna is

directive, it means that it possesses a gain G_t in a determined direction, the target's direction. So, what we end up with in a lossless medium is the radiated power amplified by the gain, and in order to be a density is then divided by the sphere's surface area.

$$\text{Power density directive antenna} = \frac{P_t G_t}{4\pi R_S^{\,2}} \ \text{W/m}^2 \tag{2.5}$$

When the electromagnetic wave with the power density described in (2.5) collides with the target at range R the incident energy is scattered in various directions, one of which leads back towards the RADAR, this energy is the backscattered energy [20]. So, from all the radiated energy in first place, the backscattered energy represents only a portion of the initial. This portion or quantity can be referred to as the radar cross section represented by φ. Worth noting that φ isn't equal to the physical cross-sectional area of the target, instead it represents an equivalent area that can be used to relate incident power density at the target to the reflected power density at the receiver [20]. The φ expression is proportional to the relation between the reflected and incident electric fields E_r and E_t .

$$\varphi = 4\pi R_S^{\,2} \left(\frac{|E_r|}{|E_t|} \right)^2 \tag{2.6}$$

The backscattered power density is then given by:

$$\text{Backscattered power density} = \frac{P_t G_t}{4\pi R_S^{\,2}} \frac{\varphi}{4\pi R_S^{\,2}} \ \text{W/m}^2 \tag{2.7}$$

We can further specify that the RADAR's receiving antenna only uses the energy from a given effective aperture area A_e, meaning that the power received by the radar is:

$$\mathrm{P}_r = \frac{P_t G_t}{4\pi R_S^{\,2}} \frac{\varphi}{4\pi R_S^{\,2}} \mathrm{A}_e \ \text{W/m}^2 \tag{2.8}$$

When the same antenna is used to both transmit and receive, a relation between the gain G and the effective area A_e is verified, from where we can retrieve A_e [20].

$$G_t = \frac{4\pi A_e}{\lambda^2} \Leftrightarrow A_e = \frac{G_t \lambda^2}{4\pi} \tag{2.9}$$

By defining the maximum range $R = R_{\max}$ of a RADAR as the value for which the receiver verifies the minimum measurable value $P_r = S_{\min}$ we can write:

$$S_{\min} = \frac{P_t G_t}{4\pi R_{\max}^{\ 2}} \frac{\varphi}{4\pi R_{\max}^{\ 2}} \mathrm{A}_e \tag{2.10}$$

From where the maximum range expression emerges as:

$$S_{\min} = \frac{P_t G_t \varphi \mathrm{A}_e}{(4\pi)^2 R_{\max}^{\ 4}} \Leftrightarrow R_{\max} = \left(\frac{P_t G_t \varphi \mathrm{A}_e}{(4\pi)^2 S_{\min}} \right)^{\frac{1}{4}} \tag{2.11}$$

With the minimum detectable value $S_{\min}$ being:

$$S_{\min} = kT_0 B F_n \left(\frac{S}{N} \right)_{\min} \tag{2.12}$$

Where: k is the Boltzmann constant, T_0 the temperature, B the receiver bandwidth, F_n the noise factor and $\left(\frac{S}{N} \right)_{\min}$ the minimum value of signal-to-noise-ratio

The noise factor F_n will contribute to a more accurate definition of the total noise and is given by:

$$F_n = \frac{N_0}{kT_0 B G_n} \tag{2.13}$$

With N_0 being the output noise and G_n the available gain.

2.5 - Pulsed vs Continuous

Regarding the waveforms used by RADARs, we can split them in two major groups. Pulsed or continuous waveforms. The choice of one of these types of waveforms will have consequences in the parameters presented above. For instance, in terms of range estimation, while using a pulsed waveform, which consists of periodic and short power pulses and silent periods, the RADAR is able to receive the reflected signals in these silent periods and time mark them for RADAR to perform the range estimation [22]. This however wouldn't work with a RADAR transmitting a continuous waveform, which would lack the silent periods for the RADAR to time mark the signal.

Pulsed Waveform

While using pulsed waveforms we are able to estimate range. As said previously this is due to the silent period of the transmission. The transmitted pulse has a time duration τ (usually in the microseconds order) following this, comes the silent period. During this time, in order to avoid interference, the reflected signal has to return to the radar before the next pulse is transmitted.

The overall repetition happens according to the pulse repetition frequency period, $T_{PRF} = \tau + \text{silent period}$. That is the reason why the range is heavily dependent on the T_{PRF}. Figure 20 shows a practical automotive scenario.

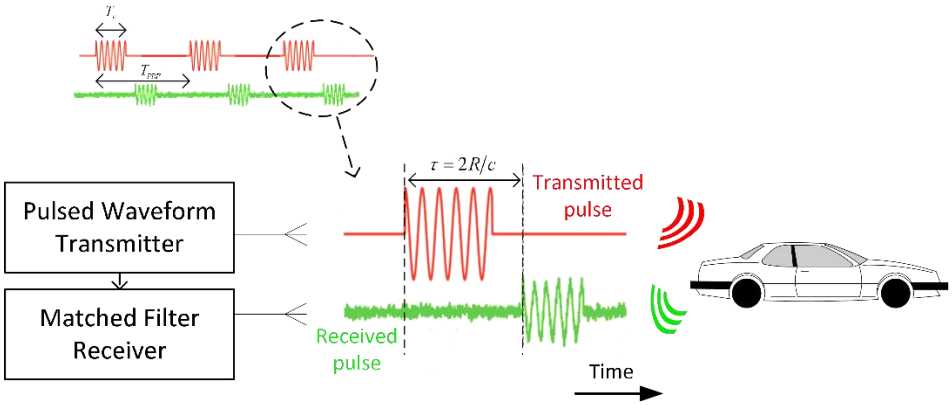

Figure 20- Pulsed waveform scenario [22].

Continuous waveform

Continuous wave RADAR systems are constantly transmitting an illuminating signal and at the same time receiving its echo scattered by the target. Although CW RADARs don't excel in range estimation, they do in detecting small variations, thus making them appropriate to use upon moving targets. Let us say we apply a continuous signal to a stationary target. What will happen is that the frequency of the received echo will remain immutable. However, when applying the same transmitted signal to a moving target, we will notice that the frequency of the echo signal is altered. This change is none other than the expression of the previously presented Doppler effect hence making this waveform perfect to measure velocity accurately. Figure 21 shows the basic operation method of a CW radar system.

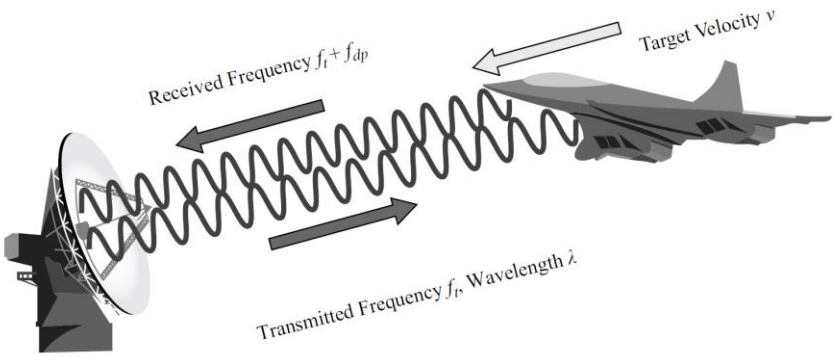

Figure 21- Operation of a CW radar system [7].

Chapter 3
OFDM in RADAR

This chapter starts by presenting a general description of the orthogonal frequency division multiplexing (OFDM) waveform and why it is used in RADAR. After this a more detailed vision of OFDM is presented where all the concepts involved are addressed, then an explanation on how OFDM can be of use to a RADAR system through the analysis of its parameters.

3.1 - Why OFDM

In order to achieve the desired multifunction feature (sensing and communication) simultaneously it is necessary to resort to integrated waveforms. This has been a highly researched area and some conclusions have already been taken from there.

Multicarrier waveforms constitute a flexible candidate for the joint radar and communication systems. These waveforms are already being used as the basis of several communication systems (e.g., IEEE 802.11 a/g/n, Long Term Evolution (LTE), and 5G New Radio (NR)) and have also become popular for RADARs [23]. Furthermore, it is shown in [24]- [25] that OFDM waveforms present a good fit for radar applications, since they lead to improvements in terms of parameter estimation (e.g., Doppler effect and range), target detection, spectral efficiency and radar resolution.

3.2 - Introduction to OFDM

To explain in a short sentence, OFDM can be seen as a special case of multicarrier transmission, where a single data stream with high rate is transmitted over a number of lower-rate subcarriers [26]. OFDM ends up bringing innumerous advantages, not only does it bring the necessary robustness for a dual transmitting system but also a much greater efficiency in terms of bandwidth usage compared to the other techniques. For instance, a classical parallel-data system sees its band divided into N frequency subchannels with each of these being modulated with a separate symbol, then the N subchannels are frequency multiplexed, and in order to reduce its intercarrier interference each subcarrier is isolated from the others so that no overlap happens. Although it solves the interference problem, it does so at the expense of extra bandwidth, meaning it creates a new problem, inefficiency. This is shown in the figure 22 below in which (a) represents the FDM scenario and (b) the OFDM.

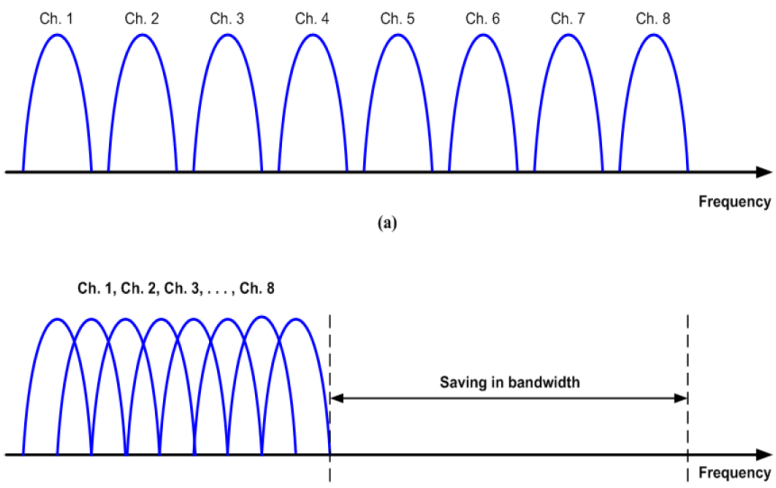

Figure 22- OFDM efficiency vs FDM [27].

3.3 - How OFDM works

Let us now better describe OFDM's operation method. The first thing needed is multiple carriers, a common technique was based on a bank of filters, each filter was a band-pass that when applied to the input signal would return it in multiple components, however and in order to further expand the number of carriers the bank of filters gave place to the use of fast Fourier transform (FFT) algorithms. In figure 23 we can observe how OFDM divides the single high rate data stream into multiple lower rate data streams.

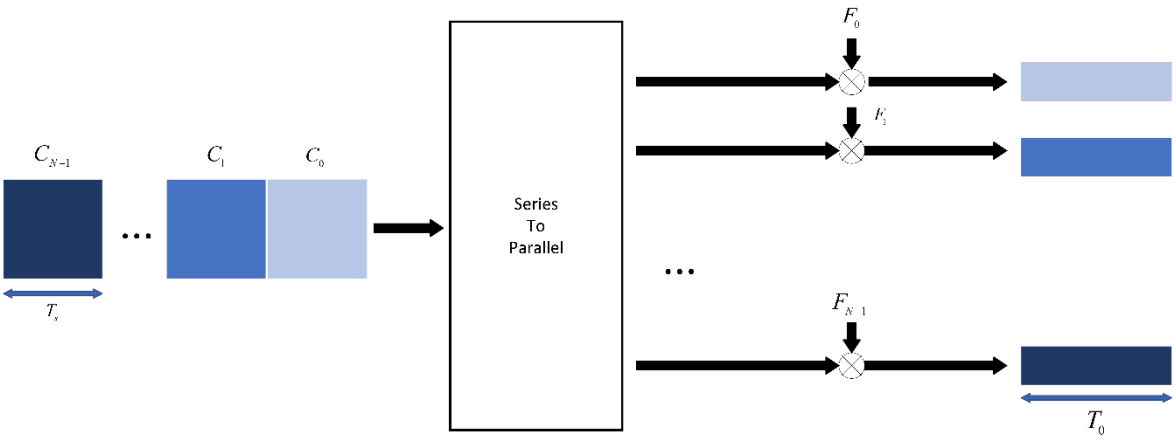

Figure 23 -OFDM Series to parallel.

The OFDM signal generated uses the inverse fast Fourier transform (IFFT) and later the demodulation is done through FFT as described in figure 24 for a QAM case.

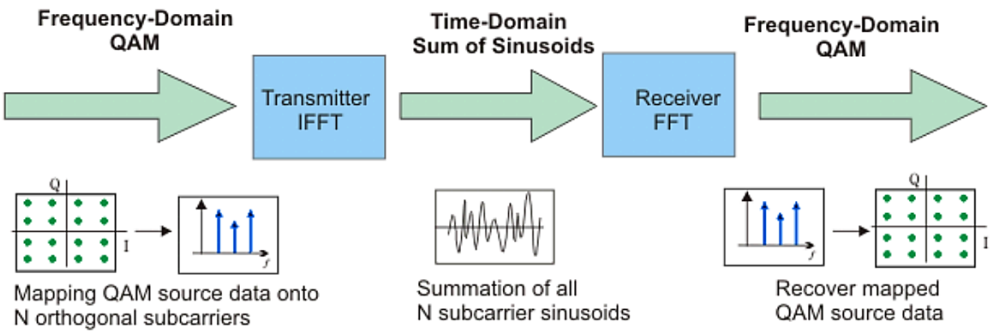

Figure 24- Simplified OFDM block diagram [28].

The OFDM signal can be described as a set of closely spaced FDM subcarriers. In the frequency domain each transmitted sub-carrier is a sinc function, these have side lobes that end up overlapping with other sub-carriers's side-lobes [28], that is where orthogonality comes in. By arranging them and get these frequencies orthogonally spaced, the individual peaks of each one will stay lined up with the nulls of the other subcarriers, this can be visualized in figure 25. As so, even though there is a visual overlapping of sub-carriers in the same channel, it presents no interference at all, allowing the system to fully recover the original signal.

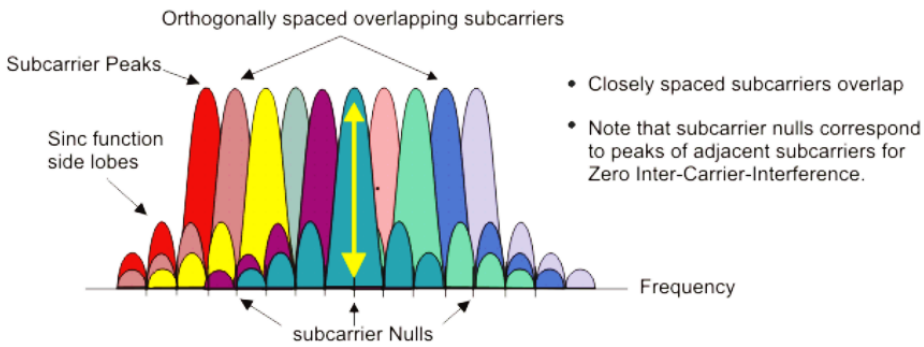

Figure 25- OFDM signal [28].

The sub-carrier modulation is commonly achieved through phase shift keying (PSK) or QAM, whereas the orthogonality happens due to the correct sub-carrier spacing Δf choice, which corresponds to the inverse of the OFDM symbol duration $1/T = 1/(N/B) = B/N$, with N being the number of sub-carriers and B the bandwidth.

Furthermore, the mathematical condition to achieve orthogonality is given by:

$$\int_0^T s_i(t)\, s_j(t)\, dt = \begin{cases} c & i = j \\ 0 & i \neq j \end{cases} \tag{3.1}$$

3.4 - OFDM Symbol

As previously mentioned, the sub-carriers are transmitted in parallel across the frequency and overlapped in time, this is presented in figure 26.

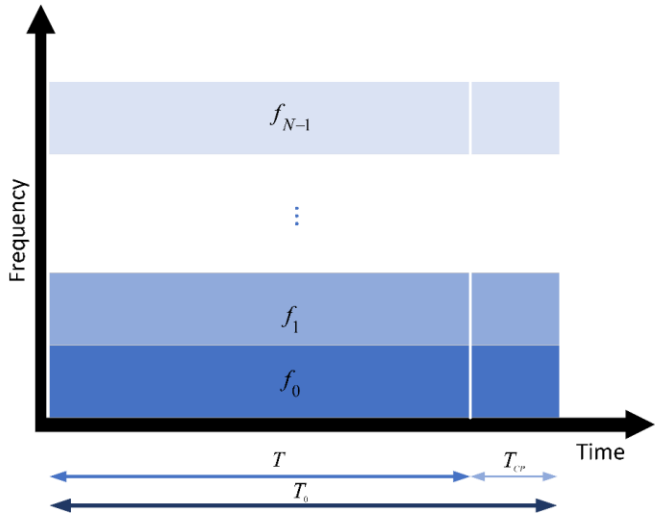

Figure 26 -OFDM subcarriers through time.

Let us assume to have a group of complex symbols $c_{k,l}$, these symbols will be transmitted across the N multiple sub-carriers. This is repeated for each of the M transmitted symbols. Each set of these M transmitted symbols across every sub-carrier is called an OFDM symbol, and as we continuously keep transmitting OFDM symbols we create what is called an OFDM frame. Both concepts are shown in the figure 27.

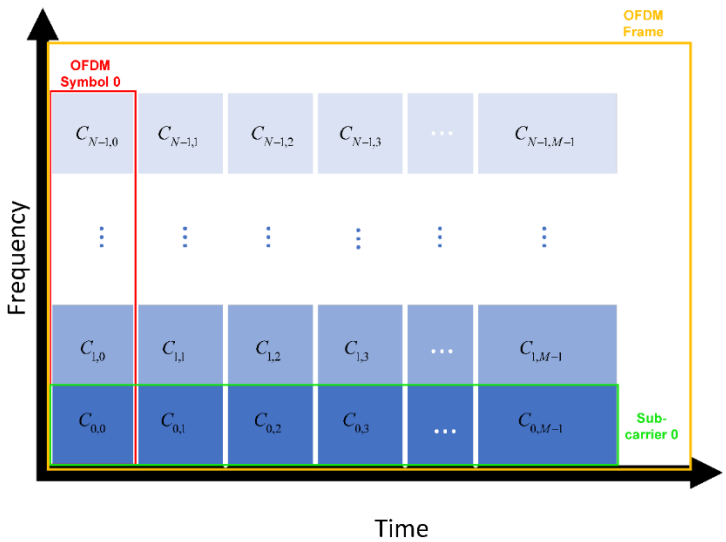

Figure 27 -OFDM Frame.

Let us now describe the indexes for each frame dimension, being k the sub-carrier index and l the symbol index, with k going from 0 to $N-1$ and l through 0 to $M-1$.

Each $c_{k,l}$ is then modulated into a T duration rectangular pulse shape as follows

$$rect(t) = \begin{cases} 1, & 0 < t < T \\ 0, & otherwise \end{cases} \tag{3.2}$$

The sub-carriers' frequencies are described by adding the sub-carrier separation Δf times the index k

$$f_k = f_0 + k\Delta f \tag{3.3}$$

Moreover, we can describe the first complex baseband OFDM symbol $s(t)$ (index $l = 0$), through the following mathematic expression

$$s(t) = \sum_{k=0}^{N-1} c_{k,0} e^{j2\pi k\Delta f t} \tag{3.4}$$

The modulation of the OFDM signal is then efficiently performed through the inverse fast Fourier transform. In order to do this, the IFFT length has to be equal to the number of sub-carriers, the time variable t also has to be replaced by the sampling period $n\frac{T}{N}$ and since $T = \frac{1}{\Delta f}$ we end up with $t = \frac{n}{N\Delta f}$.

With the mentioned substitutions we are now able to express the discrete version of the first OFDM symbol of the frame, which is given by

$$s(n) = s(nT/N) = \sum_{k=0}^{N-1} c_{k,0} e^{j2\pi\frac{kn}{N}}, n = \{0,1,...,N-1\} \tag{3.5}$$

This reinforces the idea that the discrete time signal for the OFDM symbols is given by the IFFT of the modulated symbol.

As so it is proven that it is possible to recover the original sequence $c_{k,l}$ using the FFT with a N/T rate over the N samples, the global procedure goes as follows

$$s(n) = IFFT(c_{k,l}) \Rightarrow c_{k,l} = FFT(s_n) \tag{3.6}$$

3.5 - Cyclic prefix

As with any other communication technology, the OFDM signal presents vulnerabilities in terms of delay and distortion, so there is always a necessity to mitigate these phenomena. One way to act on this matter is by using a cyclic prefix. The way this works is, for each OFDM symbol there is a guard interval inserted before. While it's duration, T_{CP} may vary (usually is a fraction of the symbol duration T , typically $1/4$ or $1/8$) it has to be greater than the channel maximum delay. In this guard interval a copy of the end of the symbol is inserted at the beginning of the symbol, see figure 28 and figure 29. This preserves the orthogonality of the subcarriers and prevents inter-symbol interference (ISI) between successive OFDM symbols [29].

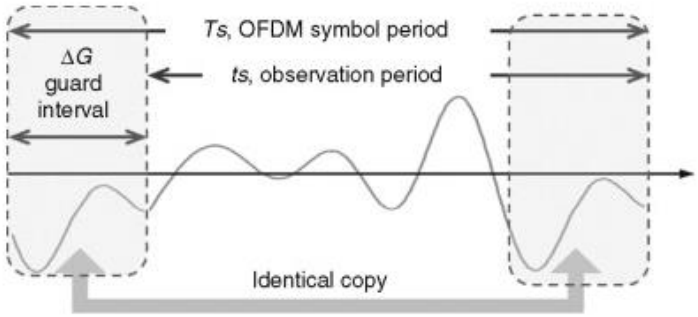

Figure 28-Copy of the last part of the OFDM symbol [29].

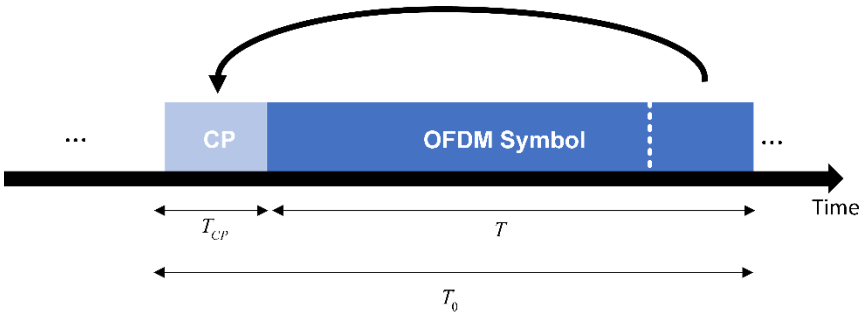

Figure 29 – Time increment due to the CP addition.

This naturally increases the symbol length to $T_0 = T + T_{CP}$ as shown in figure 29. Although the benefits ultimately surpass the drawbacks.

3.6 - Transmitter and receiver block diagrams

In this section we group the processes described in the above sections. For the sake of simplicity let us disregard the parameters related to the RF front-end. Table 1 presents the relevant parameters

Table 1- OFDM parameters

N	**Number of subcarriers**
M	Number of OFDM symbols
Δf	Sub-carrier spacing
$T = 1/\Delta f$	OFDM symbol duration
T_{CP}	Duration of cyclic prefix
$T_0 = T_{CP} + T$	Total duration of OFDM symbol
$N_{Total} \geq N$	IFFT length
$fs = N_{Total}\Delta f$	Sampling rate

Figure 30 depicts a typical OFDM system, starting with a bitstream in the transmitter, the first action to be performed after channel coding is the modulation, as said before, the used techniques may be PSK or QAM. The next step is where each symbol is distributed through the available sub-carriers in what can be seen as a series to parallel commutation, this is done through an inverse fast Fourier transform. After the IFFT being applied, the resulting discrete time signal is again converted to serial from parallel. The cycle prefix addition then takes place, after which the signal is ready to be sent through the channel.

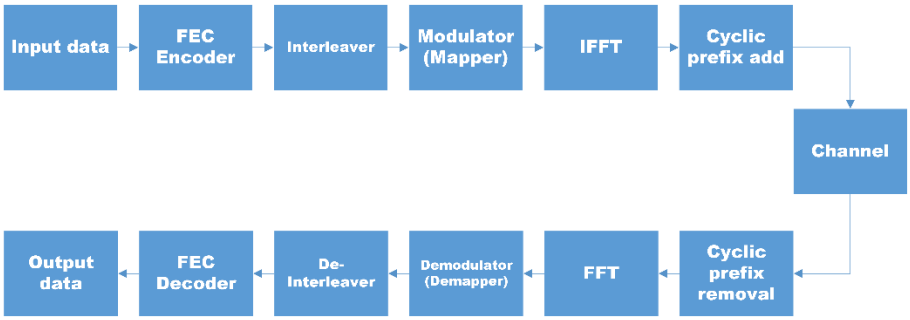

Figure 30 – OFDM system block diagram [30].

At the reception, as expected the inverse procedure happens. The first operation is the CP removal, followed by the series to parallel, FFT and parallel to series group. After this the demodulation and decoding takes place, leaving us with the fully recovered original message.

3.7 - Channel parameters and OFDM parametrization

We've briefly covered what happens in the transmitter and receiver, however the channel has to also be taken in account. As the system transmits a signal $s(t)$ it will be convolved with the time-variant fading channel impulse response function $h(t,\tau)$. Thus, for a given channel it is mandatory to adjust the signal parametrization in order to ensure that neither interference between consecutive OFDM symbols (Inter-Symbol Interference (ISI)) nor between adjacent sub-carriers (Inter-carriers interference (ICI)) happens. As so the channel itself can be seen as the main source of imposed restrictions. The main propagation characteristics that must be respected are the following: [31]

Maximum excess delay τ_e : Often, due to multipathing, the receiver ends up receiving radio waveforms at different times, the difference between the first and last arrival of a same waveform is described by τ_e. Maximum excess delay is shown in figure 31.

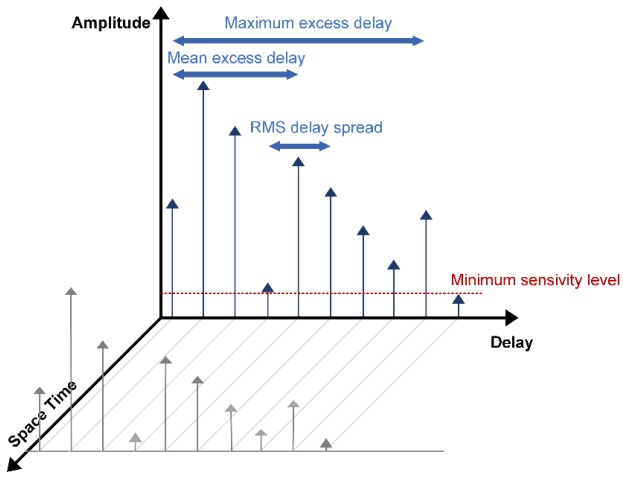

Figure 31- Channel power delay profile.

Doppler spread B_D : Represents the variation of the spectrum due to the different Doppler shifts on each multipath. It has a relation of inverse proportion with the coherence time T_C which represents the time during which the channel can be assumed to be constant.

Delay spread τ_{DS} :It is somehow similar to the excess delay. Although as per figure 31 we see that each component of the power delay profile (PDP) has an amplitude, this amplitude is based on the attenuation meaning that paths that carry more energy end by contributing more than paths with large fading. The delay spread presents then a weighted average of the channel measured with each component's contribution taken into account. The delay spread is also inversely proportional this time to the coherence bandwidth B_C , which represents the bandwidth over which a channel may be considered constant.

These presented parameters have now to go according to some pre-determined conditions so that the system performs as intended.

In order to avoid ISI, it is necessary for the time between the arrival of the first and last component of a multipath signal (maximum excess delay τ_e) to be smaller than the guard interval T_{CP} :

$$T_{CP} > \tau_e \tag{3.7}$$

It is just as important to choose a sub-carrier spacing Δf larger than the Doppler spread B_D but smaller than the coherence bandwidth of the channel B_C , this will help avoiding ICI.

$$B_D < \Delta f < B_C \tag{3.8}$$

Lastly, to prevent the spread to affect the orthogonality of the sub-carriers, the coherence time T_C must be greater than the symbol duration T :

$$T < T_C \Rightarrow \Delta f > \frac{1}{T_C} \tag{3.9}$$

3.8 - The OFDM RADAR signal

The idea now is to use the OFDM signals in order to retrieve the desired target parameters, and the reason why this works is because OFDM possesses two important properties which favor the analysis of the Doppler effect as well as the time shift, these are two of the most parameters that a radar can return. Firstly, OFDM presents a long duration signal, this helps to determine the Doppler shift very accurately and secondly it has a wide spectrum, which makes it easier to find a time shift in the received echo signal [32]. From here, and as explained previously in chapter 2, velocity and range are easily determined.

Over the time, OFDM radar signal processing has seen the rise of many approaches, one of those was designed based on the correlation of received and transmitted signals [33], other uses an algorithm which operates directly on the modulated symbols, this approach is presented in detail in [34], [35].

Below figure 32 describes the OFDM radar model.

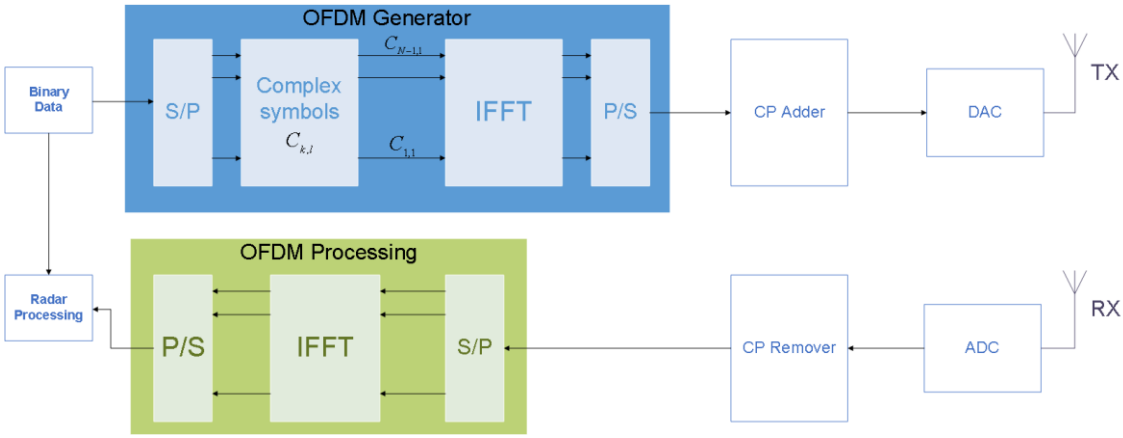

Figure 32- OFDM Basic radar block diagram.

Through the block diagram in figure 32 we can see what constitutes the transmitter and the receiver, we can further nominate two macro-blocks, the OFDM data generator block (DG), and the OFDM processing block (P).

Assuming a single transmitting antenna and single receiving antenna setup, with both antennas on a same platform, spaced by D_{ant} and a target in the far field region, the transmitted signal will be given by

$$s(t)=\sum_{l=0}^{M-1}\sum_{k=0}^{N-1}c_{k,l}e^{j2\pi k\Delta ft}rect\left(\frac{t-lT}{T}\right) \tag{3.10}$$

With k and l representing the sub-carrier and symbol indexes respectively.

The equation describes that the complex symbol $c_{k,l}$ is modulated onto the k th subcarrier and then multiplied by the rectangular function $rect\left(\frac{t-lT}{T}\right)$ whose duration is T and corresponding to the l th OFDM symbol in the time domain.

Taking a more physical perspective on what we are describing, we are sending an $s(t)$ waveform towards a target at r distance. This wave hits the target and is then backscattered back to the radar. The distance between the transmitter and receiving antenna D_{ant} is such that $D_{ant} << r$ thus we can assume the total travelled distance by $s(t)$ to be $2r$.

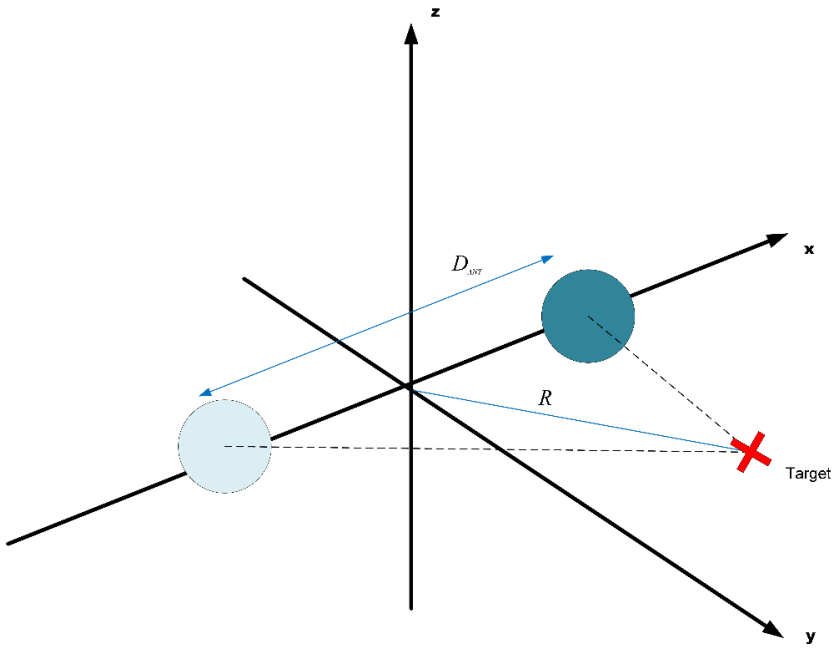

Figure 33 – Distance between antennas and target.

The time delay resulting from this roundtrip time then becomes a phase rotation once a Fourier transform is applied as per definition $F\left(s(t-\tau)\right)\Rightarrow F\left(s(t)\right)e^{-j2\pi f\tau}$ where $F\left(s(t)\right)$ denotes the Fourier transform of $s(t)$.

Considering now a moving target with radial velocity v which is translated into a Doppler shift f_D the received reflected signal is given by

$$r(t)=\sum_{l=0}^{M-1}\sum_{k=0}^{N-1}c_{k,l}e^{j2\pi(k\Delta f+f_D)(t-\tau)}rect\left(\frac{t-\tau-lT}{T}\right) \tag{3.11}$$

And since the carrier frequency is much larger than the sub-carrier spacing, we can assume that all sub-carriers are equally affected by the Doppler effect f_D , thus we can neglect the term $e^{-j2\pi f_D\tau}$. Adding to this the multi-target scenario where we have Z targets we end up with

$$r(t)=\sum_{z=0}^{Z-1}b_z e^{j\varsigma}\sum_{l=0}^{M-1}\sum_{k=0}^{N-1}c_{k,l}e^{j2\pi(k\Delta f(t-\tau_z))}e^{j2\pi f_{D,z}t}rect\left(\frac{t-\tau_z-lT}{T}\right)+w(t) \tag{3.12}$$

In this expression we have

Table 2- equation (3.12) parameter description

Attenuation	$b_z=\sqrt{\frac{c_0\varphi,z}{(4\pi)^3 r_h^4 f_c^2}}$
Random phase offset	$e^{j\varsigma}$
Time delay	$\tau_z=2\frac{r_z}{c_0}$
Doppler shift	$f_{D,z}=2\frac{v_z}{c_0}f_c$
White Gaussian Noise	$w(t)$

Where φ stands for the radar cross section, c_0 the speed of light and v_z for the relative speed of the target.

The signal processing will happen in the digital domain therefore we have to use the discrete form

$$t = \frac{nT}{N} + lT \tag{3.13}$$

With n being the sample number and varying between 0 and $N-1$.

From here we can rewrite the equation as a function of the indexes k, l assuming OFDM processing was performed.

$$r(k,l) = \sum_{z=0}^{Z-1} b_z e^{j\zeta} c_{k,l} e^{-j2\pi k\Delta f \tau_z} e^{j2\pi f_{D,z} lT} + w(k,l) \tag{3.14}$$

By then relating the transmitted and received signal it is possible to compute the values for the range and speed of the target, we will return to this ahead in this work.

3.9 - System parameters

In order to produce a fully functional and reliable RADAR, there are some parameters that must be respected. These parameters concern particularly effects that cause signal distortion like Doppler shift and multi-path propagation [35]. This information is highly relevant since it describes and characterizes the crucial functionalities of the radar system.

Maximum range: Also referred to as maximum unambiguous range, shown in figure 34, defines the maximum distance $r_{\max}$ at which a target can be detected with accuracy, in other words it describes the maximum distance from where a pulse can return and produce reliable results

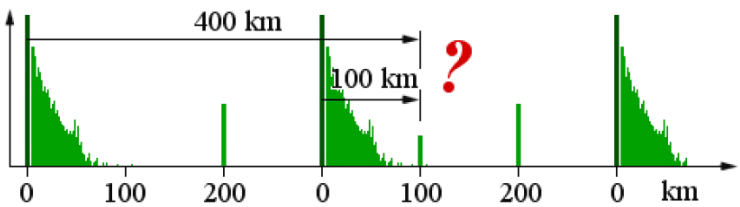

Figure 34- Maximum range ambiguity [18].

As said before, the signal takes the roundtrip time, meaning it travels the same distance twice, thus we can define the maximum unambiguous range as

$$r_{\max} = \frac{c_0 T}{2} = \frac{c_0}{2\Delta f} \tag{3.15}$$

From here, to avoid range ambiguities we can define de minimum symbol plus guard interval duration as

$$T + T_{CP} \geq \frac{2r_{\max}}{c_0} \tag{3.16}$$

Range Resolution: It is the metric which describes the minimum distance necessary for the system to be able to distinguish two separate targets. The range resolution is solely dependent on the transmitted signal's bandwidth, this also plays a significant role in determining the number of subcarriers N and the subcarrier spacing Δf [36] as it is possible to verify in the range resolution expression

$$\Delta r = \frac{c_0}{2B} = \frac{c_0}{2N\Delta f} \tag{3.17}$$

It becomes evident that the more bandwidth available, the more range resolution we'll have. It is also possible to describe the maximum range resolution $\Delta r_{\max}$ and minimum necessary bandwidth B through the relation

$$B \geq \frac{c_0}{2\Delta r_{\max}} \tag{3.18}$$

Maximum Doppler shift: Similar to the maximum unambiguous range, the Doppler shift can also present ambiguity issues, therefore it is necessary to specify the maximum frequency shift value $f_{D,\max}$ that the system is able to measure. The expression is as follows

$$f_{D,\max} = \frac{2v_{\max} f_c}{c_0} \tag{3.19}$$

Where $v_{\max} = \frac{c_0}{2Tf_c}$.

In terms of frequency, it is important to define a maximum sub-carrier spacing in order to ensure that the orthogonality isn't compromised. Δf as then to be larger than the Doppler shift caused by the target whose maximum velocity is $v_{\max}$.

$$\Delta f \gg \frac{2v_{\max}}{c_0} f_c \tag{3.20}$$

Doppler resolution: Much like the range resolution, it expresses the minimum frequency shift value which translates in a measurable velocity Δv that allows for the distinction of two different targets with two different velocities. The Doppler resolution takes into account the OFDM period T and the number of symbols M

$$\Delta v = \frac{c_0}{2MTf_c} \tag{3.21}$$

And from this expression we can define the minimum frame duration (M times the OFDM period T) for a given maximum velocity resolution $\Delta v_{\max}$

$$MT \geq \frac{c_0}{2\Delta v_{\max} f_c} \tag{3.22}$$

Chapter 4

MIMO Systems Overview

This chapter addresses the use of spatial dimension to improve the RADAR performance. We start by explaining how conventional MIMO systems work and why they are beneficial. We discuss diversity concept as well as the MIMO topologies, then a brief presentation of the Alamouti encoding takes place, followed by a more in-depth explanation of the Tarokh codification which is the one used in our work.

MIMO stands for multiple-input-multiple-output, and nowadays these systems are in the forefront of wireless research due to its potential for improving communications through the achievement of high-rate data services [37]. Given that MIMO is revealing itself as one of the best ways to achieve the necessary high throughput demanded by today's communications, we can then use this to accumulate the benefits of MIMO and OFDM by merging both techniques. In order to do this a step frequency technique is applied where each subcarrier is transmitted through one of the elements of the MIMO system [38] granted that the number of subcarriers is higher than the number of elements.

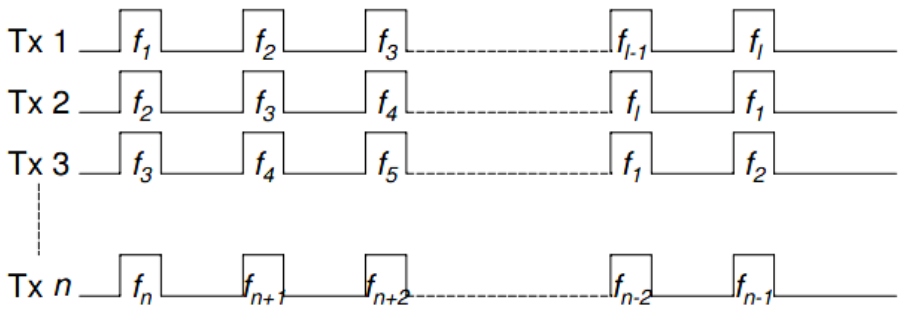

Figure 35- Step frequency sequence [38].

This technique used by OFDM communication systems to separate the sub-carriers can also be employed for MIMO RADAR, which relying on the use of multiple transmitters and receivers, sense the environment and the targets in it. To achieve this, MIMO RADAR uses multiple antennas which transmit correlated or uncorrelated waveforms [39].

The following section goes through the basics of the MIMO systems, explores its concepts and its configurations.

4.1 - MIMO systems

MIMO can be seen as an answer to the multipath scattering problem in the communication channels. By making use of its multiple antennas setup, a MIMO system is capable of whether improving its data rate capacity, by performing spatial multiplexing (sending different symbols through different antennas), or

improving its diversity (the flow of the same information through different independent paths [40]) which will lead to a better signal to noise ratio (SNR) and consequently a lower bit error rate (BER), thus bringing more reliability to the communication.

This naturally represents a great improvement since a given system is now able to increase the data rate or signal to noise ratio [41], without the need of additional bandwidth or transmitting power.

4.2 - Diversity

As a transmitted signal travels towards the receiver, it usually experiences destructive processes. Common phenomena like multiple reflections end up being the cause of distortion, delay and attenuation. These effects have a negative impact in the communication system's performance ultimately resulting in a higher chance of errors in the communication itself. Therefore, through diversity we can bring some robustness to the system. The existence of many independent paths between two points ensures that, even when one or more of the available paths is in poor conditions to deliver the message, there is always another path which likely will not be in the same unfavorable condition. This way, the communication is done through multiple parallel paths, minimizing the chance of destructive phenomena.

The diversity can be achieved in three main domains.

Spatial diversity: The simplest concept, as explained before, represents the different physical paths between the transmitter and receiver. This concept is easily understood in the following sub-chapters where we go through the multiple antenna physical configurations available.

Time diversity: The idea here is to send the same information in different time slots, this interval time has to be bigger than the channel's coherence time. Worth noticing that in a single transmitting antenna this means repeating L times the information sent, thus decreasing the data rate by a factor L which is the main drawback of time diversity.

Frequency diversity: The diversity here happens through the RF spectrum, with the same information being transmitted across different spaced frequencies, each independent from the others. In this case it is necessary to increase the bandwidth L times to achieve a diversity order of L, which is not the best option for wireless communications.

4.3 - MIMO configurations

Based on the number of transmitting and/or receiving antennas we can split the MIMO topologies in four classes:

SISO

Single input and single output, it consists in the most basic configuration, has one transmitting antenna and one receiving antenna.

Figure 36 - SISO system.

Its simplicity represents both its advantage and its disadvantage. It requires no additional processing; however, it is very vulnerable to fading due to not having any spatial diversity.

SIMO

Single input multiple output, in this configuration we have one transmitting antenna and multiple receiving antennas. We get diversity in the reception at the expense of some additional processing power in regards to the SISO configuration, although not as simple it proves to be less vulnerable to fading effects.

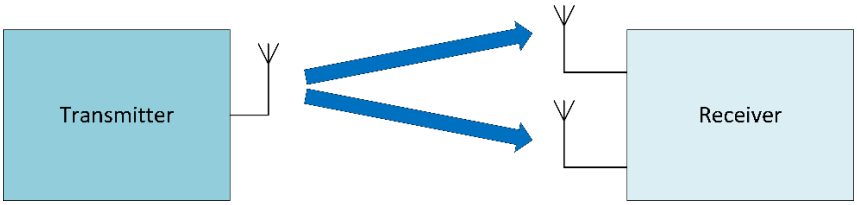

Figure 37 - SIMO system.

The idea behind the techniques commonly used in receiver diversity scenarios seek to get the best possible signal at the reception, to achieve that the system utilizes the signal replicas at disposal to either combine or choose the best one to keep. Two similar techniques are maximal ratio combining (MRC) and equal gain combining (EGC) both combine all the paths although MRC optimizes the weights in order to maximize the output SNR whereas EGC gives equal weights to every component leading to a slightly lower performance. Selection combining (SC) is also an option, although it has the term combining in its name this technique simply compares the amplitude of each channel and opts for the one with the highest SNR.

MISO

Multiple input single output is the inverse of the SIMO configuration, has multiple transmitting antennas and one receiving antenna. In this case the spatial diversity and processing happen on the transmitting side.

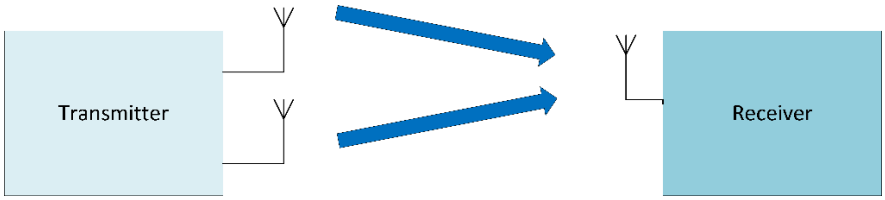

Figure 38 - MISO system.

In this case, the idea of transmitting diversity is to send redundant information through many antennas without interference, to make this possible it becomes necessary to use a pre-coder before the information is sent. This technology is widely used nowadays in digital television, wireless local area networks (WLANs) and mobile communications [42].

MIMO

This last configuration merges its predecessors, by using multiple transmitting and receiving antennas we achieve spatial diversity at both ends. MIMO configuration supports the simultaneous transmission of several data streams both in time and frequency. However, in order for this configuration to bring more robustness to the system, more processing is needed, this happens because it is now necessary to distinguish the data travelling in the different established paths, this is done through coding on the spatial channels which we will go more in detail in the next sections.

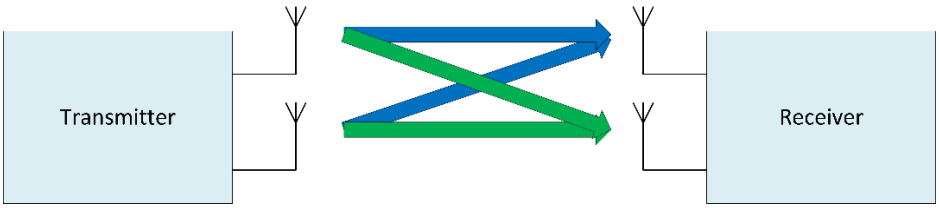

Figure 39 - MIMO system.

4.4 - MIMO orthogonality

Orthogonality has to be seen as a great advantage amidst all communication systems. This property means that there is no interference between two or more given orthogonal signals. It is therefore crucial to assign each one to a specific antenna. For instance, a structural modification was proposed in [43] where the idea was, instead of having all subcarriers active, as in any typical classic OFDM system, we would only have a set of subcarriers active based on the number of available channels. The idea is depicted in figure 40, 41 and 42.

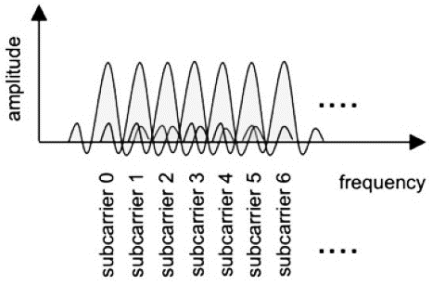

Figure 40 -All sub-carriers active.

Figure 40 shows the scenario with all the six subcarriers active.

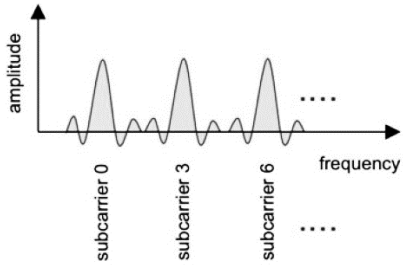

Figure 41 -Three active sub-carriers.

Figure 41 presents the modified OFDM waveform where we only have three available channels thus three subcarriers active

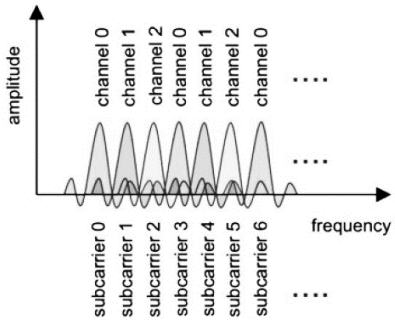

Figure 40 – Superimposition of all transmitted signals.

In figure 42 we have the superimposition of all transmit signals at the receiver, all of them through the three available channels. The main idea is to distribute the N subcarriers through all the available channels. Lastly in figure 43 we have a full example.

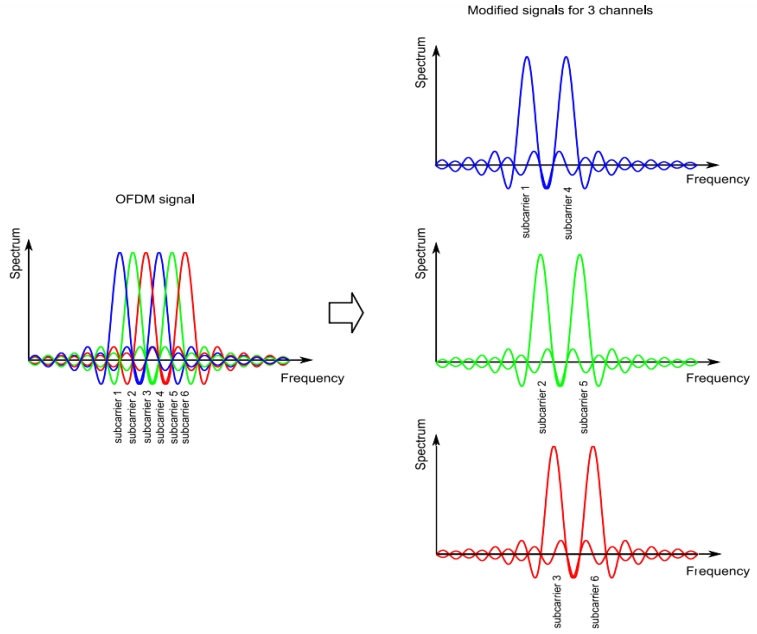

Figure 41 - Subcarrier assignment to generate orthogonal signals [44].

In this work however, in order to attain orthogonality, we took a different approach. We opted to make use of the space-time/frequency block codes (STBC/SFBC) given the robustness and diversity that this technique can introduce in the system. Next section addresses STBC in detail.

4.5 - Space-time/frequency block codes

As discussed earlier, the use of multiple antennas in reception, transmission or both, results in diversity. Which means that either in space, time or frequency we have different versions of the same signal travelling through the system. These can later be combined in order to reduce fading effects or even attain antenna gain. To make this possible, some details have to be respected, for instance the channels have to be independent, meaning that the space between antennas has to be enough so that each channel presents no interference to others.

For the downlink (MISO systems) the spatial diversity can be achieved by a simple combination of the transmit replicas. A more sophisticated signal processing at the transmitter side should be done. One of the most used schemes are the so-called space-time or space-frequency block codes (STBC/SFBC). The simplest code being the Alamouti scheme [45] that can be used for 2 transmit antennas and an arbitrary number at the receiver side, assuming complex constellation.

The **Alamouti scheme**, as described in [45] encodes a block of two symbols, say s_1 and s_2 in two time slots or two frequencies and two antennas. In the first time slot, s_1 and s_2 are transmitted through transmitting

antenna 1 (Tx_1) and Tx_2 respectively. In the second instant $-s_2^*$ is transmitted through Tx_1 and s_1^* is transmitted through Tx_2. Table 3 along with the matrix S presented in 4.1 schematize the described procedure.

$$S = \begin{bmatrix} s_1 & -s_2^* \\ s_2 & s_1^* \end{bmatrix} \tag{4.1}$$

Table 3 - Alamouti scheme

Time	Ant1	Ant2
t	s_1	s_2
$t+T$	$-s_2^*$	s_1^*

Let us assume that the channel between the first antenna Ant1 and the receiver antenna is h_1 and the channel between Ant2 and the receiver antenna is h_2. We also assume that the two channels are time invariant through the duration of the transmission of the two symbols. Below we have the full scheme.

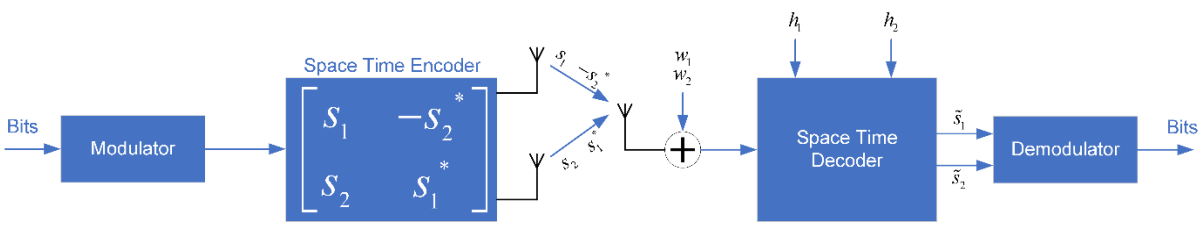

Figure 42- Alamouti block scheme.

We can now write the expressions for the received signals r_1 and r_2 at the two instants t and $t+T$, where T stands for the symbol duration and w for the noise at the reception

$$r_1 = r(t) = h_1 s_1 + h_2 s_2 + w_1 \tag{4.2}$$

$$r_2 = r\left(t+T\right) = -h_1 s_2^{\ *} + h_2 s_1^{\ *} + w_2 \tag{4.3}$$

By using a matrixial form we get

$$\begin{bmatrix} r_1 \\ r_2 \end{bmatrix} = \begin{bmatrix} s_1 & -s_2^{\ *} \\ s_2 & s_1^{\ *} \end{bmatrix} \begin{bmatrix} h_1 \\ h_2 \end{bmatrix} + \begin{bmatrix} w_1 \\ w_2 \end{bmatrix} \tag{4.4}$$

However, we can re-write the same expression in order to only depend on the symbols s_1 and s_2 pushing the complex and signal properties to the channel itself, this way we get

$$\begin{bmatrix} r_1 \\ r_2^{\ *} \end{bmatrix} = \begin{bmatrix} h_1 & h_2 \\ h_2^{\ *} & -h_1^{\ *} \end{bmatrix} \begin{bmatrix} s_1 \\ s_2 \end{bmatrix} + \begin{bmatrix} w_1 \\ w_2 \end{bmatrix} \tag{4.5}$$

The above equation can be rewritten as

$$\mathbf{r} = \mathbf{Hs} + \mathbf{w} \tag{4.6}$$

Where $\mathbf{H}$ represents the overall channel matrix.

The data symbols can now be estimated by making then use of the Hermitian matrices' properties.

As so by multiplying $\mathbf{H}^H$ in both members we get

$$\begin{bmatrix} h_1^{\ *} & h_2 \\ h_2^{\ *} & -h_1 \end{bmatrix} \begin{bmatrix} r_1 \\ r_2^{\ *} \end{bmatrix} = \begin{bmatrix} h_1^{\ *} & h_2 \\ h_2^{\ *} & -h_1 \end{bmatrix} \begin{bmatrix} h_1 & h_2 \\ h_2^{\ *} & -h_1^{\ *} \end{bmatrix} \begin{bmatrix} s_1 \\ s_2 \end{bmatrix} + \begin{bmatrix} h_1^{\ *} & h_2 \\ h_2^{\ *} & -h_1 \end{bmatrix} \begin{bmatrix} w_1 \\ w_2 \end{bmatrix} \tag{4.7}$$

In a simpler notation

$$\mathbf{H}^H \begin{bmatrix} r_1 \\ r_2^{\ *} \end{bmatrix} = \mathbf{H}^H \mathbf{H} \begin{bmatrix} s_1 \\ s_2 \end{bmatrix} + \mathbf{H}^H \begin{bmatrix} w_1 \\ w_2 \end{bmatrix} \tag{4.8}$$

Since $\mathbf{H}^H \mathbf{H} = \|\mathbf{h}\|^2 \mathbf{I}$ where $\|\mathbf{h}\|^2 = |h_1|^2 + |h_2|^2$ we get

$$\mathbf{H}^H \begin{bmatrix} r_1 \\ r_2^{\ *} \end{bmatrix} = \begin{bmatrix} s_1 \\ s_2 \end{bmatrix} \|\mathbf{h}\|^2 \mathbf{I} + \mathbf{H}^H \begin{bmatrix} w_1 \\ w_2 \end{bmatrix} \tag{4.9}$$

From where we can retrieve the detected symbols as function of the channel, the transmitted symbol and of course the noise

$$\begin{cases} \tilde{s}_1 = \|\mathbf{h}\|^2 s_1 + \mathbf{H}^H w_1 \\ \tilde{s}_2 = \|\mathbf{h}\|^2 s_2 + \mathbf{H}^H w_2 \end{cases} \tag{4.10}$$

An important concept to have present is the scheme's code rate. The Alamouti 2x1 configuration described above, has a code rate of one meaning that each antenna in the system transmits one symbol per time slot. Generally, we can say that the rate R of a STBC is defined as the ratio between the number of symbols the encoder takes as its input, N_S and the number of time slots used for the transmission, N_P [40]. This is translated through

$$R = \frac{N_S}{N_P} \tag{4.11}$$

However, Alamouti only works for a pair of transmitting antennas, when we seek solutions for more than that we have to give something in return so to speak. The available options are more complex codes which present a rate lower than one, meaning that we need more time slots to transmit the data symbols, a good example are the **Tarokh codes**.

To better illustrate it, let us look at the 4x1 Tarokh scheme, in which four symbols (s_1, s_2, s_3, s_4) are transmitted over four transmitting antennas through the duration of eight time slots, thus with a code rate $R = \frac{N_S}{N_P} = \frac{4}{8} = \frac{1}{2}$.

$$\begin{array}{cc} & \text{Time slots / Frequencies} \\ & \begin{array}{cccccccc} \boxed{1} & \boxed{2} & \boxed{3} & \boxed{4} & \boxed{5} & \boxed{6} & \boxed{7} & \boxed{8} \end{array} \\ \mathbf{S} = & \begin{bmatrix} s_1 & -s_2 & -s_3 & -s_4 & s_1^* & -s_2^* & -s_3^* & -s_4^* \\ s_2 & s_1 & s_4 & -s_3 & s_2^* & s_1^* & s_4^* & -s_3^* \\ s_3 & -s_4 & s_1 & s_2 & s_3^* & -s_4^* & s_1^* & s_2^* \\ s_4 & s_3 & -s_2 & s_1 & s_4^* & s_3^* & -s_2^* & s_1^* \end{bmatrix} \begin{array}{c} \boxed{1} \\ \boxed{2} \\ \boxed{3} \\ \boxed{4} \end{array} \quad \text{Antennas} \end{array}$$

Figure 43 – Tarokh coding scheme.

Similarly, to the logic followed in the Alamouti section, h_{1-4} defines the channels between each transmitting antenna and the receiving one. We can define the received signals at each of the eight instants y_{1-8} as

$$
\begin{aligned}
y_1 &= h_1 s_1 + h_2 s_2 + h_3 s_3 + h_4 s_4 + n_1 \\
y_2 &= -h_1 s_2 + h_2 s_1 - h_3 s_4 + h_4 s_3 + n_2 \\
y_3 &= -h_1 s_3 + h_2 s_4 + h_3 s_1 - h_4 s_2 + n_3 \\
y_4 &= -h_1 s_4 - h_2 s_3 + h_3 s_2 + h_4 s_1 + n_4 \\
y_5 &= h_1 s_1^* + h_2 s_2^* + h_3 s_3^* + h_4 s_4^* + n_5 \\
y_6 &= -h_1 s_2^* + h_2 s_1^* - h_3 s_4^* + h_4 s_3^* + n_6 \\
y_7 &= -h_1 s_3^* + h_2 s_4^* + h_3 s_1^* - h_4 s_2^* + n_7 \\
y_8 &= -h_1 s_4^* - h_2 s_3^* + h_3 s_2^* + h_4 s_1^* + n_8
\end{aligned}
\tag{4.12}
$$

Considering $\mathbf{y}$ as the vector constituted by the received signals y_{1-8} , $\mathbf{H}$ as the overall channel matrix with the four possible channels h_{1-4} and the vector $\mathbf{s}$ as defined above, we get:

$$
\mathbf{y} = \mathbf{H}\mathbf{s} + \mathbf{n} \tag{4.13}
$$

Further following the logic used in the Alamouti case we can retrieve the soft decisions through

$$
\begin{aligned}
\tilde{\mathbf{s}}_1 &= y_1 h_1^* + y_2 h_2^* + y_3 h_3^* + y_4 h_4^* + y_5^* h_1 + y_6^* h_2 + y_7^* h_3 + y_8^* h_4 \\
\tilde{\mathbf{s}}_2 &= y_1 h_2^* - y_2 h_1^* - y_3 h_4^* + y_4 h_3^* + y_5^* h_2 - y_6^* h_1 - y_7^* h_4 + y_8^* h_3 \\
\tilde{\mathbf{s}}_3 &= y_1 h_3^* + y_2 h_4^* - y_3 h_1^* - y_4 h_2^* + y_5^* h_3 + y_6^* h_4 - y_7^* h_1 - y_8^* h_2 \\
\tilde{\mathbf{s}}_4 &= -y_1 h_4^* - y_2 h_3^* + y_3 h_2^* - y_4 h_1^* - y_5^* h_4 - y_6^* h_3 + y_7^* h_2 - y_8^* h_1
\end{aligned}
\tag{4.14}
$$

Which is the same as

$$
\tilde{\mathbf{s}} = \mathbf{H}^H \mathbf{H}\mathbf{y} = \|\mathbf{h}\|^2 \mathbf{s} + \mathbf{H}^H \mathbf{n} \tag{4.15}
$$

Where

$$
\|\mathbf{h}\|^2 = |h_1|^2 + |h_2|^2 + |h_3|^2 + |h_4|^2 \tag{4.16}
$$

Therefore, the first detected symbol $\tilde{s}_1$, similarly to the other three, can be written as

$$
\tilde{s}_1 = \sum_{m=1}^{4} |h_m|^2 s_1 + n_1 h_1^* + n_2 h_2^* + n_3 h_3^* + n_4 h_4^* + n_5^* h_1 + n_6^* h_2 + n_7^* h_3 + n_8^* h_4 \tag{4.17}
$$

Although it achieves a diversity order of four it does so at the expense of doubling the bandwidth.

4.6 - Antenna setup and virtual array

The configuration of MIMO RADAR antennas has to be taken in consideration since it directly affects its performance. For instance, [46] mentions the relation between multiple widely spaced antennas and the performance improvement observed. This comes naturally as a consequence of exploiting the multiplexing diversity thanks to the multiple channels available. With that being said, the importance of the number of antennas in a system becomes evident, it is then important to maximize it through all the techniques at our disposal.

Through the use of the virtual array concept, it is possible to achieve just that. The logic behind it tells us that we can virtually consider to have a higher number of receiving antennas than we physically have. Although it looks slightly weird, it does make sense. When we have a MIMO system with P transmitting antennas and Q receiving antennas, considering the definition of channel as the transmitter-target-receiver path what we have is a total of $P \times Q$ channels, given that each transmitter will have a path towards every receiver.

The virtual array itself is the denomination given to the set of receiving antennas in the equivalent scenario where we have one transmitting antenna and $P \times Q$ receiving ones. Within this technique, we now have to pay attention to the distance between antennas, d_{ant} ,which by being $d_{ant} = \lambda/2$ in both transmit and receiving antennas results in the case shown in figure 46.

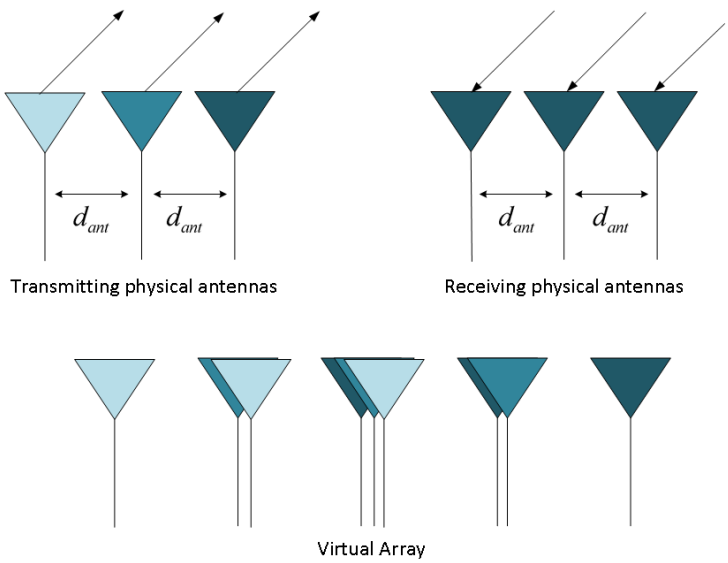

Figure 44 - Virtual array concept for a MIMO system.

However, in this situation we end up with a five-element virtual array instead of nine. To solve this issue, we return to the wide spaced antennas previously mentioned. By spacing the transmitting antennas with a greater distance, namely $d_{ant} = Q \times \lambda/2$ while maintaining the receiver antenna spacing, we obtain the

maximum number of non-repetitive terms as shown in figure 47. Thus, reaching the virtual array with $P \times Q$ elements mentioned earlier.

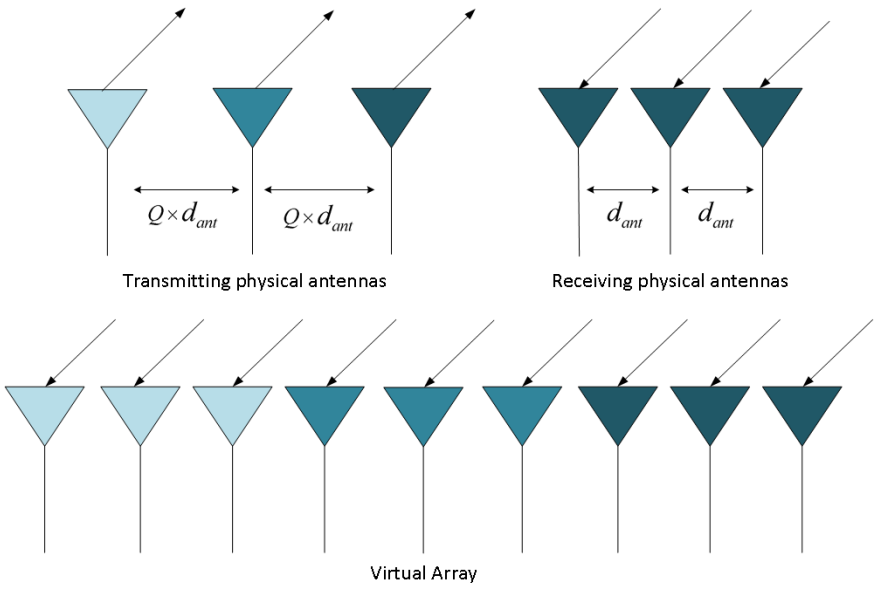

Figure 45 - Virtual antenna array properly spaced.

4.7 - Direction of arrival or Angle estimation

With a SISO system we would not be able to estimate a signal's direction of arrival (DOA), this happens because unlike the range or speed estimations, which have delay and Doppler effect respectively as means to make the estimation, the DOA relies on the existence of at least two receiving antennas. It does so because multiple receiving antennas imply multiple paths, with multiple distance differences, taking the example of figure 48.

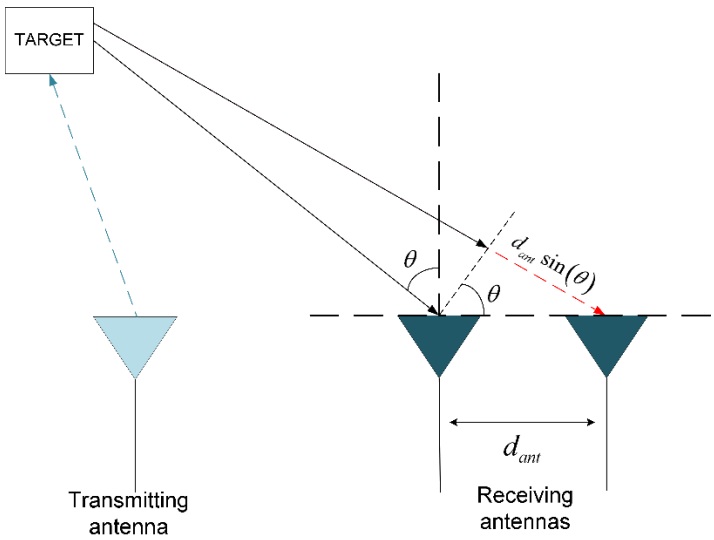

Figure 46 - Angle of arrival estimation.

In this case we have two receiving antennas spaced by d_{ant}. This spacing will ultimately be translated in an additional distance that the signal will have to travel from the target to the second antenna in relation to the first. This additional value pictured in the figure in red has the value of $d_{ant}\sin(\theta)$. Lastly this additional travel distance will result in a phase difference w at the second receiving antenna.

$$w = \frac{2\pi}{\lambda} d_{ant} \sin(\theta) \tag{4.18}$$

From this phase difference it is then possible, by manipulating the expression, to retrieve the DOA or the estimated angle whose range goes from -90° to 90°.

$$\theta = \arcsin\left(\frac{w\lambda}{2\pi d_{ant}}\right) \tag{4.19}$$

4.8 - OFDM MIMO Radar signal waveform

Let us now rewind and return to the OFDM frame presented in section 3.4. There we presented a structure which describes the distribution of symbols through frequencies. The core concept is that a OFDM symbol is transmitted by making use of a set of available frequencies N, meaning the symbol itself is represented by a group of subcarriers carefully spaced. This way $c_{k,l}$ describes the complex symbol l in the k th sub-carrier.

We can now turn this structure into a matrix and rearrange it into F_{Tx} as shown in figure 49.

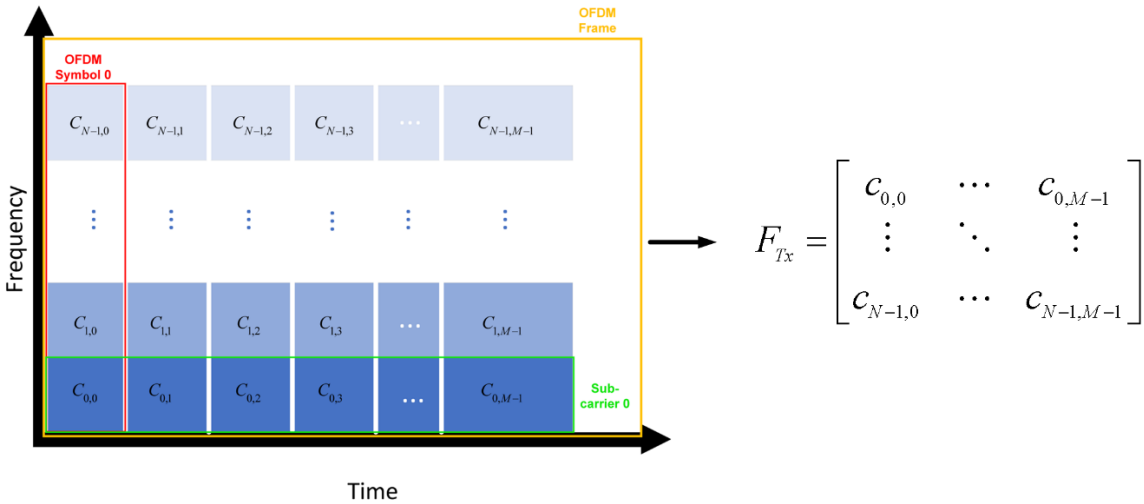

Figure 47 -Transforming the OFDM frame into the F matrix.

Through F_{Tx} we have now a full description of the OFDM frame where each row now represents a different sub-carrier, while each column represents an OFDM symbol. Regarding the modulation alphabet in this work, we used QPSK and 16-QAM.

As per [47] we can further specify that in a $P \times Q$ transmit and receive antenna scenario a Tx frame contains M OFDM symbols and each of the P transmitting antennas will use a set of N/P sub carriers, this can be visualised in figure 50 where we're considering four transmitting antennas.

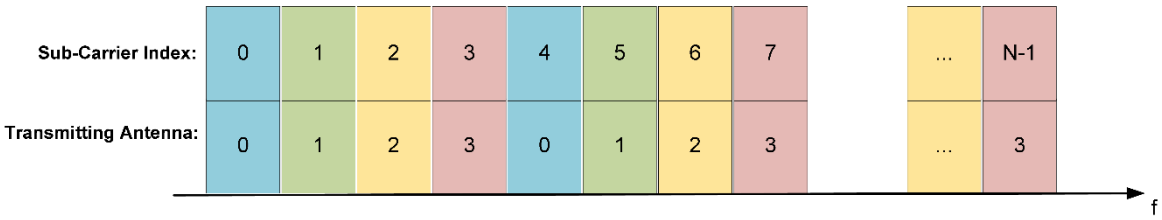

Figure 50 -Distribution of the sub-carriers through the transmitting antennas.

In this case of four transmitting antennas, we see that the fourth, eight and every $i \times 4$ th for $i = 1, 2, 3 ... N-1$ sub carrier is allocated to the fourth transmitting antenna. By generalizing we can say that every k_p th sub-carrier is allocated to the p th antenna, where P is the number of the antenna, which ranges $0 \le P \le N-1$ and k_p is the index of every last subcarrier (p th) transmitted in each frame $k_p = p + (i \times P)$ and i the sub-carrier index of the sub-carriers allocated to one transmitting antenna $0 \le i \le (N/P) - 1$.

Similar to what happened in section 3.8 although with the introduction of F_{Tx} it is now possible to re-write the transmitted signal through every p th antenna as

$$s_p(t) = \sum_{l=0}^{M-1} \sum_{i=0}^{N-1} F_{Tx,p}(k,l) \cdot e^{j2\pi k_p \Delta f t} \cdot rect\left(\frac{t - lT}{T}\right) \tag{4.20}$$

where

$$F_{Tx,p}(k,l) = \begin{cases} F_{Tx}(k,l) & ,k = p + (i \times P), 0 \le i \le (N/P) - 1 \\ 0 & else \end{cases} \tag{4.21}$$

By the receiving side every receiving antenna then receives the interleaved signals of all the transmitting antennas in order to recreate the transmitted signal. At each q th antenna we get the transmitted signal with the expected effects of delay, frequency shift and noise from each target z.

$$F_{Rx,q}(k,l) = \sum_{p=0}^{P-1} F_{Tx,p}(k,l) \sum_{z=0}^{Z-1} b_z \cdot e^{-j2\pi k\Delta f \tau_{p,q,z}} \cdot e^{j2\pi f_{D_{p,q,z}} lT} + W_q(k,l) \tag{4.22}$$

Where $\tau_{p,q,z} = \frac{r_{p,z} + r_{q,z}}{c_0}$ is the round-trip time delay, with $r_{p,z}$ and $r_{q,z}$ representing the distances between the antennas and the target z, and $f_{D_{q,p,z}} = \frac{2v_{rel,p,q,z} f_c}{c_0}$ representing the frequency shift relative to a given target z.

Chapter 5

Implemented STBC in MIMO-OFDM RadCom

Efficiency, this word represents the ultimate motor force for the appearance of the whole RadCom concept. The search for efficient ways to perform sensing and communication simultaneously along with the new possibilities that come from there is what keeps fueling the ongoing research on this topic. With both systems well solidified in our day-to-day routines, we now start to face some challenges which naturally require an answer. The shrinking availability of the radio frequency spectrum directly contrasts with its growing demand. At the same time, we keep observing a non-stop growing number of communication-capable devices, services, and applications emerging before our eyes. The course of action reveals itself clearly, radar and communication should no longer keep a competitive relation over the limited common resource required to its functions. Such competition represents a waste of spectrum that has no place in the future IoT reality [23].

We start this chapter by recalling the main motivations behind the ongoing research on RadCom. We also present a brief discussion about a prior approach based on Alamouti coding. We then start by analyzing the simplest SISO-OFDM RADAR scenario. Afterwards, we introduce the periodogram, presenting its working method and the purpose of its use. We then move to a MIMO-OFDM RADAR scenario, where we later add the communication capability through the use of STBC. Lastly, we compare and analyze the obtained results. In order to create the proposed joint RadCom system, it is necessary to rely on a waveform capable of accommodating both operations without presenting interference in between them. This is accomplished through the use of OFDM as the common waveform since it has already been widely pointed as suitable for this purpose. In previous approaches, Alamouti coding was used to integrate the communication in the RADAR system. It is a full rate code that brings orthogonality and diversity to the system, however, there was still room to improve. The Alamouti code is tied to a two transmitting antennas scheme, but this limitation can be overcome if we are willing to sacrifice some code rate. As such, through the use of other STBC techniques, it is then possible to upgrade that aspect by making use of more antennas, thus reaching higher diversity order. In this dissertation, we use Tarokh codes that allow us to equip the terminals with more antennas and thus boost the overall system performance. This code preserves the orthogonality property, and along with the already mentioned OFDM waveform makes it possible to achieve a fully functional RadCom system. As a result, we can observe several improvements which ultimately result in a more robust system. The higher SNR consequently lowers the BER and increases the detection probability, making the system capable of better coping with the scattering and other destructive distortions present in all wireless communication systems. At the same time the RADAR functionality experiences an increment in terms of angle resolution thanks to the greater number of transmission antennas. In order to evaluate the performance of the developed schemes, a simulation platform was implemented in MatLab.

5.1 - OFDM SISO Radar

Starting with the simplest case, ,i.e. with a SISO-RADAR only system, we build the foundations of the future iterations. First, a single transmitter single receiver monostatic radar is implemented. Since this configuration does not meet the minimum requirements to measure angles, which is having at least two receiving antennas, this system measures only the range, and the velocity of the target. No other signal sources are considered in the simulation, therefore the only distortion in the received signal is the additive white Gaussian noise.

Figure 51 shows the representation of the first version simulated which consists in a single transmitter and a single receiver classic monostatic setup. The transmitter is responsible for sending the OFDM signal $s(t)$ which after hitting the target(s) will be reflected towards the receiver. $r(t)$ then represents the received signal which can be the reflected signal of one target or a superposition of the reflected signal of a variety of Z targets

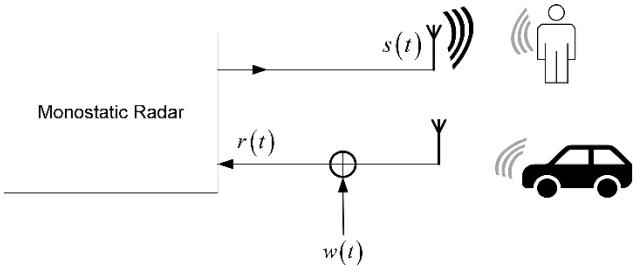

Figure 48 - Monostatic Radar Schematic.

The modulated symbols are organized in the matrix F_{Tx} where the rows and columns represent the sub-carriers and OFDM symbols respectively. We can visualize the concept in figure 52.

$$F_{Tx} = \begin{bmatrix} c_{0,0} & \cdots & c_{0,N-1} \\ \vdots & \ddots & \vdots \\ c_{N-1,0} & \cdots & c_{N-1,M-1} \end{bmatrix}$$

Sub-carrier 0

Symbol 0

Figure 49 -Matrix F with first sub-carrier and symbol identified.

Recalling from section 3.8, we can see that both the delay and the Doppler shift are represented through exponentials as follows

$$r(t) = \sum_{z=0}^{Z-1} b_z e^{j\varsigma} \sum_{l=0}^{M-1} \sum_{k=0}^{N-1} c_{k,l} e^{j2\pi(k\Delta f(t-\tau_z))} e^{j2\pi f_{D,z} t} rect\left(\frac{t-\tau-lT}{T}\right) + w(t) \tag{5.1}$$

By introducing the OFDM frame F_{Tx} (presented in figure 52) into the received signal equation we get the received frame F_{Rx},

$$F_{Rx}(k,l)=\sum_{z=0}^{Z-1} b_z F_{Tx}(k,l)\cdot e^{-j2\pi\tau_z\Delta fk} e^{j2\pi f_{D,z}lT}+W(k,l) \tag{5.2}$$

Further recalling, τ_z stands for the delay, which causes a phase shift in every sub-carrier which is expressed through $e^{-j2\pi\tau_z\Delta fk}$ with k being the subcarrier index ranging from $[0, N-1]$. f_D represents the Doppler frequency shift, and since it represents a variation of frequency, each subcarrier will be affected differently, the higher the frequency the more affected the sub-carrier. However, in this model given that $f_C >> B$ we can neglect that detail and assume a uniform frequency variation throughout the sub-carriers. Therefore f_D can be seen as a modulation of each row of F_{Tx} with a complex sinusoid given by $e^{j2\pi f_{D,z}lT}$. Lastly $W(k,l)$ is the matrixial form of the AWGN whose elements are complex.

We now have both the transmitting and receiving matrices which represent no interest to the parameters we want to retrieve. As so we can divide them and isolate the wanted parameters, the delay τ_z and the frequency shift f_D. By proceeding to a element-wise matrixial division we get $F(k,l)$.

$$F(k,l)=\frac{F_{Rx}}{F_{Tx}}=\sum_{z=0}^{Z-1} b_z\cdot e^{-j2\pi\tau_z\Delta fk} e^{j2\pi f_{D,z}lT}+\frac{W(k,l)}{F_{Tx}(k,l)} \tag{5.3}$$

$F(k,l)$ is the representation of the wanted parameters across all symbols $c_{k,l}$. Having this information in a single matrix is what will later allow radar processing to generate radar imaging through a periodogram which is discussed in the next section.

5.2 - Spectral estimation problem

The use of periodograms allow RADARs to process its information into a visual representation. This happens due to the fact of periodograms being a well understood method to identify sinusoids. In a simpler one-dimension case, the use of a periodogram to identify a sinusoid is an already standard procedure, since it is already a well-known and explored technique. Being $s(k)$ a discrete-time signal with N samples of length its periodogram is given by

$$Per_{s(k)}(f) = \frac{1}{N}\left|\sum_{k=0}^{N-1} s(k) e^{-j2\pi fk}\right|^2 \tag{5.4}$$

It is possible to further simplify this expression when it comes to digital systems by firstly quantifying the frequency in regular intervals with the use of the N_{Per} parameter which has a higher value than N [31].

$$Per_{s(k)}(f) = \frac{1}{N}\left|\sum_{k=0}^{N-1} s(k) e^{-j2\pi \frac{nk}{N_{Per}}}\right|^2 \tag{5.5}$$

Which is equivalent to applying the fast Fourier transform to the signal. [31]

$$Per_{s(k)}(n) = \frac{1}{N}\left|FFT_{N_{Per}}\left[s(k)\right]\right|^2 \tag{5.5}$$

As in our case the input signal $s(k)$ is the earlier obtained two-dimension matrix $F(k,l)$, some readjustments have to be made in order to properly obtain its periodogram. A solution to this question is shown below as proposed in [48], where l denotes the symbols (columns) and k the sub-carriers (rows). It is important to keep in mind that these two dimensions present great importance since they allow us to respectively estimate range and velocity from a given target.

$$Per(n,m) = \frac{1}{NM}\underbrace{\left|\sum_{k=0}^{N_{Per}-1}\left(\overbrace{\sum_{l=0}^{M_{Per}-1}(F)_{k,l}\, e^{-j2\pi\frac{lm}{M_{per}}}}^{N \text{ FFTs of length } M_{Per}}\right) e^{j2\pi\frac{kn}{N_{per}}}\right|^2}_{M_{Per} \text{ IFFTs of length } N_{Per}} \tag{5.6}$$

It is important to choose a value of N_{Per} and M_{Per} higher than N and M respectively since it will increase the number of supporting points of the discrete periodogram and hence the accuracy at which frequencies can be estimated. Overall, this will increase the estimation accuracy at higher values of SNR [48], in this work we used a factor of eight for both parameters ($N_{Per} = 8N, M_{Per} = 8M$).

As described in the two-dimension periodogram expression, the operation consists in FFTs across every row and IFFTs across every column. This process is preceded by a zero-padding process row and column-wise as described in figure 53. The matrix's final dimension ends up being $N_{Per} \times M_{Per}$.

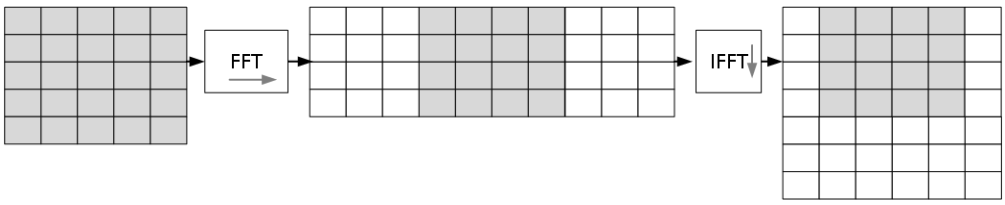

Figure 50 -Calculation of the periodogram. The grey area indicates periodogram elements with n<Nmax and |m|<Mmax.

Lastly we know that a sinusoid's presence in the input matrix $F(k,l)$ will translate into a peak value in the periodogram, therefore we know we are in the presence of an abrupt frequency oscillation which we can identify in terms of coordinates, for instance, if we observe a peak value for $Per(a,b)$ we can conclude that F has a column oscillation of $\Omega_d = \frac{2\pi a}{N_{Per}}$ and a row oscillation of $\Omega_v = \frac{2\pi b}{M_{Per}}$. And by multiplying these oscillation factors by the range and speed expressions presented in section 3.9 we get the distance estimation d and speed estimation v

$$d = \overbrace{\frac{c_0 T}{2}}^{r_{unambiguous}} \cdot \overbrace{\frac{a}{N_{Per}}}^{oscillation} \tag{5.6}$$

$$v = \overbrace{\frac{c_0}{2Tf_c}}^{v_{\max}} \cdot \overbrace{\frac{b}{M_{Per}}}^{oscillation} \tag{5.7}$$

5.3 - OFDM MIMO Radar

In order to measure the direction of arrival (DOA) of a signal, the minimum requirement is to have at least two receiving antennas in the system. Therefore, by using a MIMO configuration we ensure not only the angle estimation capability but we also benefit from the earlier mentioned diversity introduced in the system.

Picking up where we left off, in section 4.7, the received frame at the q th antenna is given by

$$F_{Rx,q}(k,l)=\sum_{p=0}^{P-1}F_{Tx,p}(k,l)\sum_{z=0}^{Z-1}b_z\cdot e^{-j2\pi k\Delta f\tau_{p,q,z}}\cdot e^{j2\pi f_{Dp,q,z}lT}+W_q(k,l) \tag{5.8}$$

Where:

- b_z is the attenuation factor
- $\tau_{p,q,z}=\dfrac{r_{p,z}+r_{q,z}}{c_0}$ is the round-trip time delay, with $r_{p,z}$ and $r_{q,z}$ represent the distance between the transmitting and receiving antennas and the target z respectively
- $f_{D_{q,p,z}}=\dfrac{2v_{rel,p,q,z}f_c}{c_0}$ represents the frequency shift relative to the target z

Considering a MIMO topology with $P\times Q$ antennas let us now also recur to the virtual array concept mentioned in section 4.6. By using that we are left with a $1\times PQ$ setup as shown in figure 54.

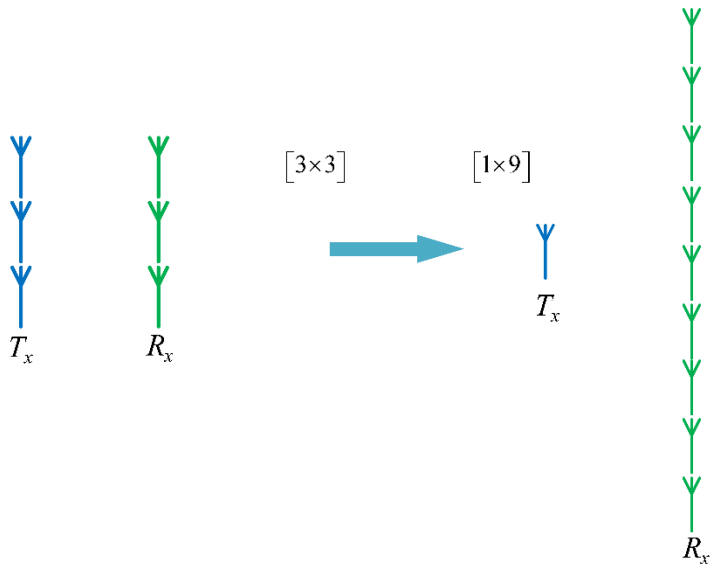

Figure 51 -Virtual array concept.

Following the same procedure as in (5.3) we remove the parameters with no interest by dividing element-wise the receiving frame in the q th antenna from the transmitted frame, obtaining

$$F_q(k,l)=\frac{F_{Rx,q}}{F_{Tx}}=\sum_{z=0}^{Z-1}b_z\cdot e^{-j2\pi\tau_{q,z}\Delta fk}e^{j2\pi f_{D,q,z}lT}+\frac{W_q(k,l)}{F_{Tx}(k,l)} \tag{5.9}$$

According to the concept presented in section 4.7, the signal has to travel increasingly more distance as we go through each antenna element, therefore we can say that each antenna presents an additional delay. Following that thought we can separate the delay $\tau_{z,q}$ in two components, τ_z which is the base delay from the target to the first antenna of the virtual array, and τ_{ant} which is the additional distance relative to the q th antenna.

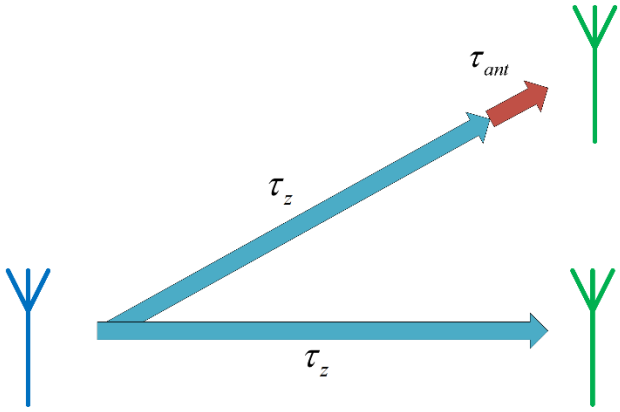

Figure 52 – Representation of the additional distance travelled.

The base delay is given by $\tau_z = \frac{2d_z}{c_0}$ with d_h being the distance between Tx antenna and target, whereas the additional delay uses the additional distance travelled expression presented in 4.7 $d_{ant}\sin(\theta)$ and presents itself as $\tau_{ant} = (q-1)\frac{d_{ant}\sin(\theta_z)}{c_0}$ where d_{ant} represents the antenna separation which in this case is $\frac{\lambda}{2}$.

The method to calculate the range and speed in this configuration stands similar to the one used in the SISO system, with the addition that the processing is done through all antenna elements. Therefore, we define the matrix responsible for mapping the delay and Doppler effect relative to the q th antenna as

$$G_q(k,l) = \underbrace{\sum_{k=0}^{N-1}\left(\overbrace{\sum_{l=0}^{M-1}(F)_{k,l}\, e^{-j2\pi\frac{lm}{M}}}^{N\text{ FFTs of length M}}\right) e^{j2\pi\frac{kn}{N}}}_{M\text{ IFFTs of length N}} \tag{5.10}$$

Which means that we will have a matrix mapping all the delay and Doppler effects throughout each of the Q antennas.

$$\mathbf{G}(k,l)=\begin{bmatrix} G_1(k,l) \\ \dots \\ G_Q(k,l) \end{bmatrix} \tag{5.11}$$

And in order to map each angle of incision throughout the antennas we will have another matrix

$$\mathbf{B}(\theta)=\begin{bmatrix} 1 \\ e^{-j2\pi(\sin(\theta)d_{ant}/\lambda)} \\ \dots \\ e^{-j2\pi((Q-1)\sin(\theta)d_{ant}/\lambda)} \end{bmatrix} \tag{5.12}$$

What we did was mapping the relevant parameters in two separate matrixes $\mathbf{G}$ and $\mathbf{B}$. We are then able to group the two matrixes by recurring to the Frobenius inner product (notation: $\langle a,b \rangle$), obtaining the single matrix $\mathbf{H}$. This matrix concentrates all the relevant information within itself and mapped through the indexes k,l and θ. We can express the matrix $\mathbf{H}$ as,

$$\mathbf{H}(k,l,\theta)=\langle \mathbf{G}(k,l),\mathbf{B}(\theta) \rangle \tag{5.13}$$

Where the angle of the target detection is $-90^{o}<\theta<90^{o}$.

5.4 - OFDM MIMO STBC RadCom system

With a well-established radar functionality, we are now in conditions to present the detailed joint RADAR and communication system implemented in this work. We start by modulating the data in the RadCom transmitter. The next step is the STBC where a Tarokh code is considered. Here we make use of the orthogonal code and send the information through the multiple antennas accordingly to the presented Tarokh scheme, thus introducing diversity in the system. At the reception, we receive this same data with added channel effects, from there we can later retrieve information relative to the channel itself as well as recover the sent data. The overall idea is to represent a system that will keep the sensing feature active whilst now performing communication at the same instant.

The general concept is depicted below in figure 56.

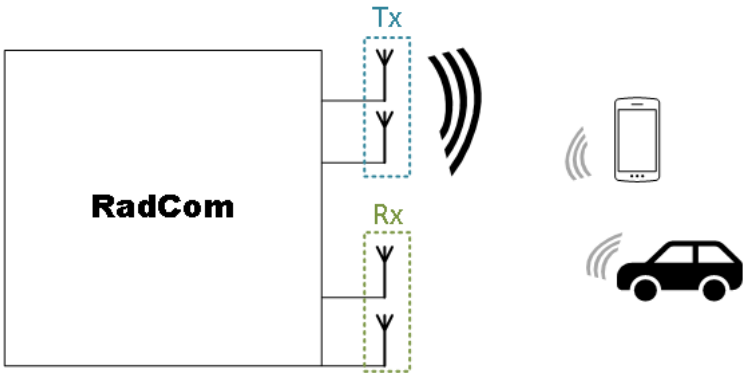

Figure 53 - RadCom scheme.

The RadCom system generates and encodes the transmitting data through the use of Tarokh coding. The generated signal is responsible for carrying out the two functionalities. Communicate with a mobile device equipped with a receiving antenna, and at the same time 'hit' the target(s) and return to the RadCom device. Despite the fact that these two systems share a common waveform, the processing differs from one to the other. In a classic monostatic radar, the used waveform is well known while the channel is not, therefore it is estimated through some estimation algorithm (e.g., periodogram). On the other end, in a communication receiver, the opposite happens. The channel has to be previously estimated, and only then the detection of the transmitted symbols can take place, this happens so that later the estimated channel effects (estimated a priori) can be reverted.

5.4.1 TRANSMITTER

Starting with the transmitter, where we considered a four transmitting antennas setup, the main functions to be performed are OFDM modulation and the space-time encoding as shown in figure. 57.

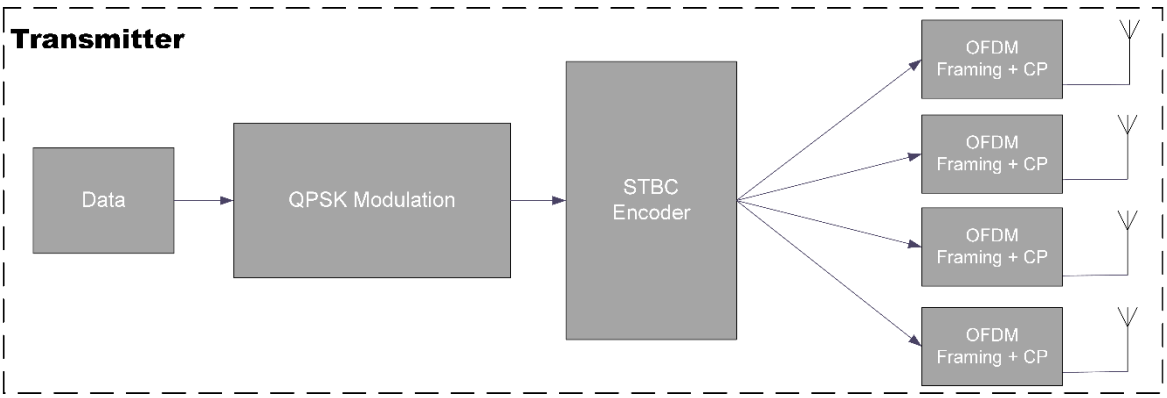

Figure 54 - Transmitter Block.

First, the bits are mapped in a QPSK or 16-QAM modulation scheme. In order to illustrate this, let us consider the QPSK case.

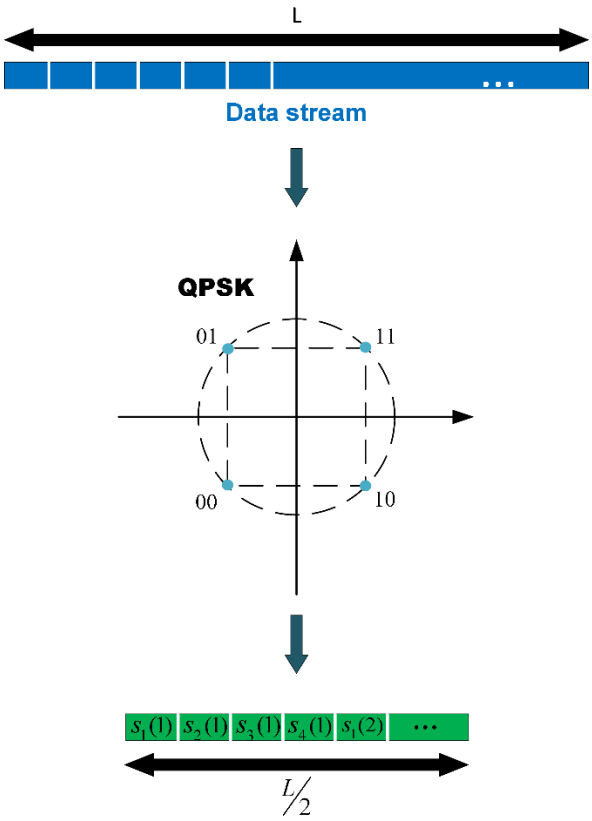

Figure 55-QPSK modulation process.

After the modulation, blocks of four symbols s_1, s_2, s_3, s_4 are taken and encoded into eight instants and four antennas per iteration, as will be explained next.

Through space-time block coding a data stream is encoded in blocks whose dimensions are space (between antennas) and time/frequency (slots). This process allows multiple redundant copies of the data stream to be sent through the different antennas thus bringing diversity to the process. Considering the first four modulated symbols $s_1(1), s_2(1), s_3(1), s_4(1)$ let us now define the Tarokh coding scheme as a matrix $\mathbf{C}$, where for the sake of simplicity we omit the indexes and so we denote $s_x(1)$ as s_x.

$$\mathbf{C} = \overbrace{\begin{bmatrix} s_1 & -s_2 & -s_3 & -s_4 & s_1^* & -s_2^* & -s_3^* & -s_4^* \\ s_2 & s_1 & s_4 & -s_3 & s_2^* & s_1^* & s_4^* & -s_3^* \\ s_3 & -s_4 & s_1 & s_2 & s_3^* & -s_4^* & s_1^* & s_2^* \\ s_4 & s_3 & -s_2 & s_1 & s_4^* & s_3^* & -s_2^* & s_1^* \end{bmatrix}}^{\text{Time/Frequency Slots}} \left.\vphantom{\begin{bmatrix} s \\ s \\ s \\ s \end{bmatrix}}\right\} \text{Antennas} \tag{5.14}$$

From the first to the fourth transmitting instants Ts_1 to Ts_4 (time slot 1 to 4), regarding the first four modulated symbols and ignoring channel effects, the transmitting data is given by

$$
\begin{aligned}
Ts_1 &= \{s_1, s_2, s_3, s_4\} \\
Ts_2 &= \{-s_2, s_1, -s_4, s_3\} \\
Ts_3 &= \{-s_3, s_4, s_1, -s_2\} \\
Ts_4 &= \{-s_4, -s_3, s_2, s_1\}
\end{aligned}
\tag{5.15}
$$

For the remaining four transmitting instants Ts_5 to Ts_8 (time slot 5 to 8), the same pattern repeats itself although in its conjugate form denoted by * in the coding scheme. What we are doing is basically go through each matrix element column by column.

$$
\begin{aligned}
Ts_5 &= \{s_1^*, s_2^*, s_3^*, s_4^*\} \\
Ts_6 &= \{-s_2^*, s_1^*, -s_4^*, s_3^*\} \\
Ts_7 &= \{-s_3^*, s_4^*, s_1^*, -s_2^*\} \\
Ts_8 &= \{-s_4^*, -s_3^*, s_2^*, s_1^*\}
\end{aligned}
\tag{5.16}
$$

This process then repeats itself with the next set of four modulated symbols $s_1(2), s_2(2), s_3(2), s_4(2)$, and keeps repeating until the last group of four symbols is processed. The concept can be visualized in figure 58 where we can see the modulated data continuously being added to the s_1, s_2, s_3, s_4 arrays.

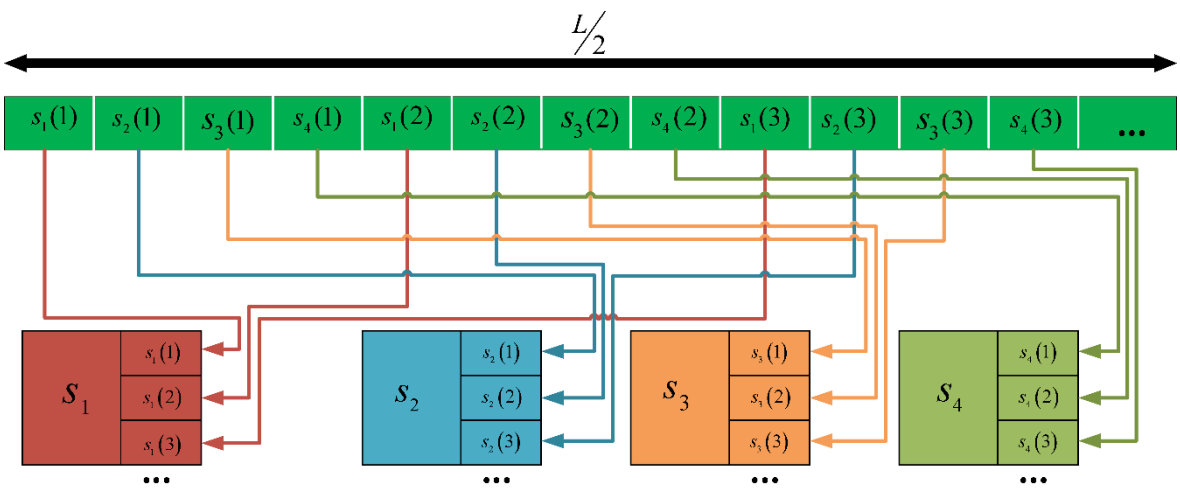

Figure 56 – Tarokh encoding process.

As we saw, for each four symbols we have eight transmission slots meaning that each antenna will transmit the double of the processed data symbols, therefore this code has a rate of $R = 1/2$. Furthermore, for each data stream an IFFT is performed and a cycle prefix added, accordingly to the OFDM waveform.

The following receiver operations are presented separately in two parts, one for the communication processing and one for the RADAR processing.

5.4.2 Communication receiver

Starting with the communication functionality, figure 60 gives a generic overview of its block diagram.

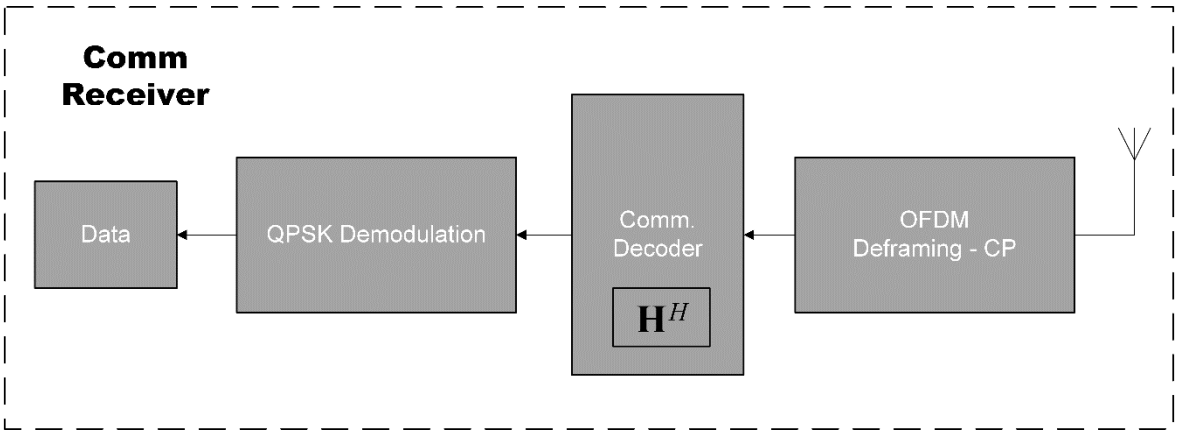

Figure 60 -Receiver block scheme.

Considering now the communication terminal, which is non-co-located with the transmitter, the focus falls on estimating the received data. This happens under the assumption that the channel is already known (estimated). The operations comprised in this block start with the OFDM deframing. Followed a decoding stage in which is possible to use the previously estimated channel matrix $\mathbf{H}$ to revert its own effects from the signal thus isolating it. This process will be explained further in this section. The last operation of the receiver is a QPSK and 16-QAM demodulation.

This communication receiver might represent a mobile device such as a cellphone for instance. This system is responsible for acquiring the data sent by the RadCom transmitter, and process it in order to recover the payload.

The received signal $\mathbf{r}_{k,l}$ at the time slot l and the k th sub-carrier can be given by,

$$\mathbf{r}_{k,l} = \mathbf{C}_{k,l}\mathbf{h}_{\mathrm{k,l}} + \mathbf{n}_{k,l} = \mathbf{H}_{k,l}\mathbf{c}_{k,l} + \mathbf{n}_{k,l} \tag{5.17}$$

Where $\mathbf{h}_{k,l}$ represents the channel effect vector, $\mathbf{n}_{k,l}$ the white Gaussian noise vector and the channel's coherence time higher than the duration of eight OFDM symbols. This takes place after the CP removal and after applying the FFT.

$\mathbf{C}_{k,l}$ represents the coding matrix for the subcarrier k and the block l with $k=\{0,...,N-1\}$ and $l=\{0,...,M-1\}$. This concept was earlier described. The first column of $\mathbf{C}_{k,l}$ represents the signal to be transmitted through the first antenna. Second, third and fourth columns follow the same logic being transmitted through the second third and fourth antennas, respectively

$$\mathbf{C}_{k,l}=\begin{bmatrix} s_1 & s_2 & s_3 & s_4 \\ -s_2 & s_1 & -s_4 & s_3 \\ -s_3 & s_4 & s_1 & -s_2 \\ -s_4 & -s_3 & s_2 & s_1 \\ s_1^* & s_2^* & s_3^* & s_4^* \\ -s_2^* & s_1^* & -s_4^* & s_3^* \\ -s_3^* & s_4^* & s_1^* & -s_2^* \\ -s_4^* & -s_3^* & s_2^* & s_1^* \end{bmatrix} \tag{5.18}$$

After comes the soft-decision, in order to do so we group the channel response components into the matrix $\mathbf{H}_{k,l}$ which becomes

$$\mathbf{H}_{k,l}=\begin{bmatrix} h_{k,l}(1) & h_{k,l}(2) & h_{k,l}(3) & h_{k,l}(4) \\ -h_{k,l}(1) & h_{k,l}(2) & -h_{k,l}(3) & h_{k,l}(4) \\ -h_{k,l}(1) & h_{k,l}(2) & h_{k,l}(3) & -h_{k,l}(4) \\ -h_{k,l}(1) & -h_{k,l}(2) & h_{k,l}(3) & h_{k,l}(4) \\ h_{k,l}(1)^* & h_{k,l}(2)^* & h_{k,l}(3)^* & h_{k,l}(4)^* \\ -h_{k,l}(1)^* & h_{k,l}(2)^* & -h_{k,l}(3)^* & h_{k,l}(4)^* \\ -h_{k,l}(1)^* & h_{k,l}(2)^* & h_{k,l}(3)^* & -h_{k,l}(4)^* \\ -h_{k,l}(1)^* & -h_{k,l}(2)^* & h_{k,l}(3)^* & h_{k,l}(4)^* \end{bmatrix} \tag{5.19}$$

By applying the Hermitian of $\mathbf{H}$ on both sides of the received signal equation (5.17) we get the soft decision $\tilde{\mathbf{c}}_{k,l}$

$$\tilde{\mathbf{c}}_{k,l}=\mathbf{H}_{k,l}{}^H\mathbf{r}_{k,l}=\mathbf{H}_{k,l}{}^H\mathbf{H}_{k,l}\mathbf{c}_{k,l}+\mathbf{H}_{k,l}{}^H\mathbf{n}_{k,l} \tag{5.20}$$

By now exploiting the Hermitian property $\mathbf{H}_{k,l}{}^H\mathbf{H}_{k,l}=\left\|\mathbf{h}_{k,l}\right\|^2\mathbf{I}$ where $\left\|\mathbf{h}_{k,l}\right\|^2=\left[\left|h_{k,l}(1)\right|^2+\left|h_{k,l}(2)\right|^2+\left|h_{k,l}(3)\right|^2+\left|h_{k,l}(4)\right|^2\right]$ and the fact that the identity matrix multiplied by another given matrix results in that same given matrix, we obtain the soft decision expression

$$\tilde{\mathbf{c}}_{k,l} = \left\|\mathbf{h}_{k,l}\right\|^2 \mathbf{c}_{k,l} + \mathbf{H}_{k,l}{}^{H}\mathbf{n}_{k,l} \tag{5.21}$$

5.4.3 RADAR receiver

Relatively to the RADAR functionality, figure 61 gives us a generic overview.

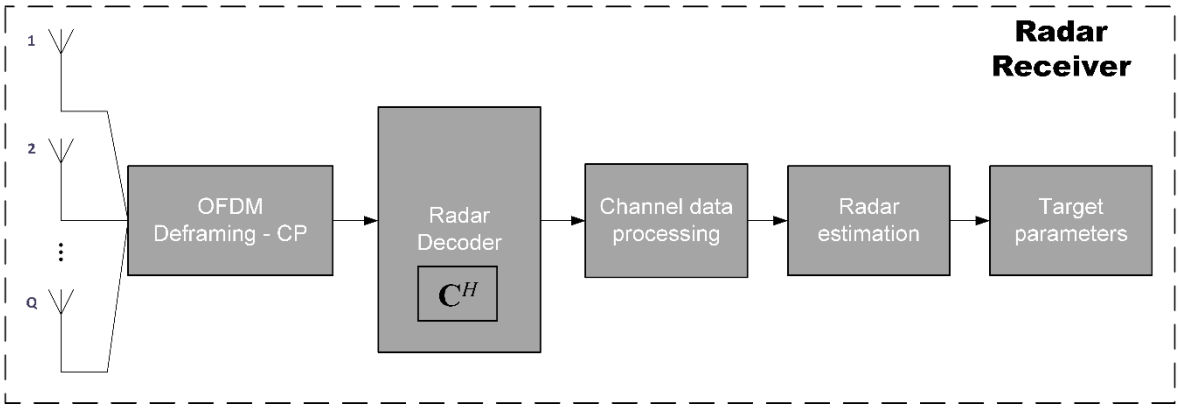

Figure 57- Radar receiver block diagram.

The objective now is to retrieve the channel effect matrix $\mathbf{H}$ so that its parameters can be estimated. In order to achieve this, we use an approach similar to the one used in the communication receiver. Firstly, an OFDM deframing takes place. Next comes the decoding block. By this time knowing the coded sent data $\mathbf{C}_{k,l}$ (e.q. 5.18), we can then cancel it, thus isolating the wanted channel effect matrix $\mathbf{h}_{k,l}$, this process will be addressed next in this section. After this stage we are in possession of the isolated channel effects parameters, and from here the RADAR processing and estimation takes place.

We express the received signal at the Q th receiving antenna element as

$$\mathbf{r}_{k,l}{}^{q} = \mathbf{C}_{k,l}\mathbf{h}_{k,l}{}^{q} + \mathbf{n}_{k,l} \tag{5.22}$$

With $\mathbf{r}_{k,l}{}^{q}$ denoting the OFDM received signal and $\mathbf{h}_{k,l}{}^{q}$ the channel frequency response between the transmitting antennas and the qth receiving element. $\mathbf{C}_{k,l}$ and $\mathbf{n}_{k,l}$ represent the already described coding matrix and noise components respectively.

Contrasting with the communication terminal, here the objective is to recover the channel matrix $\mathbf{H}_{k,l}$. However, the process to attain it shares some similarities with the previous. We start by defining the channel estimate towards the q th antenna $\tilde{\mathbf{h}}_{k,l}{}^{q}$ recurring to the Hermitian coding matrixes $\mathbf{C}_{k,l}{}^{H}$

$$\tilde{\mathbf{h}}_{k,l}{}^{q} = \mathbf{C}_{k,l}{}^{H}\mathbf{r}_{k,l} = \mathbf{C}_{k,l}{}^{H}\mathbf{C}_{k,l}\mathbf{h}_{k,l}{}^{q} + \mathbf{C}_{k,l}{}^{H}\mathbf{n}_{k,l} \tag{5.23}$$

By knowing the equality $\mathbf{C}_{k,l}{}^{H}\mathbf{C}_{k,l} = \mathbf{I}$ we can further write the full matrixial form for all channel components' soft decision as

$$\tilde{\mathbf{H}}_{k,l} = \mathbf{C}_{k,l}{}^{H}\mathbf{R}_{k,l} = \mathbf{H}_{k,l} + \mathbf{C}_{k,l}{}^{H}\mathbf{N}_{k,l} \tag{5.24}$$

where $\mathbf{R}$ is composed by all the receiving signal at each of the Q receiving antennas $\mathbf{R}_{k,l} = \left[\mathbf{r}_{k,l}{}^{1},\ldots,\mathbf{r}_{k,l}{}^{Q}\right]$ and $\mathbf{N}$ by the noise components at each of the Q receiving antennas $\mathbf{N}_{k,l} = \left[\mathbf{n}_{k,l}{}^{1},\ldots,\mathbf{n}_{k,l}{}^{Q}\right]$

We now have the channel estimation for each path for each transmitting antenna in the matrixial form.

By vectorizing the channel estimation transposed matrix $\mathbf{H}_{k,l}{}^{T}$ we obtain the channel response in a single vector $\mathbf{a}_{k,l}\left(p\right)$ in the following format

$$\mathbf{a}_{k,l}\left(p\right) = e^{j2\pi T_0 f_D l} e^{-j2\pi k\Delta f\tau} e^{-j2\pi p\phi} \tag{5.25}$$

By now making use of the virtual array concept presented earlier in sections 4.6 and 5.3, where an $P\times Q$ antenna setup can be approached as a $1\times PQ$, let us now assume a setup with one transmitting antenna and a uniform linear array (ULA) of 4Q receiving ones, each spaced by $\lambda/2$. This way, after vectorizing $\tilde{\mathbf{H}}_{k,l}{}^{T}$, we obtain $\tilde{\mathbf{a}}_{k,l}\left(p\right)$, which represents the channel response of the virtual setup with the one transmitting antenna and the 4Q receiving antennas.

From here, and as mentioned earlier it is possible to retrieve the Doppler frequency $f_D = 2v/\lambda$, the delay $\tau = 2R/c_0$ and the angle $\phi = \sin\left(\theta\right)$. With T_0 being the OFDM symbol duration, Δf being the subcarrier spacing and c_0 the speed of light.

For each OFDM symbol we generate a N sized vector, and by grouping each of these we obtain a square matrix of dimension $N\times M$ (Number of subcarriers $\times$ Number of OFDM symbols) shown in figure 62. By further concatenating these resulting two-dimension matrixes, one for each receiving antenna we attain a three-dimension matrix $\mathbf{G}_{k,l,p}$ as per figure 63.

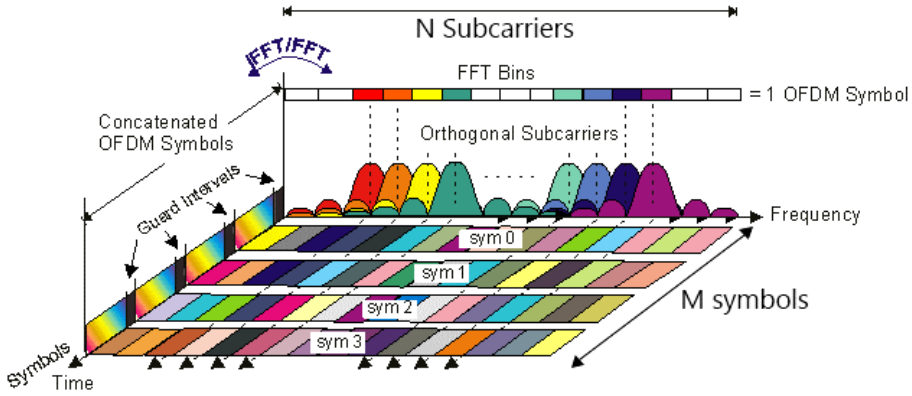

Figure 58- Graphic presentation of the OFDM frame in both domains [49].

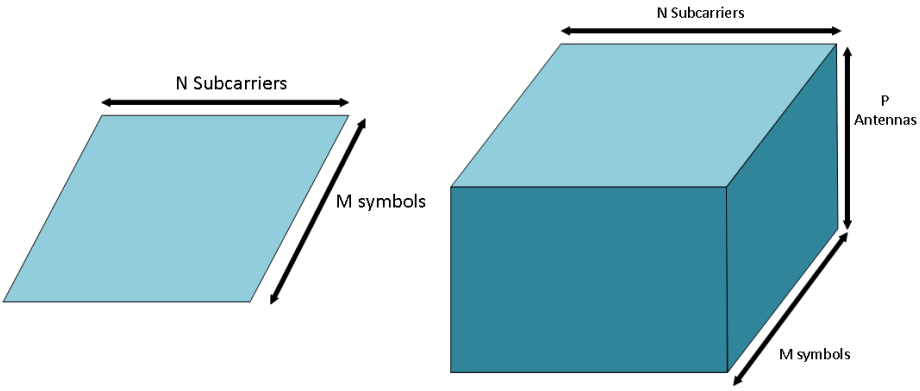

Figure 59 – Three-dimension frame.

We now have a full structure that maps all the parameters which are accessible through the k, l, p indexes. We can then proceed as described in section 5.2, 5.3 in order to obtain the radar parameters.

5.5 - Numerical results

This section presents and evaluates the obtained results for both the OFDM SISO and MIMO radar and the RadCom system. Some initial parameters worth mentioning are the operation frequency of both systems which is 24GHz ISM mmWave band, which has been used for research purposes as it is deregulated, and the bandwidth B=93.1 MHz. The systems' maximum unambiguous range is given by

$R = c_0/2\Delta f = Tc_0/2 = 1649m$ and the range resolution, fully dependent on the bandwidth has the value of $\Delta r = c_0/2B = 1.61m$. The number of subcarriers is $N_c = 1024$. All these parameters and other related to the OFDM waveform are summarized in table 4.

Table 4 - Experimental parameters

Unambiguous Range R	$1649m$
Range resolution Δr	$1.61m$
Velocity resolution Δv	$4.44\,m/s$
Number of subcarriers N_c	1024
Subcarrier spacing Δf	$90.09kHz$
Number of OFDM symbols M	128

Following the same order used to present the systems functionalities, we first present the results for the OFDM SISO radar system, followed by the MIMO radar, capable of angle estimation, and lastly, we go through the results of the proposed implemented RadCom system.

5.5.1 OFDM SISO Radar

We start by presenting the results obtained for the OFDM SISO RADAR. Three scenarios are considered.

The first being the simplest, one target case. The target parameters and set resolutions are shown in table 5.

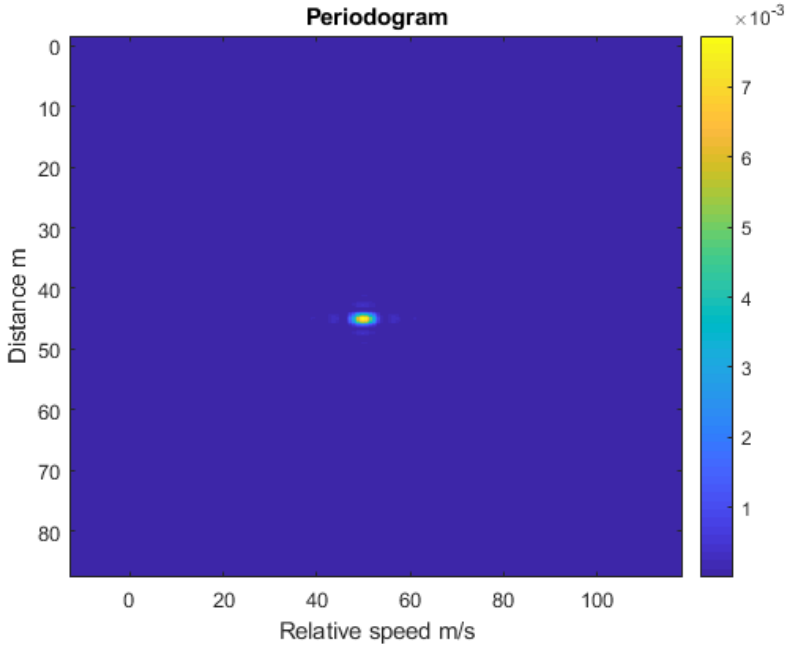

Figure 60 -OFDM SISO one target.

Table 5 - Example 1

Distance	45 m
Speed	50 m/s
Range resolution	1.61 m
Speed resolution	4.44 m/s

- Following with a multi-target scenario in the same unchanged system (same resolution values), where target1 is the one in the lower half of the picture and target 2 the one in the upper half.

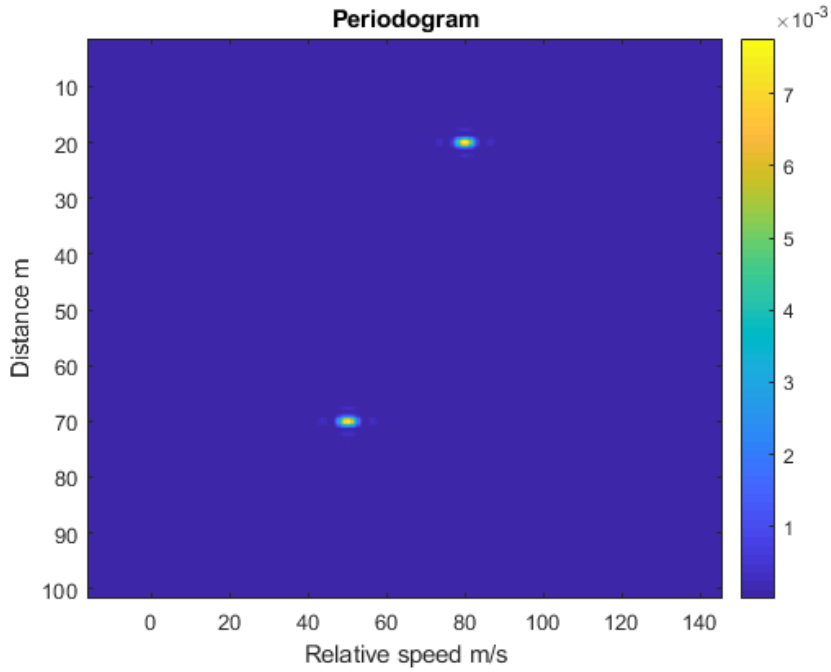

Figure 61 -OFDM SISO two targets.

Table 6 - Example 2

Distance Target1	70 m
Speed Target1	50 m/s
Distance Target2	20m
Speed Target2	80 m/s

- In this system's last example, while maintaining the previous settings we add a third target. The targets disposition from left to right is target1, target3 and target2.

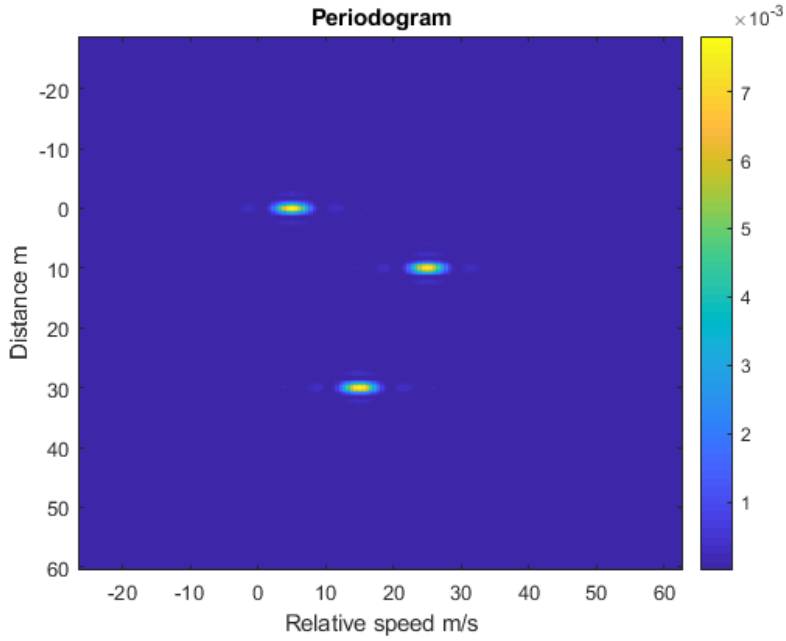

Figure 62 – OFDM SISO three targets.

Table 7 - Example 3

Distance Target1	0 m
Speed Target1	5 m/s
Distance Target2	10m
Speed Target2	25 m/s
Distance Target3	30 m
Speed Target3	15 m/s

As we can see, with this middle range configuration, the OFDM SISO RADAR system is fully capable of acquiring multiple target's distance and velocity. Since we set a range resolution of 1.61m, and the distance between all targets is way above that value. The RADAR shows no difficulties identifying each target with accuracy. The same happened with the velocity estimation. We can further conclude that the number of sub-carriers and symbols matches this scenario, otherwise we would see a distorted image in terms of speed resolution which is what happens when those parameters are too low.

5.5.2 OFDM MIMO Radar

Moving to the multiple antenna scenario we will now be able to estimate the angle along with the range. The way the results will be presented is also through three scenarios, however this time we will keep doubling the number the antennas of the system in each example.

All the following three scenarios will share the same target parameters shown in table 8.

Table 8 - Example 4 OFDM MIMO parameters

Distance Target1	20 m
Angle Target1	10º
Distance Target2	10 m
Angle Target2	50º
Distance Target3	60 m
Angle Target3	25º

- In the following cases we have $Q = 10, 20, 40$ receiving antennas, respectively

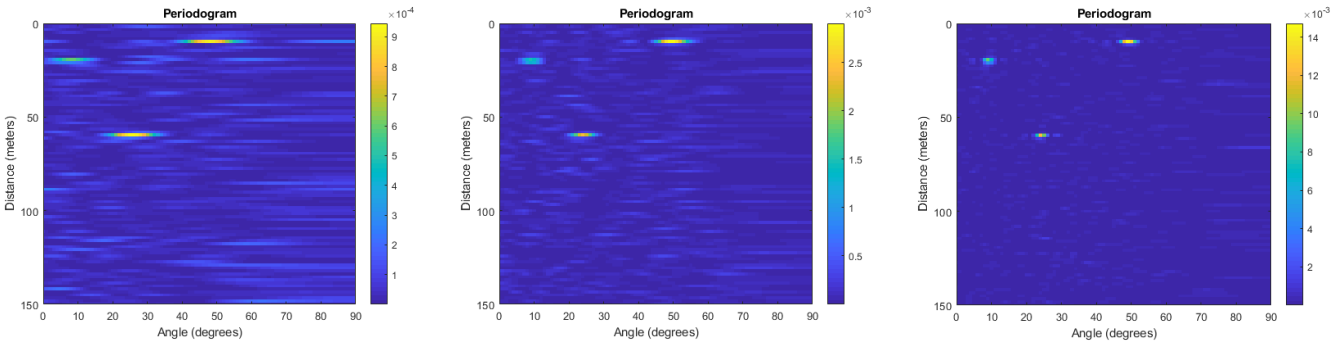

Figure 63 -MIMO-OFDM RADAR, 10 / 20 / 40 receiving antenas.

As we can verify, in figure 66 the 10 receiving antennas setup results in a poor angle resolution, therefore it becomes challenging to read the angle value with accuracy. In the second scenario, the number of antennas is doubled to 20, and the results show some improvement, although still being far from optimal. Lastly with 40 receiving antennas we see a much-improved angle resolution in which we can read with ease the angle values. It becomes clear how the number of antennas highly influences the system's performance. This happens due to the fact of the angle resolution being obtained through $180/Q$ where Q is the number of receiving antennas. Therefore, across the three cases we can see the angle resolution changing from 18° to 9° and 4.5^{o}.

5.5.3 OFDM MIMO QPSK RadCom

Lastly, we present the results for the RadCom system with $Q = 20$ receiving antennas and 128 OFDM symbols. In a first instance using QPSK modulation, we once more will be increasing the number of targets throughout the scenarios, describing their respective parameters and average BER performance.

- Starting with the one target scenario.

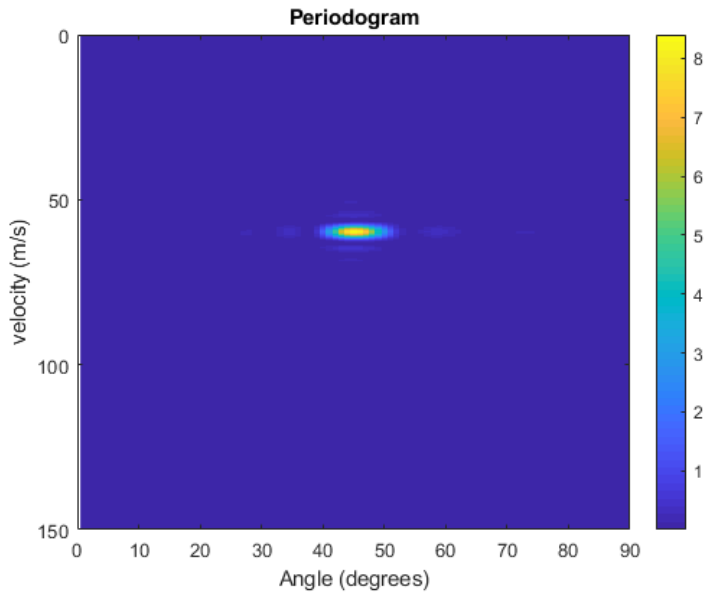

Figure 64 – OFDM MIMO RadCom one target.

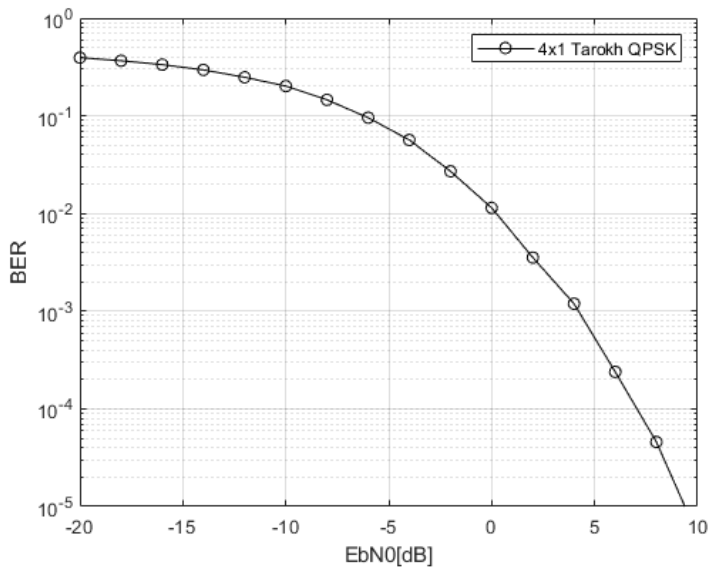

Figure 65 - OFDM MIMO RadCom one target BER performance.

Table 9 - Example 5

Speed	60 m/s
Angle	45º
Speed resolution	4.44 m/s
Angle resolution	9º

- Two target scenario follows

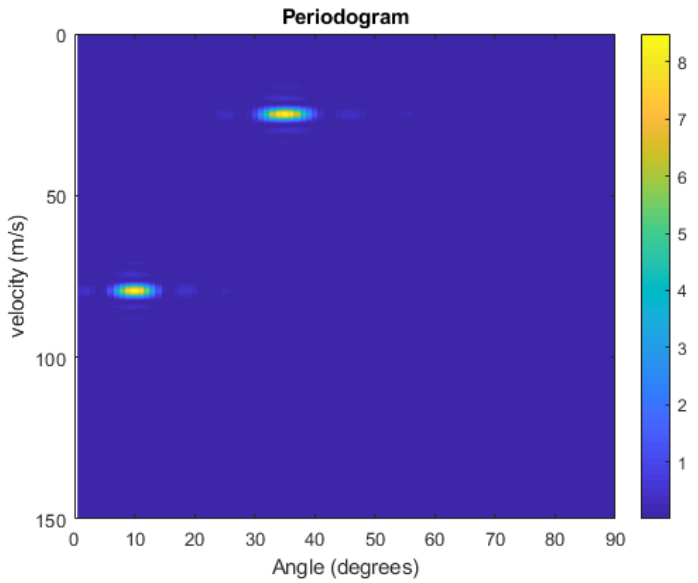

Figure 70 – OFDM MIMO RadCom two targets.

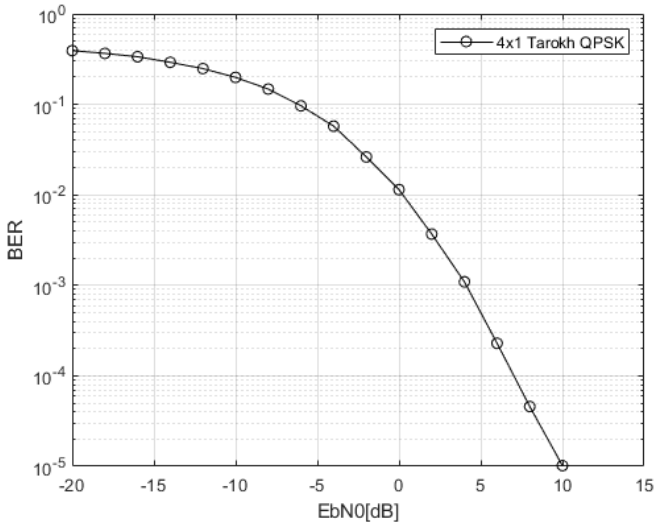

Figure 66 - OFDM MIMO RadCom two targets BER performance.

Table 10 - Example 6 OFDM MIMO RadCom two targets' parameters

Speed Target1	25 m/s
Angle Target1	35º
Speed Target2	80 m/s
Angle Target2	10º
Speed resolution	4.44 m/s
Angle resolution	9º

In both cases it is possible to observe a good RADAR estimation, with the displayed targets easily matching the described target parameters presented in the parameter tables. Again, in this case, the number of received antennas was 20, by increasing this value, we would be able to attain an even better angle resolution. We can also verify the successful inclusion of the communication functionality in the system, and analyze its BER through figure 70 and 72. A more detailed comparison of BER curves is presented in the end of this chapter.

5.5.4 OFDM MIMO 16-QAM RadCom

We now present the 16-QAM implementation. We consider the same structure as the above presented QPSK.

- One target scenario

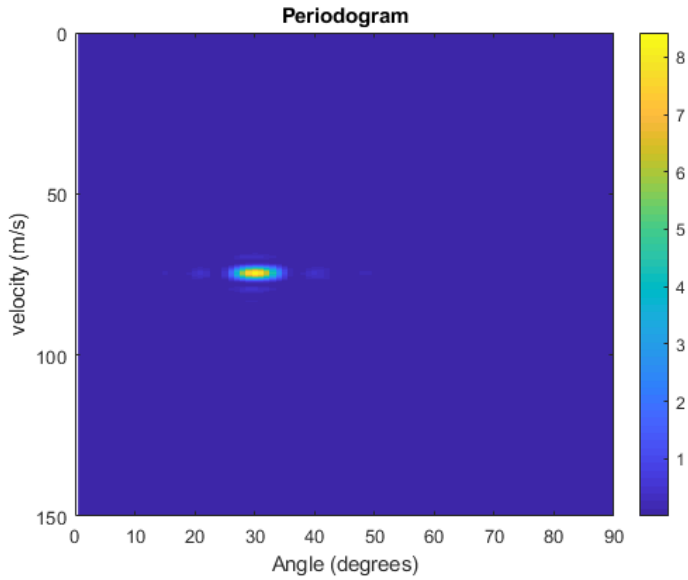

Figure 67 - OFDM MIMO 16-QAM RadCom one target.

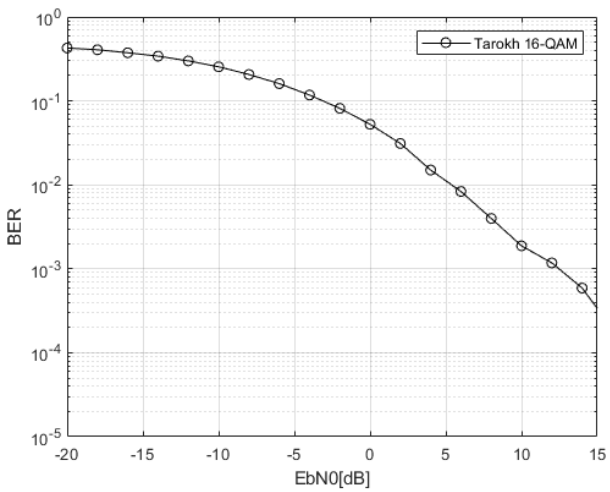

Figure 68 - OFDM MIMO 16-QAM RadCom one target BER performance.

Table 11 - Example 7 OFDM MIMO 16-QAM RadCom one target parameters

Speed	75 m/s
Angle	30º
Speed resolution	4.44 m/s
Angle resolution	9º

- Two target scenario

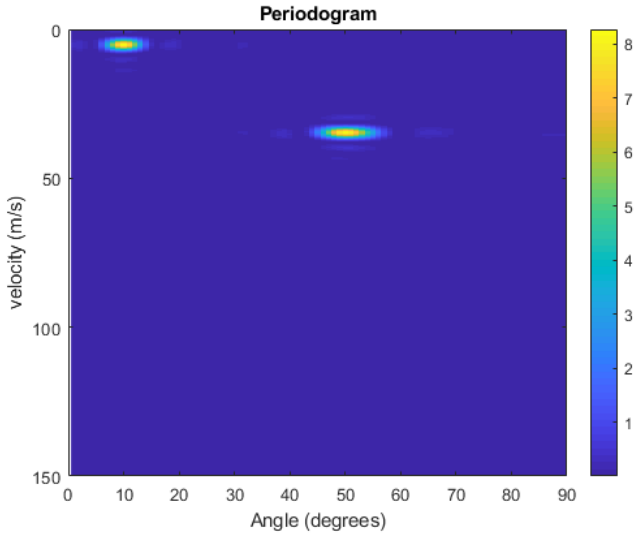

Figure 69 - OFDM MIMO 16-QAM RadCom two target.

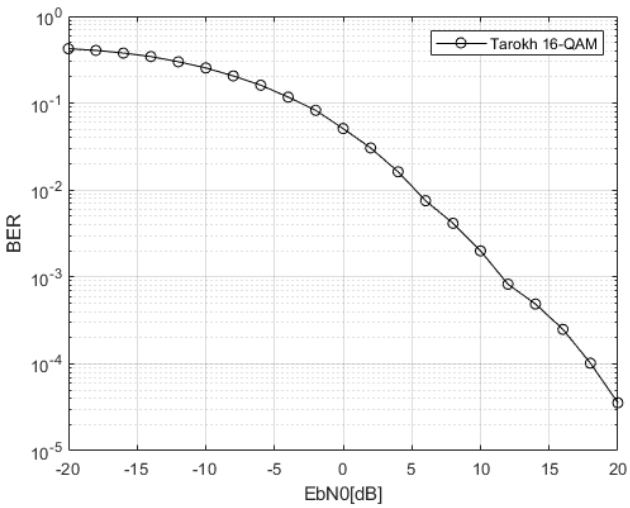

Figure 70 - OFDM MIMO 16-QAM RadCom two target BER performance

Table 12 - Example 8 OFDM MIMO 16-QAM RadCom two target parameters

Speed Target1	5 m/s
Angle Target1	35º
Speed Target2	10 m/s
Angle Target2	50º
Speed resolution	4.44 m/s
Angle resolution	9º

Again, through the displayed images we can confirm the correct RADAR detection for both the one and two target scenarios. We can also notice, by analyzing the BER curve of both scenarios, that the 16-QAM implementation presents a slightly lower performance in relation to the QPSK, this comparison is explicitly presented next.

In figure 77 we present the BER comparison between all the presented implementations including also two Alamouti based 2×1 implementations (QPSK and 16-QAM) non discussed in this work.

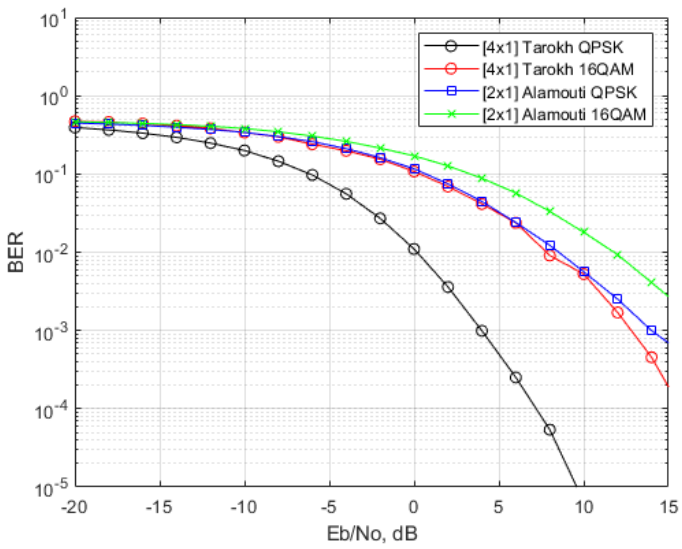

Figure 71 – BER performance comparison between QPSK and 16QAM implementations.

As we analyze the average BER comparison, we can visualize the impact of a greater diversity degree in the system, with the 4×1 Tarokh implementation outperforming the 2×1 Alamouti system by presenting a steeper slope in its curve. We can then conclude that the communication functionality integrated in this shared platform presents a viable performance level. Lastly, we can affirm that the proposed integration of RADAR and communication functionalities in an OFDM MIMO RadCom system was achieved.

.

Chapter 6
Conclusion

In this section, we summarize and present the conclusions of this work, as well as some topics for possible future development.

6.1 - Conclusions

The presented dissertation follows the need of convergence between the two already well-known and consolidated systems, the RADAR and communication. Although the fact that each of them has already solidified its position in our world and are totally independent of the other, the possibility of merging both is seen as a great benefit in terms of general efficiency, and as key technology for 6G. With the pace at which wireless communications is evolving, we struggle to equally evolve in efficiency. The finite resource at our disposal, the radio frequency spectrum, has to be carefully managed in order to support all the functionalities already attached to it, and since we cannot grow or produce spectrum, the solution is to use it in a smarter way. Joining functionalities is exactly that, a way to free some space in an increasingly more crowded space.

The first chapter served as an introduction to the work, while at the same time provided us information on the evolution of the mobile communication techniques. Here we can grasp the context of how a new generation arises and the changes that it can bring with it. This is exactly what we aim to do with the joint RadCom system and 5G. We also briefly discussed the RADAR topologies as well as the motivations behind this work.

The second chapter was focused on RADARs. Here a brief overview of how RADARs work was shown, followed by the possible detection scenarios in a practical RADAR system. Later in the chapter we presented the mathematic expressions for each radar measurement and lastly, we explored the pulsed and continuous wave RADARs, its differences and applications.

The third chapter presents the most important aspects of the Orthogonal Frequency Division Multiplexing. Starting with the basic functionalities and later explaining why it is beneficial to use it. We then identify the OFDM symbol structure along with the information that it carries.

The fourth chapter goes through some MIMO aspects. We explore diversity and how to attain it, we also went through the mathematic processes behind the Alamouti and Tarokh codification techniques. Later in the chapter a brief virtual array concept is presented as well as all the possibilities coming from its use.

The fifth chapter served as the meeting point for all the previous presented concepts, here we presented how we can merge the two systems. We presented the missing pieces such as the periodogram and from there we started presenting case scenarios, starting with a simpler case of a SISO RADAR and moving onto more

complex setups. From there results were presented for multiple scenarios along with how the processing happened.

It is consensual that a RadCom system brings a lot of solutions to some of the problems rising in the near future. The merging of two important functionalities into a single system represents advantages not only in terms of cost and size, but also in terms of performance and spectrum usage efficiency. This becomes possible by making use of OFDM as the common waveform, and Tarokh coding as the process to secure the communication, the use of this STBC introduces diversity and orthogonality to the system, thus improving its performance. In order to evaluate the performance of this joint system a simulation platform was created, there we started with a simpler scenario of a SISO RADAR, and kept increasing the complexity, finally reaching the MIMO RadCom system.

The evaluation of the presented results led to the following main conclusions.

- The flexibility in terms of sub-carrier allocation provided by the use of OFDM proves itself useful in the RADAR functionality, furthermore by being able to cope with good resolution values, OFDM presents itself as a good option for this system.
- The simulation shown that is possible to perform RADAR imaging through the use of the proposed system.
- It is possible to estimate with the desired accuracy, target parameters such as range, speed and angle. by tuning the proposed system parameters.
- It was clearly shown that RADAR and communication can coexist without presenting interference to the other. In other words, it is possible to establish communication whilst performing a sensing operation.
- Through the presenting simulations we could observe that Tarokh presents good performance levels and can be seen as a viable coding option for a RadCom system.

6.2 - Future work

This work fits in a very searched topic, and as such there is always more work to be done. We believe that some possible next steps in this area are:

- The practical application of the presented techniques. The implementation in hardware, (e.g. FPGA) and performance evaluation in a practical scenario.
- Exploring the combinations of new codifications and modulations and compare them performance wise. In this work we used the Tarokh four antenna, $1/2$ code rate, however there are other variants with different code-rates, which can be worth to exploring.

- Testing the RadCom system's diversity and robustness limits. The system was designed to present no interference within its two functionalities; however, it would be of interest to know how it would perform in a scenario where multiple RadCom terminals deployed. Study the interferences between them and develop strategies to minimize them.
- Extending this study to other common waveforms besides OFDM. Although OFDM presents itself as a good choice for this system, it would be interesting to compare its performance to other common waveforms. Some worth mention are the generalized frequency division multiplexing (GDFM) and filter bank multicarrier (FBMC), these can reveal themselves as viable options and its study could represent some relevant future work.

.

Bibliography

[1] L. Ashiho, "Mobile technology: Evolution from 1G to 4G," *Electronics for you,* vol. 6, pp. 968--976, 2003.

[2] J. M. Sanchez, "Mobile revolution: From 2G to 5G," in *2021 IEEE Colombian Conference on Communications and Computing (COLCOM)*, Cali, Colombia, 2021.

[3] Q. K. U. D. Arshad, A. U. Kashif and I. M. Quershi, "A Review on the Evolution of Cellular Technologies," em *16th International Bhurban Conference on Applied Sciences and Technology*, Islamabad, Pakistan, 2019.

[4] Ericson, "Ericsson Mobility Report," November 2016. [Online]. Available: https://www.ericsson.com/en/mobility-report/reports. [Accessed on 16 May 2021].

[5] J. Navarro-Ortiz, P. Romero-Diaz, S. Sendra, P. Ameigeiras, J. J. Ramos-Munoz and J. M. Lopez-Soler, "A Survey on 5G Usage Scenarios," *IEEE Communications Surveys & Tutorials,* vol. 22, nº 2, pp. 905-929, Secondquarter 2020.

[6] M. Benisha, R. Prabu and V. Bai, "Requirements and challenges of 5G cellular systems," in *2016 2nd International Conference on Advances in Electrical, Electronics, Information, Communication and Bio-Informatics (AEEICB)*, Chennai, India, 2016.

[7] W. L. Melvin and J. A. Scheer, *Principles of modern radar*, Scitech publishing, 2014.

[8] W. Wiesbeck, L. Sit, M. Younis, T. Rommel, G. Krieger and A. Moreira, "Radar 2020: The Future of Radar Systems," in *2014 International Radar Conference*, Lille, France, 2014.

[9] C. Sturm, T. Zwick and W. Wiesbeck, "An OFDM System Concept for Joint Radar and Communications Operations," in *Vehicular Technology Conference Spring 2009 - IEEE 69th Vehicular Technology Conference*, 2009.

[10] B. K. Chalise, M. G. Amin and B. Himed, "Performance Tradeoff in a Unified Passive Radar and Communications System," *IEEE Signal Processing Letters,* vol. 24, nº 9, pp. 1275-1279, 2017.

[11] B. Paul, A. R. Chiriyath e D. W. Bliss, "Survey of RF Communications and Sensing Convergence Research," *IEEE Access,* 2016.

[12] F. Liu, C. Masouros, A. P. Petropulu, H. Griffiths and L. Hanzo, “Joint Radar and Communication Design: Applications, State-of-the-Art, and the Road Ahead,” *IEEE Transactions on Communications,* vol. 68, nº 6, pp. 3834-3862, 2020.

[13] H. H. Meinel, “Evolving Automotive Radar - from the very beginnings into the future,” in *The 8th European Conference on Antennas and Propagation*, Stuttgart, 2014.

[14] “Tesla,” [Online]. Available: https://www.tesla.com/autopilot%20. [Accessed on 14 06 2021].

[15] D. Arminas, “Case proven for C-V2X, says German trial,” *Its International*, 2020.

[16] L. Leyva, J. Maciel, D. Castanheira, A. Silva e A. Gameiro, “Alamouti coding scheme and virtual array concept for joint radar and communication systems,” in *2020 12th International Symposium on Communication Systems, Networks and Digital Signal Processing (CSNDSP)*, Porto, Portugal, 2020.

[17] H. Griffiths, P. Knott e W. Koch, “Christian Hülsmeyer: Invention and Demonstration of Radar, 1904,” *IEEE Aerospace and Electronic Systems Magazine,* vol. 34, nº 8, pp. 56-60, 2019.

[18] C. Wolff, “Radar Basics,” [Online]. Available: https://www.radartutorial.eu/01.basics/Range%20Resolution.en.html. [Accessed on 29 06 2021].

[19] D. R. M. O'Donnell, “Introduction to Radar Systems – Lecture 5 – Detection of Signals,” MIT Lincoln Laboratory, 25 07 2018. [Online]. Available: https://www.youtube.com/watch?v=PmEHxluUWuc. [Accessed on 29 06 2021].

[20] M. I. Skolnik, *Radar Handbook*, McGraw Hill, 1990.

[21] M. A. Richards, *Fundamentals of radar signal processing*, McGraw-Hill Education, 2005.

[22] S. M. Patole, M. Torlak, D. Wang and M. Ali, “Automotive radars: A review of signal processing techniques,” *IEEE Signal Processing Magazine,* vol. 34, nº 2, pp. 22-35, 2017.

[23] L. Leyva, D. Castanheira, A. Silva, A. Gameiro and L. Hanzo, “Cooperative multi-terminal radar and communication: A new paradigm for 6G mobile networks,” *IEEE Vehicular Technology Magazine,* pp. 2 - 11, 11 October 2021.

[24] L. Zheng, M. Lops, Y. C. Eldar and X. Wang, “Radar and Communication Coexistence: An Overview: A Review of Recent Methods,” *IEEE Signal Processing Magazine,* vol. 36, nº 5, pp. 85-99, 2019.

[25] K. V. Mishra, M. R. B. Shankar, V. Koivunen, B. Ottersten and S. A. Vorobyov, “Toward Millimeter-Wave Joint Radar Communications: A Signal Processing Perspective,” *IEEE Signal Processing Magazine,* vol. 36, nº 5, pp. 100-114, 2019.

[26] R. Prasad, OFDM for wireless multimedia communications, Boston: Artech House.

[27] H. L. Zayed, A.-E. Zikry, F. Newagy and S. Mahmood, “Effect of switching loads on the power line communication(PLC) modems inside direct local area network (dlan),” 2014.

[28] “Concepts of orthogonal frequency division multiplexing (ofdm) and 802.11 wlan,” Keysight Technologies, [Online]. Available: https://rfmw.em.keysight.com/wireless/helpfiles/89600b/webhelp/subsystems/wlan-ofdm/content/ofdm_basicprinciplesoverview.htm. [Accessed on 06 07 2021].

[29] A. Zaidi et. al, “Multicarrier waveforms,” in *5G - Physical layer*, Academic press, 2018, pp. 119-158.

[30] “RF Wireless World,” [Online]. Available: https://www.rfwireless-world.com/. [Accessed on March 2021].

[31] M. Braun, “OFDM radar algorithms in mobile communication networks,” 2014.

[32] T. Kh, “OFDM signal constellation processing on Radar applications,” *Armenian Journal of Physics,* vol. 6, pp. 204-208, 2013.

[33] N. Levanov, “Multifrequency radar signals,” in *Record of the IEEE 2000 International Radar Conference*, 2000.

[34] Y. L. Sit, C. Sturm e T. Zwick, “Doppler estimation in an OFDM joint radar and communication system,” em *German Microwave Conference*, Darmstadt, Germany, 2011.

[35] S. C, P. E, Z. T e W. W, “A novel approach to OFDM radar processing,” in *IEEE Radar Conference*, Pasadena, CA, USA, 2009.

[36] A. Ganis, E. Miralles, C. Heller, U. Prechtel, A. Meusling, H.-P. Feldle, M. Loghi, F. Ellinger in V. Ziegler, “A system concept for a 3D real-time OFDM MIMO radar for flying platforms,” in *German Microwave Conference*, Bochum, Germany, 2016.

[37] E. Tsakalaki, O. Alrabadi, E. de Carvalho and G. F. Pedersen, “Multiplexing Index and MIMO Band Index: Two Novel Metrics for MIMO Antenna Evaluation,” in *7th European Conference on Antennas and Propagation*, 2013.

[38] B. J. Donnet and I. D. Longstaff, “Combining MIMO Radar with OFDM Communications,” in *European Radar Conference*, 2006.

[39] M. Lesturgie, “T06 - MIMO Radar,” in *IEEE Radar Conference*, 2014.

[40] A. Silva and A. Gameiro, “Multiple Antenna Systems,” *Comunicações sem fios DETI, Universidade de Aveiro,* 2017.

[41] Y. Liu, G. Liao and Z. Yang, “Range and angle estimation for MIMO-OFDM integrated radar and communication systems,” in *CIE International Conference on Radar*, 2016.

[42] TechTarget, “Search Mobile Computing,” [Online]. Available: https://searchmobilecomputing.techtarget.com/definition/MISO. [Accessed on 09 08 2021].

[43] C. Sturm, Y. L. Sit, M. Braun and T. Zwick, “Spectrally interleaved multi-carrier signals for radar network applications and MIMO-Radar,” *IET Radar Sonar and Navigation,* 2013.

[44] T. T. Nguyen, “Design and Analysis of Superresolution Algorithm and Signal Separation Technique for an OFDM-based MIMO Radar,” *Master Thesis,* 31 10 2012.

[45] S. Alamouti, “A simple transmit diversity technique for wireless communications,” *IEEE Journal on Selected Areas in Communications,* vol. 16, nº 8, pp. 1451 - 1458, 1998.

[46] A. M. Haimovich, R. S. Blum e L. J. Cimini, “MIMO Radar with Widely Separated Antennas,” *IEEE Signal Processing Magazine,* vol. 25, nº 1, pp. 116 - 129, 2008.

[47] B. Nuss, L. Sit, M. Fennel, J. Mayer, T. Mahler and T. Zwick, “MIMO OFDM radar system for drone detection,” *18th International Radar Symposium (IRS),* pp. 2155-5753, June 2017.

[48] M. Braun, C. Sturm and F. K. Jondral, “Maximum likelihood speed and distance estimation for OFDM radar,” in *2010 IEEE Radar Conference*, Arlington, VA, USA, 2010.

[49] M. Sadegh, April 2013. [Online]. Available: https://msnourbakhsh.ece.iut.ac.ir/content/simulation-ofdm-system-using-matlab-m-file. [Accessed on 9 June 2021].

[50] “FADING CHANNELS AND MOBILE COMMUNICATION,” IIT KHARAGPUR, 12 07 2021. [Online]. Available: http://fcmcvlab.iitkgp.ac.in/exp10/Theory/exp10.pdf.

[51] Y. Jiang, H. Sun, S. Sambhwani and J. Hou, “Uplink Closed Loop Transmit Diversity for HSPA,” *Qualcomm Inc,* 2010.

[52] E. Dahlman, S. Parkvall and J. Sköld, “Downlink Physical-Layer Processing,” *4G LTE-Advanced Pro and The Road to 5G,* pp. 93-168, 2016.